THE EFFECT OF MONOCROTALINE PYRROLE ON CELL PROLIFERATION AND DNA SYNTHESIS *IN VITRO* AND *IN VIVO*

By

Patrick Bruce Lappin

A DISSERTATION

Submitted to
Michigan State University
in partial fulfillment of the requirements
for the degree of

DOCTOR OF PHILOSOPHY

Department of Pathology
Institute for Environmental Toxicology

1997

ABSTRACT

THE EFFECT OF MONOCROTALINE PYRROLE ON CELL PROLIFERATION AND DNA SYNTHESIS *IN VITRO* AND *IN VIVO*

By

Patrick Bruce Lappin

Monocrotaline pyrrole [MCTP], a toxic pyrrolizidine alkaloid metabolite, causes pulmonary hypertension *in vivo* and inhibits cell proliferation *in vitro*. It has been hypothesized that pulmonary endothelial cell [EC] injury after MCTP is the forerunner of vascular leak and arterial medial remodeling in the lung, processes which may be exacerbated by MCTP-induced alterations in the cellular proliferative response to injury. The research described herein was designed to identify the effects of MCTP on cell replication processes *in vitro* and *in vivo*.

The disruption of cell proliferation by MCTP *in vitro* was characterized by the analysis of treated EC cell cycle progression. Bovine endothelial cells [BECs] were chemically synchronized and exposed to MCTP during limited cell cycle phases prior to, during or after DNA synthesis. Using fluorescence activated cell sorting [FACS] flow cytometry, cells exposed to MCTP during the initiation of DNA synthesis were arrested prior to mitosis but continued to synthesize DNA, a pattern not identified in other treatment groups. The disconnection of DNA synthesis and mitosis implied that MCTP caused the disruption of a premitotic checkpoint.

In vivo, the impact MCTP on EC proliferation and DNA synthesis was measured as the change in cell density and the nuclear incorporation of bromodeoxyuridine [BrdU], respectively. Within 3 days of MCTP administration, ECs lining small muscular arteries exhibited an increase in DNA synthesis which persisted through day 7. By day 8 there was no increase in the EC density in arteries from MCTP-treated rats, indicating that increased DNA synthesis induced by this toxicant was not followed by cell proliferation.

Using techniques described for the *in vivo* evaluation of ECs, an increase in medial thickness of pulmonary arteries after MCTP administration was characterized as vascular smooth muscle cell [VSMC] hypertrophy, based on an increase in medial thickness and enlargement of VSMCs. VSMCs actively synthesized DNA for up to 8 days after MCTP but did not undergo cell division, suggesting that MCTP may induce VSMC mitogenesis but block subsequent proliferation.

In summary, MCTP alters cell proliferation and DNA synthesis *in vitro* and *in vivo*. Cultured endothelial cells undergo inhibition of mitosis but continue to synthesize DNA, a pattern which is cell cycle phase-dependent. After MCTP exposure *in vivo*, pulmonary artery endothelial and smooth muscle cells have a persistent increase in DNA synthesis but do not proliferate. Interestingly, the cycle phase most responsive to the effects of MCTP *in vitro* constitutes the predominant cell cycle phase of both endothelial and smooth muscle cells in pulmonary arteries *in vivo*, suggesting similar mechanisms may be at work.

"Trust in the Lord with all your heart,
and do not rely on your own insight.
In all your ways acknowledge Him,
and He will make your path straight.

Proverbs 3:5-6
Holy Bible
New Revised Standard Version

To my wife, Robin, and my children, Christopher and Katharine

Your patients and understanding
provided the avenue,
your support and encouragement
were my vehicle.

Without you this endeavor would
not have been possible.

ACKNOWLEDGEMENTS

My deepest appreciation goes to my research advisor, mentor and fast friend, Dr. Robert Roth, who took a chance by providing a space in his laboratory for "one more pathologist". His encouragement fueled my interest in research, an area many veterinary practitioners think little about.

I would like to thank members of my guidance committee, Dr. Thomas Bell, Dr. Robert Dunstan, Dr. N. Edward Robinson and Dr. Patrick Venta. Each provided an area of expertise and wisdom which helped me to endure the total Ph.D. experience. A special thanks goes to Drs. Bell and Dunstan for their motivation during ACVP board exam preparation and their encouragement to pursue a Ph.D. degree, and to Dr. Barbara Steficek, for her endless supply of positive reinforcement.

Dr. Pamela Fraker and Dr. Louis King provided me the facilities and aptitude for the development and performance of all of the flow cytometry work. Their patients and concern for detail is greatly appreciated.

Our laboratory was filled with a group of wonderful individuals who contributed their time and talents unselfishly over my tenure, and to whom I have established a 'family' bond. Thanks go to Dr. Marc Bailie, for his never-ending enthusiasm, Dr. Patricia Ganey, for her compassion and encouragement, Dr.

Paul Jean, for his ability to motivate and contribute great ideas, Dr. Patricia Titoff and Dr. James Wagner, my sounding boards during difficult times and Dr. Duane Hill, my spiritual brother. Special thanks also go to Ms. Amanda Hutchins, Ms. Kerry Ross and Ms. Terese Schmidt for their tireless assistance in my experiments and maintenance of the tissue culture facility.

I cannot express sufficient acclamation to the staff of the MSU Clinical Center histology laboratory, Cathy Campbell, Leann Lumbert, Amy Porter, and Josselyn Miller for the effort they expended in the preparation of tissue sections essential for my research. Their dedication to detail as well as their interest and sense of humor were the ideal ingredients for a great working relationship.

Aside from the countless professional acknowledgments, I want to thank members of Cornerstone United Methodist Church for their interest and encouragement during my second academic career. They taught me that nothing is impossible if it was done with the Lord.

Last, but far from least, I want to express my love for my wife Robin, my son Christopher, and my daughter Katharine, who suffered most from my absence. They continued to be there for me, supporting my cause, providing motivation and showing me their love in spite of my inability to spend much quality time with them. I will forever be in their debt.

TABLE OF CONTENTS

		Page
LIST OF TABLES		xii
LIST OF FIGURES		xiii
LIST OF ABBREVIATIONS		xv
CHAPTER 1 - INTRODUCTION		1
I.	Pyrrolizidine Alkaloids	2
	A. Botanical Background	2
	B. Human and Animal Exposure	2
	C. Chemical Structure	4
	D. Pathophysiology of Toxic PAs	4
	E. PAs: Summary	8
II.	Monocrotaline and Monocrotaline Pyrrole	8
	A. Metabolism of MCT	9
	1. Pathways of MCT Bioconversion	10
	a. Nontoxic Metabolites of MCT	12
	b. Pyrrolic Intermediates of MCT	13
	c. Detoxification of MCTP	15
	2. Variability in the Metabolism of MCT	16
	B. Pathophysiology of MCT *In Vivo*	18
	1. MCT-induced Hepatotoxicity	20
	a. Acute Hepatotoxicity	20
	b. Chronic Hepatotoxicity	22

Table of Contents (cont.)

			Page
	2.	Cardiopulmonary Toxicity after MCT	24
		a. Clinical Effects /Necropsy Results	25
		b. Pulmonary Pathophysiology	27
		1. Early Events	27
		2. Delayed Events	30
		3. Late Events	33
C.	MCTP-induced Pneumotoxicity		34
	1.	Low Dose MCTP	35
	2.	High Dose MCTP	37
D.	Factors Contributing to PH after MCT/MCTP		38
	1.	Vasoreactivity after MCT/MCTP	39
	2.	Vasoactive Agents and MCT\MCTP	40
		a. EC-associated Mediators	40
		b. Platelet-derived Mediators	43
	3.	Pathways of Cell Growth/Metabolism	44
	4.	Mitogenic Growth Factors	46
	5.	Pharmacologic Intervention Studies: Interpretation	48
E.	Effects of MCTP on Cells *In Vitro*		49
	1.	Cell Viability and Morphology	49
	2.	Cell Enlargement and Proliferation	51
F.	Human Cardiopulmonary Disease		53
	1.	Primary Pulmonary Hypertension [PPH]	54
	2.	Acute Respiratory Distress Syndrome [ARDS]	56
G.	Summary		58
III.	Cell Injury, Repair and Altered Repair Responses		61
A.	Response to a Growth Stimulus		61

Table of Contents (cont.)

		Page
1.	Permanent, Labile and Stable Cells	61
2.	Optimal Repair of Injury	62
a.	Vascular Intima	63
b.	Vascular Media	66
c.	Vascular Adventitia	69
B.	MCT[P]-induced Vascular Injury	70
1.	Incomplete Repair	70
2.	Vascular Medial Hypertrophy	74
C.	Inhibition of Cell Proliferation	76
1.	The Cell Cycle	77
2.	Control of the Cell Cycle	79
3.	The Cell Cycle and MCTP-induced Injury	84
D.	Summary	85
IV.	Research Goals	89
CHAPTER II -	THE RESPONSE OF PULMONARY ENDOTHELIAL CELLS TO MONOCROTALINE PYRROLE: CELL PROLIFERATION AND DNA SYNTHESIS *IN VITRO*	93
	Summary	94
	Introduction	95
	Materials and Methods	98
	Results	108
	Discussion	130
CHAPTER III -	PULMONARY VASCULAR ENDOTHELIAL CELL DNA SYNTHESIS AND CELL PROLIFERATION *IN VIVO* AFTER MONOCROTALINE PYRROLE EXPOSURE	142
	Summary	143
	Introduction	144
	Materials and Methods	145
	Results	151
	Discussion	158

Table of Contents (cont.)

	Page
CHAPTER IV - HYPERTROPHY AND PROLONGED DNA SYNTHESIS IN SMOOTH MUSCLE CELLS CHARACTERIZE PULMONARY ARTERIAL WALL THICKENING AFTER MONOCROTALINE PYRROLE ADMINISTRATION TO RATS	166
Summary	167
Introduction	168
Materials and Methods	170
Results	176
Discussion	185
SUMMARY AND CONCLUSIONS	195
BIBLIOGRAPHY	204

LIST OF TABLES

		Page
TABLE 1:	Density of smooth muscle cells in pulmonary arteries of MCTP-treated rats.	181
TABLE 2:	Medial thickness of pulmonary arterial walls after exposure of rats to MCTP.	183

LIST OF FIGURES

		Page
Figure 1:	Basic pyrrolizidine alkaloid structure.	5
Figure 2:	Metabolic products of monocrotaline.	11
Figure 3:	Vascular repair after endothelial cell injury.	65
Figure 4:	Potential VSMC responses to MCTP and endothelial cell injury.	68
Figure 5:	Stages of the cell cycle.	78
Figure 6:	Cell cycle checkpoints.	80
Figure 7:	MCTP-induced endothelial cell injury and hypothetical cell cycle effect.	88
Figure 8:	Cell cycle phase distributions.	109
Figure 9:	BrdU incorporation.	111
Figure 10:	Cell cycle progression of unsynchronized BECs.	113
Figure 11:	Cell cycle progression of synchronized BECs.	115
Figure 12:	Cell cycle pattern in unsynchronized BECs exposed to vehicle or MCTP.	118
Figure 13:	Cell cycle phase distribution in unsynchronized BECs treated with vehicle or MCTP.	119
Figure 14:	Cell cycle pattern in synchronized BECs exposed to vehicle or MCTP.	120
Figure 15:	Cell cycle phase distribution in synchronized BECs treated with vehicle or MCTP.	122

List of Figures (cont.)

		Page
Figure 16:	Cell cycle kinetic pattern in untreated, synchronized BECs.	123
Figure 17:	Progression of BrdU+ BECs after removal of APH.	126
Figure 18:	Progressive entry of untreated, synchronized BECs into the cell cycle.	128
Figure 19:	Cell cycle kinetic pattern after exposure of synchronized BECs to vehicle or MCTP.	129
Figure 20:	Effect of MCTP exposure [0-4 hours after APH removal] on the cell cycle kinetic pattern.	132
Figure 21:	Effect of MCTP exposure [4-8 hours after APH removal] on the cell cycle kinetic pattern.	134
Figure 22:	Markers of lung injury after MCTP.	153
Figure 23:	Photomicrographs of lung from vehicle- or MCTP-treated rats.	155
Figure 24:	BrdU incorporation in pulmonary artery endothelial cells after vehicle or MCTP administration.	157
Figure 25:	Representative photomicrographs showing the relative BrdU incorporation in pulmonary vascular endothelial cells.	160
Figure 26:	Density of endothelial cells lining small pulmonary arteries.	161
Figure 27:	Medial thickness of small pulmonary arteries from rats treated with vehicle or MCTP.	178
Figure 28:	DNA synthesis [BrdU labeling index] of pulmonary vascular smooth muscle cells [VSMCs].	180
Figure 29:	The frequency distribution of small pulmonary artery diameters.	184
Figure 30:	The medial thickness ratio of small pulmonary arteries.	186

LIST OF ABBREVIATIONS

ACE	Angiotensin-Converting Enzyme
ANOVA	Analysis of Variance
APC	Alveolar Pneumocyte [Type I Pneumocyte]
APH	Aphidicolin
ARDS	Acute Respiratory Distress Syndrome
BALF	Bronchoalveolar Lavage Fluid
BEC	Bovine Pulmonary Artery Endothelial Cell
BrdU	2-Bromo-5-Deoxyuridine
BSA	Bovine Serum Albumin
Cdk	Cyclin-dependent Kinase
cRBC	Chicken Red Blood Cell
DFMO	α-Difluoromethylornithine
DMEM	Dulbecco's Modified Eagle's Medium
DMF	N,N'-Dimethylformamide
DNA	Deoxyribonucleic Acid
EC	Endothelial Cell
ECG	Electrocardiograph
EDRF	Endothelium-Derived Relaxing Factor
EDTA	Ethylenediaminetetraacetic acid
EGF	Epidermal Growth Factor
ET-1	Endothelin-1
ETOH	Ethanol
FACS	Fluorescence-Activated Cell Sorting
FBS	Fetal Bovine Serum
FITC	Fluorescein Isothiocyanate
HBSS-CM	Hanks Balanced Salt Solution with Calcium and Magnesium
HBSS-w/o-CM	Hanks Balanced Salt Solution without Calcium and Magnesium
5-HT	5-Hydroxytryptamine [serotonin]
ip	Intraperitoneal
iv	Intravenous
Hg	Mercury
LDH	Lactate Dehydrogenase
LW/BW	Lung Weight/Body Weight Ratio

List of Abbreviations (cont.)

MCT	Monocrotaline
MCTP	Monocrotaline Pyrrole
MCT[P]	Monocrotaline or Monocrotaline Pyrrole
M199	Medium 199
MMC	Mitomycin C
ODC	Ornithine Decarboxylase
PA	Pyrrolizidine Alkaloid
PAF	Platelet Activating Factor
PBS	Phosphate-Buffered Saline
PDGF	Platelet-Derived Growth Factor
PEC	Porcine Pulmonary Artery Endothelial Cell
PGI_2	Prostaglandin I_2 [Prostacyclin]
PH	Pulmonary Hypertension
PI	Propidium Iodide
PPH	Primary Pulmonary Hypertension
PSF	Penicillin, Streptomycin, Fungizone
REC	Rat Pulmonary Vascular Endothelial Cell
RNA	Ribonucleic Acid
RV/[LV+S]	Right Ventricle Weight/[Left Ventricle Weight+ Interventricular Septum Weight]
SCE	Sister Chromatid Exchange
TBS	Tris-buffered Saline
TGF-β	Transforming Growth Factor-Beta
VOD	Veno-occlusive Disease
VSMC	Vascular Smooth Muscle Cell

Chapter I

INTRODUCTION

I. Pyrrolizidine Alkaloids

A. Botanical Background

One in ten of the plants found throughout the world contain one or more alkaloid compounds, some of which are harmful (Culvenor, 1980). The ingestion of plants containing alkaloids may be intentional, as with psychotropic drugs [ie, cocaine], or accidental, through the ingestion of contaminated foods and herbal medicaments. As many as 3% of the world's flowering plants, including the genera *Heliotropium*, *Senecio* and *Crotalaria* contain pyrrolizidine alkaloids [PAs] (Zalkow et al, 1979; Culvenor, 1980; Smith and Culvenor, 1981), many of which have been associated with acute and chronic injury in both humans and animals (Mattocks, 1986; Huxtable, 1989). The ubiquitous distribution of plants containing these alkaloids provides a readily avaliable source of contamination of both human and animal foods (Bull et al, 1968).

B. Human and Animal Exposure

PAs intoxication occurs in humans with the use of some traditional medicinal herbs or "bush teas" (Stuart and Bras, 1957; McGee et al, 1976; Stillman et al, 1977; Huxtable, 1980; Arseculeratne et al, 1981; Roitman, 1981; Ridker et al, 1985; Arseculeratne et al, 1985; Kumana et al, 1985; Sperl et al, 1995), or following the consumption of contaminated foods (Mohabbat et al,

1976; Tandon et al, 1976; Ghanem and Hershko, 1981; Ridker et al, 1985). Acute or chronic liver injury have been most often reported, but sporadic cases of pulmonary artery injury have also been attributed to PA intoxication (Heath et al, 1975; McGee et al, 1976). The accidental ingestion of PAs leading to liver disease has also been reported in horses (Lessard et al, 1986; Mendel et al, 1988), pigs (Harding et al, 1964; Hooper and Scanlan, 1977; Peckham et al, 1974), cattle (Johnson and Molyneux, 1984; Odriozola et al, 1994) and other ruminants (Goeger et al, 1982; Seaman, 1987; Winter et al, 1990).

The administration of PA compounds to experimental animals has been used to characterize the mechanism of toxicant bioactivation and to study injury to the liver or lung which ensues. PA toxicosis has been most extensively studied in the rat (Christie, 1958; Hayashi and Lalich, 1967; Kay et al, 1967; Newberne and Rogers, 1973; Meyrick et al, 1980; Bruner et al, 1983; Wilson et al, 1989). Other species have been exposed to a variety of PA compounds to examine variability in metabolism and toxicologic effect, including mice (Rosenfeld and Beath, 1945; Hooper, 1974), monkeys (Allen et al, 1967; Chesney and Allen, 1973), cattle (Bras et al, 1957; Dickenson et al, 1976; Johnson et al, 1985; Pringle et al, 1991), dogs (Atkinson et al, 1977; Miller et al, 1978; Epstein et al, 1992), pigs (McGrath et al, 1975; Hooper and Scanlan, 1977), chickens (Allen et al, 1970; Hooper and Scanlan, 1977) and trout (Hendricks et al, 1981). The results and conclusions derived from these and

similar studies have been the subject of several review papers (McLean, 1970; Huxtable, 1990).

C. Chemical Structure

The basic structure of all naturally occurring PAs is an hydroxylated 1-methylpyrrolizidine composed of two, fused five-member rings (necine or pyrrolizidine nucleus) with a common nitrogen at the bridgehead (position 4 of the pyrrolizidine nucleus) and unsaturation at the 1-2 position of the 3-pyrroline ring as shown in Figure 1 (Mattocks, 1972b; Mattocks, 1986). Toxic PAs are unsaturated necines with branching ester groups at positions 7 and/or 9 of the pyrrolizidine nucleus (Schoental and Mattocks, 1960; Culvenor et al, 1962; Cheeke, 1988; Winter and Segall, 1989). The conformation of each base alkaloid [pyrrolizidine ring and attached ester groups] dictates the relative cytotoxicity of each PA (Schoental and Mattocks, 1960; Mattocks, 1972b; Kim et al, 1993); monoesterified PAs are the least toxic, whereas cyclic diesters are associated with the greatest toxicity (Winter and Segall, 1989).

D. Pathophysiology of Toxic PAs

The alkaloid base extracted from leaves, seeds and stems of a PA-containing plants may be directly injurious to cells (Sullman and Zuckerman,

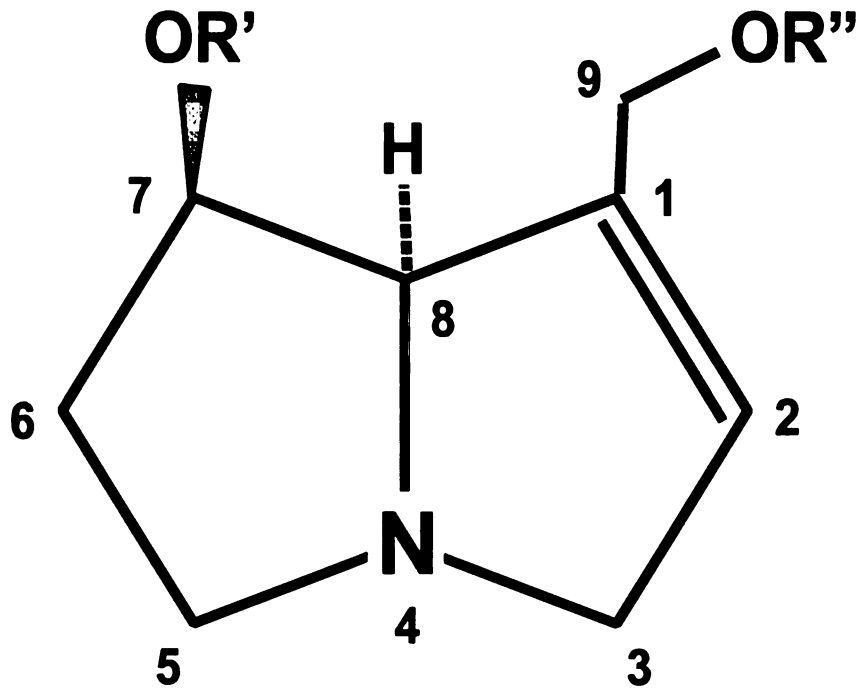

Figure 1. Basic pyrrolizidine alkaloid structure.

Fused, 5-member rings with a common nitrogen at position 4 [bridgehead] constitute the core structure of pyrrolizidine alkaloids. The addition of carboxylic acid residues at R' and R" dictate the ability to produce toxicity. Cyclic diesters formed from esterification with dicarboxylic acids demonstrate the greatest toxicity.

1969; Baybutt et al, 1994) but it is generally considered to produce little toxicity without metabolic modification of that base (Frayssinet and Moulé, 1969; Mattocks, 1971; Mattocks, 1972b; Armstrong et al, 1972). *In vivo*, the liver is responsible for metabolism of the parent alkaloid (Mattocks, 1968; Hilliker et al, 1983; Lafranconi and Huxtable, 1984), a process which results in the formation of both nontoxic and toxic intermediates (Mattocks, 1968; Mattocks, 1971b; Monks et al, 1990). Toxic PA metabolites cause injury which is dose- (Bull and Dick, 1960; Lalich and Merkow, 1961; Plestina and Stoner, 1972; Hurley and Jago, 1975; Lalich et al, 1977; Cheeke and Pierson-Goeger, 1983; Okada et al, 1995c) and species-dependent (McLean, 1970), and can be influenced by the age and sex of the exposed individual (Chesney and Allen, 1973b; Cheeke and Pierson-Goeger, 1983; Cheeke, 1989).

The liver is most often affected after PA exposure (Davidson, 1935; Christie, 1958; Barnes et al, 1964; Jago, 1970), by virtue of its proximity to sites of reactive metabolite formation (McLean, 1970). Acute, hepatic necrosis and hemorrhage are seen after a large dose of a toxic PA (Christie, 1958; Culvenor et al, 1976), whereas smaller, single or multiple doses result in more limited acute cell death but produce chronic persistent injury to the liver and other organs (Davidson, 1935; Barnes et al, 1964; Jago, 1970; McLean, 1970; Culvenor et al, 1976; Odriozola et al, 1994). Cells of lungs (Davidson, 1935; Harris et al, 1942; Kay et al, 1967; Wagenvoort et al, 1974a; Meyrick and Reid,

1979), kidney (McGrath et al, 1975; Hooper and Scanlan, 1977; Kurozumi et al, 1983), heart (Rosenfeld and Beath, 1945; Lalich and Merkow, 1961) spleen and thymus [ie, immunocytes] (Deyo and Kerkvliet, 1990; Deyo and Kerkvliet, 1991; Deyo et al, 1994) may also be affected by PA exposure.

In addition to the cytotoxic effects produced by PA intoxication, these compounds are genotoxic (Williams and Mori, 1980; Bruggeman and Vanderhoeven, 1985; Mori et al, 1985; Sanderson and Clark, 1993), mutagenic (Green and Christie, 1961; Martin et al, 1972; Yamanka et al, 1979; Wehner et al, 1979; Müller et al, 1992), carcinogenic (Newberne and Rogers, 1973; Allen et al, 1975; Schumaker et al, 1976; Hirono et al, 1977; Mattocks and Cabral, 1982; Candrian et al, 1985), and cause the inhibition of mitosis (Davidson, 1935; Peterson, 1965; Downing and Peterson, 1968; Svoboda et al, 1971; Peterson et al, 1972; Mattocks and Legg, 1980). The property of mitotic inhibition prompted testing of indicine N-oxide as an anticancer drug in the late 1970's (Powis et al, 1979; Kovach et al, 1979). It has been hypothesized that PA exposure results in the inhibition of proliferation through mitotic arrest and thereby delays repair, substantially contributing to the progressive nature of PA-induced disease (Schoenthal and Magee, 1959; McGrath and Duncan, 1975; Reindel and Roth, 1991).

E. PAs: Summary

PAs are a class of plant-derived alkaloid toxins which are associated with morbidity and mortality in both humans and animals. PA intoxication in humans is most often the result of intentional or accidential ingestion. Although hepatic injury is a major effect of PA intoxication, other tissues are susceptable to both acute cytotoxicity and chronic disease. Chronic injury may be an effect of altered repair processes associated with PA-induced inhibition of mitosis. Among the hundreds of potentially harmful PAs, several have been studied extensively, not only for their impact on human health, but in experimental animals as models of human pulmonary diseases.

II. Monocrotaline and Monocrotaline Pyrrole

PA-containing plants of the family Leguminosae comprise several species including *Crotalaria* (Bull et al, 1968; Huxtable, 1989). *Crotalaria spectabilis* is common to central and southern India, Jamaica, and the southeastern United States (Huxtable, 1989; Kay and Heath, 1969). A closely related species, *C. fulva*, is also abundant in India, Sri Lanka, Indonesia and the Caribbean. Both plant species have been associated with poisoning of humans and animals (Bras et al, 1957; Stuart and Bras, 1957; Pringle et al, 1991).

C. spectabilis contains several types of PAs including monocrotaline (MCT), spectabiline and retusine (Huxtable, 1989). MCT is a cyclic diester of the pyrrolizidine, retronecine, and is the primary PA constituent of *C. spectabilis* (Bull et al, 1968; Culvenor, 1980; Smith and Culvenor, 1981). Other alkaloids extracted from *C. spectabilis* are considered toxic but have been less well characterized (Huxtable, 1989). The harmful effects of *C. spectabilis* have been well documented (Lalich and Merkow, 1961; Kay et al, 1967; Peckham et al, 1974; Smith and Heath, 1978; Meyrick and Reid, 1979; Meyrick et al, 1980). The leaves and seeds of the *C. spectabilis* plant contain the greatest amount of alkaloid; these constituents and purified MCT have been used to produce experimental liver and lung injury (Kay et al, 1967; Kay et al, 1971). MCT has also been used to study DNA damage produced by this alkylating agent (Petry et al, 1984; Mori et al, 1985; Müller et al, 1992).

A. Metabolism of MCT

The toxic effect of MCT *in vivo* is due to reactive intermediates derived from the structural modification of the parent alkaloid by hepatocellular metabolism (Mattocks, 1968; Mattocks, 1972b; Lafranconi and Huxtable, 1984; Buhler et al, 1990; Pan et al, 1991). The toxicity of a large dose of unmetabolized MCT applied to cultured cells has been reported (Baybutt et al,

1994; Deyo et al, 1994; Sullman and Zuckerman, 1969). Toxicity resulting from the metabolism of MCT to one or more toxic intermediates by extrahepatic cells has also been suggested (Baybutt et al, 1994; DeLeve et al, 1996). Whether the cytotoxicity of large doses of MCT applied to such cells requires metabolism or occurs by other means has not been resolved (Mattocks, 1968; Armstrong and Zuckerman, 1970; Hilliker et al, 1983; Lafranconi and Huxtable, 1984; Lafranconi et al, 1985; Pan et al, 1991).

1. Pathways of MCT Bioconversion

Three major pathways responsible for the structural conversion of MCT and other PAs *in vivo* have been described: N-oxidation, hydrolysis and dehydrogenation (Mattocks, 1972b; Chesney and Allen, 1973b). Additional, less well characterized pathways which result in the conjugation of sulfur-containing amino acids or proteins to MCT or other MCT metabolites have also been described (White, 1976; Estep et al, 1990b; Huxtable et al, 1990; Monks et al, 1990; Pan et al, 1993; Yan and Huxtable, 1995b). All of the common pathways result in the production of nontoxic and readily excretable products except dehydrogenation, which produces reactive pyrrolic metabolites (McLean, 1970; Winter and Segall, 1989). An example of these common metabolic pathways with MCT is shown in Figure 2.

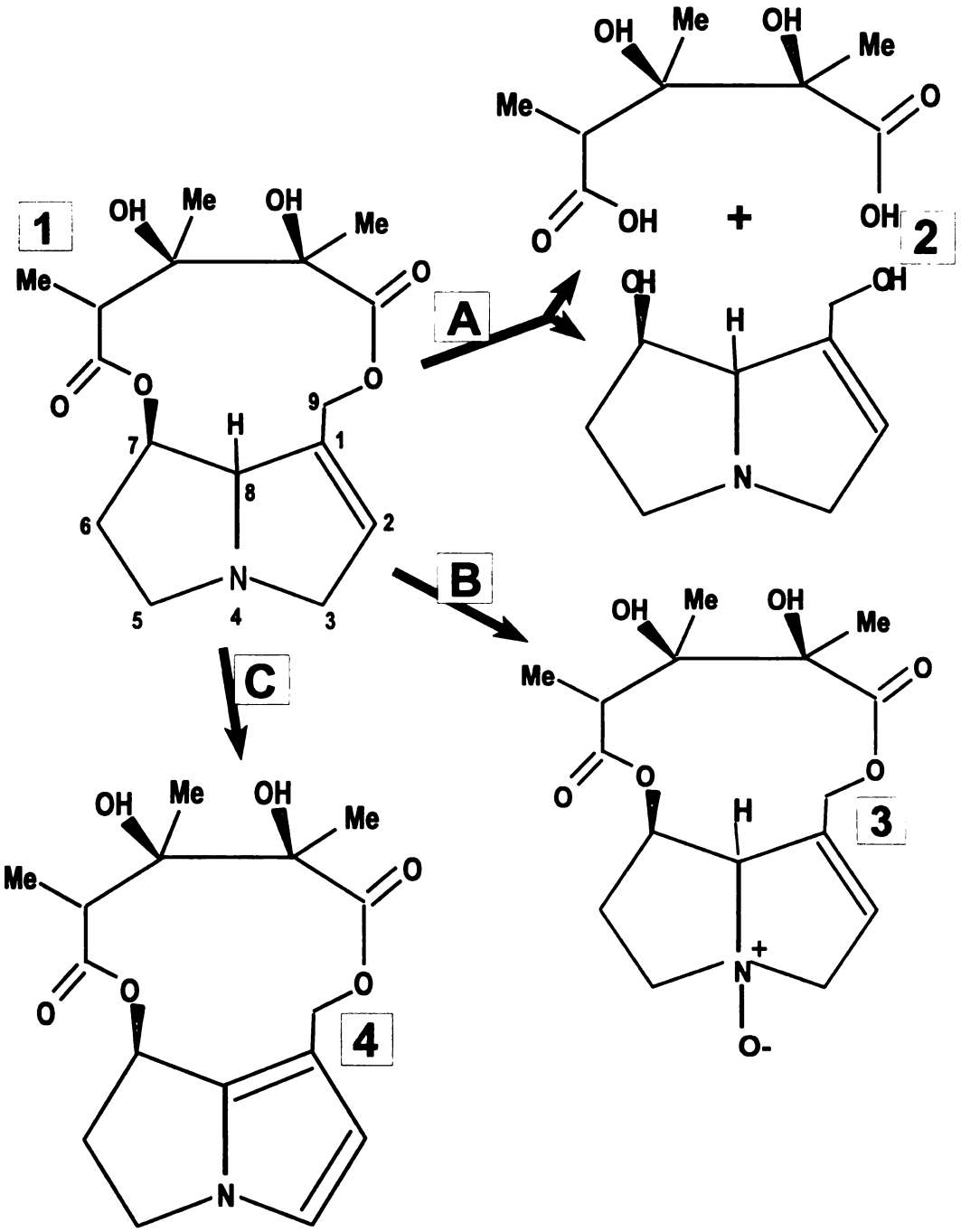

Figure 2. Metabolic products of monocrotaline.

Hydrolysis [A] and N-oxidation [B] of monocrotaline [1] result in the formation of nontoxic monocrotalic acid and retrorsine [2], and MCT N-oxide [3], respectively. Dehydrogenation [C] produces toxic monocrotaline pyrrole [4].

a. Nontoxic Metabolites of MCT

The formation of PA N-oxides is catalyzed by hepatic microsomal enzymes (Parkinson, 1995). N-oxides are highly water-soluble and readily excreted in the urine (Winter and Segall, 1989). They are considered nontoxic when administered by parenteral routes unless given in amounts equal to or greater than a dose of MCT which causes toxicity (Mattocks, 1971a; Culvenor et al, 1976). N-oxides added to microsomal preparations are generally not metabolized to reactive intermediates by P-450 enzymes (Mattocks and White, 1971; Mattocks, 1971b; Mattocks, 1972b). When given orally, however, N-oxides of some PAs can be reduced to their corresponding alkaloid base by the gastrointestinal flora, be absorbed and subsequently metabolized by hepatic microsomal enzymes to toxic pyrroles (Mattocks and White, 1971; Mattocks, 1972a).

The hydrolysis of MCT results in the formation of retronecine and monocrotalic acid [Figure 2]. Carboxylesterase enzymes in the liver are responsible for hydrolysis, and the products formed are rapidly excreted (Winter and Segall, 1989).

b. Pyrrolic Intermediates of MCT

Derivatives of esterified PAs responsible for toxicity are produced by the enzymic dehydrogenation of the necine nucleus, resulting in the formation of a pyrrole [see Figure 2] (Mattocks, 1968; Winter and Segall, 1989). This structural conversion causes a shift in molecular electrons, the loss of one or more ester groups from the PA molecule and the generation of positively-charged reactive sites (Mattocks, 1972b; Petry et al, 1984). Dehydrogenation occurs through the action of P-450 enzymes located in the microsomal fraction of hepatocytes (Williams et al, 1989; Glowaz et al, 1992; Parkinson, 1995). Two specific isoforms of P-450 responsible for the bioactivation of PAs in the male rat [UT-A and PCN-E] have been identified (Williams et al, 1989). The PCN-E form of P-450 appears more active in the formation of pyrrolic metabolites (Williams et al, 1989). In humans, P-450IIIA4 is both structurally and functionally similar to the PCN-E isoform found in the rat (Miranda et al, 1991).

Among the metabolites isolated from the medium of isolated livers perfused with MCT is monocrotaline pyrrole [MCTP or dehydromonocrotaline] (Yan and Huxtable, 1994). MCTP is highly reactive and responsible for most, if not all of the toxicity ascribed to MCT (Butler et al, 1970; Winter and Segall, 1989; Pan et al, 1993; Yan and Huxtable, 1994). MCTP and

pyrroles of other alkaloids readily bind to proteins (White, 1976; Robertson et al, 1977; Niwa et al, 1991) or DNA (Petry et al, 1984; Hincks et al, 1991). The cyclic diester structure of MCT contributes to the bifunctional alkylating ability of MCTP (Mattocks, 1968; Sullman and Zuckerman, 1969; White, 1976; Niwa et al, 1991).

Cysteinyl-, glutathione- and glutathionyl-pyrrole conjugates are also formed in the liver and found in the perfusate or bile of isolated liver preparations treated with MCT (Estep et al, 1990; Huxtable et al, 1990; Lamé et al, 1990). These conjugates have been proposed to stabilize reactive, pyrrolic intemediates sufficiently to allow transit from the liver to the lung or other tissues (White, 1976; Estep et al, 1990; Lamé et al, 1990; Pan et al, 1991; Estep et al, 1991). Such a mechanism could stabilize pyrroles which otherwise can rapidly polymerize and are inactivated in the aqueous environment of the plasma (Mattocks, 1969; Bruner et al, 1983; Mattocks and Jukes, 1990a).

In vivo, MCT metabolism and the tissue distribution of its intermediates is rapid (Mattocks, 1968; Lamé et al, 1995). A colorimetric assay [Ehrlich assay] which identifies the pyrrolic forms of PAs has been used to characterize the pharmacokinetic fate of MCT pyrrole in tissue and blood (Mattocks, 1968; Mattocks and White, 1970; Mattocks, 1986). "Metabolic" pyrroles produced by liver bioconversion are detected in the liver within 10 minutes of administration and have been identified in other tissues including the lungs, heart and kidneys within several hours (Mattocks, 1968; Mattocks and

White, 1970). "Metabolic" pyrroles persist in the liver and other tissues for up to 48 hours, while the parent alkaloid is often excreted completely within 24 hours (Mattocks, 1968). The rapid metabolism of MCT and tissue distribution of its intermediates has also been quantified by high performance liquid chromatography and gas chromatography/mass spectrophotometry (Monks et al, 1990; Lamé et al, 1990; Pan et al, 1993; Yan and Huxtable, 1994; Yan and Huxtable, 1995), and after the administration of radiolabeled MCT to rats (Estep et al, 1990a; Estep et al, 1991; Lamé et al, 1991).

c. Detoxification of MCTP

Prior to alkylation of cellular macromolecules, reactive pyrroles can be inactivated by hydrolysis and thiol-conjugation (Mattocks, 1986). MCTP is converted to dehydroretronecine and monocrotalic acid [Figure 2] by hydrolysis in basic or neutral aqueous solutions (Mattocks, 1969). Although dehydroretronecine is considerably less cytotoxic than dehydromonocrotaline (Mattocks, 1986), it can cause mitotic inhibition (Shumaker et al, 1976) and has been associated with the induction of neoplasia (Mattocks and Legg, 1980). The generation of monocrotalic acid is of little toxicologic consequence (Mattocks, 1969).

Cysteine or glutathione conjugation to pyrrolic intermediates results in the formation of polar molecules which are rapidly excreted (Pan et al, 1993; Yan and Huxtable, 1994; Yan and Huxtable, 1995a). Conjugates of MCTP comprise a sizable portion of the PA metabolites identified in bile, urine or plasma after MCT administration to rats (Yan and Huxtable, 1994). Although injury has been reported in the isolated, perfused lung after exposure to a conjugated pyrrole hydrolysis product (Huxtable et al, 1990), glutathione and cysteine pyrroles are nontoxic when administered *in vivo* (Pan et al, 1993). The enhancement of hepatic glutathione concentration through glutathione precursor supplementation reduces the proportion of reactive pyrroles in the liver, increases conjugated pyrroles in the bile and liver tissue after MCT (Yan and Huxtable, 1995b) and decreases the pneumotoxicity of MCT in rats (Yan and Huxtable, 1996).

2. Variability in the Metabolism of MCT

The sensitivity of different animals to the toxic effects of MCT and other PAs is influenced by the age, sex, and animal species. Many of these influences on sensitivity can be explained by differences in PA metabolism (Allen and Chesney, 1972; Chesney and Allen, 1973; Cheeke and Pierson-Goeger, 1983; Cheeke, 1989). Much of the variability is dictated by differences

in the type, amount and activity of enzymes necessary for PA metabolism (Cheeke and Pierson-Goeger, 1983; Kiyatake et al, 1992). Newborn rats lack sufficient P-450 monooxygenase activity to convert PAs to reactive metabolites; within 24 hours of birth the activity of PA-metabolizing P-450 enzymes increases as does the injury produced by MCT and other PAs (Mattocks and White, 1973). Male rats have more PA-metabolizing P-450 activity than do female rats, produce more pyrrolic metabolites of MCT and are more sensitive to the toxic effects of MCT (Ratnoff and Mirier, 1949; Kay et al, 1982; Williams et al, 1989). Chronic supplimentation of sex hormones can alter the gender differences in sensitivity to MCT and other PAs; female rats receiving testosterone or methylandosterone prior to MCT respond to MCT exposure in a manner similar to male rats (Goldenthal et al, 1964). Neutered males treated with estrogen prior to MCT survive longer after MCT exposure than intact males treated with MCT only (Goldenthal et al, 1964; Farhat et al, 1993).

Species-related variation in the sensitivity to PA-induced toxicity usually involves differences in the relative activity of opposing bioactivating and detoxification systems. This is evident in the comparison of the rat to the guinea pig (Chesney and Allen, 1973). The rat has functional pathways for the dehydrogenation and N-oxidation of PAs, the guinea pig has a predominance of detoxifying carboxylesterase enzymes but relatively little pyrrole-forming P-450 activity (Mattocks et al, 1986; Dueker et al, 1992a; Dueker

et al, 1992b). As such, the guinea pig is highly resistant to most PAs (Mattocks, 1972b; Cheeke, 1989); other resistant species may exhibit a similar disparity of metabolic pathways. These differences in metabolism-dictated sensitivity can be abolished by the direct administration of reactive pyrroles (Mattocks, 1972b; Chesney and Allen, 1973).

In addition to the normal constitutive activity of PA-converting pathways, the inducibility of each metabolic pathway can also dictate the response of different animal species to each PA (White and Mattocks, 1971; Williams et al, 1989; Mattocks et al, 1986). The degree of toxicity induced by pyrrolic metabolites can be altered by chemicals which up- or down-regulate the activity of PA bioconversion pathways (Allen et al, 1972; Chesney et al, 1974b; White and Mattocks, 1971; Mattocks et al, 1986). For example, the metabolism of PAs to pyrroles and ensuing toxicity can be enhanced by the induction of P-450 enzyme activity with phenobarbital (White et al, 1973; White et al, 1983). Likewise, the suppression of esterase activity, a detoxification pathway, can enhance the toxicity of a PA (Mattocks et al, 1986).

B. Pathophysiology of MCT *In Vivo*

The early 20th century marked the first association of PA exposure with toxicity in the United States (reviewed by Bull et al, 1968b). Horses in Iowa

and Nebraska developed a progressive wasting disease associated with ambulatory difficulty, coma and death. A *Crotalaria* sp. plant was abundant on farms in the region and suspected to be the cause of this condition. Several initial attempts to recreate the condition with experimental exposure to plant extracts met with failure, but *C. sagitallis* was ultimately determined to be the cause. Livestock with Winton disease, a clinical neurologic disorder were determined to have consumed hay contaminated with common ragwort, a weed which contains the alkaloid *Senecio jacobaea*. Hepatic cirrhosis was the primary lesion in affected horses and cattle seen at necropsy and hepatic dysfunction thought to be the cause of clinical signs involving the nervous system.

The involvement of specific organs in the expression of PA-associated toxicity is somewhat determined by the derivation of a particular PA. Unsaturated alkaloids extracted from *Senecio* and *Heliotropium* are almost exclusively hepatotoxic (Peterson et al, 1972), whereas those derived from *Crotalaria* sp. plants are hepatotoxic, but can induce significant pneumotoxicity (Harris et al, 1942; Barnes et al, 1964). The manifestations and severity of *C. spectabilis* or MCT intoxication are highly dependent on the cumulative dose of alkaloid administered (Jago, 1970; Huxtable et al, 1978; Shubat et al, 1989; Kim et al, 1993). The pattern of toxicity attributed to MCT is highly reproducible and not affected by the route of MCT administration (Schoental and Head, 1955).

1. MCT-induced Hepatotoxicity

Hepatotoxicity constitutes the most frequent presentation of PA intoxication in humans (Stuart and Bras, 1957; Kumana et al, 1985; Sperl et al, 1995) and several domestic animal species (Mendel et al, 1988; Odriozola et al, 1994). The liver participates in the pathogenesis of PA toxicity because of its role in the bioconversion of alkaloid to reactive and unstable intermediates (Mattocks, 1968; Mattocks, 1986).

a. Acute Hepatotoxicity

The clinical presentation of animals acutely intoxicated with MCT almost uniformly reflects the severity of liver injury. Affected animals are distressed, weak and dyspneic (Mendel et al, 1988; Odriozola et al, 1994). At necropsy, the liver is firm, congested and granular in appearance; hemorrhagic ascitic fluid may also be present (Mattocks, 1986). Hepatic parenchymal cell necrosis is the most notable histologic change in the liver, and the centrilobular and midzonal hepatocytes are the most severely affected (Bull and Dick, 1959; Jago, 1970). The hepatic sinusoids may be dilated with blood, some to an extent which obscures visualization of other parenchymal landmarks. These so-called "blood lagoons" have been proposed

as sites of hemorrhage secondary to massive sinusoidal endothelial cell damage (Barnes et al, 1964; Green and Christie, 1961). Endothelial cells lining the hepatic sinusoids, central veins and sublobular veins consistently exhibit a greater degree of damage than the adjacent hepatic parenchyma; the damaged endothelial cells are swollen and rupture acutely (Davidson, 1935). In animals which survive the acute toxic effect, endothelial cells enlarge and/or proliferate, while damaged hepatocytes may be replaced by connective tissue (Davidson, 1935; McLean, 1970). Primary injury to the microvasculature resulting in hemorrhage has also been identified in the heart and kidney after PA exposure (Rosenfeld and Beath, 1945). Injury to the vasculature or vaso-formative mesenchyme has been blamed for PA-induced malformations of the fetus in rats exposed during pregnancy (Green and Christie, 1961).

Acute PA exposure typically results in death in 1-4 days (Mattocks, 1986). In those animals which survive, clinical recovery may be followed by a prolonged course of decline, due to chronic effects of the alkaloid metabolites on hepatic cells.

Cellular metabolism is responsible for the regional pattern of injury in the liver after MCT (Mattocks, 1986). The midzonal and centrilobular portions of the liver lobule represent the areas of the liver in which hepatocytes contain the greatest relative concentration of P-450 enzymes responsible for pyrrole formation (Mattocks, 1986). Regional metabolism and

pyrrolic reactivity predisposes hepatocytes and other cells in the centrilobular and midzonal parts of the lobule to immediate alkylation, resulting in injury.

b. Chronic Hepatoxicity

MCT and similar PAs produce chronic changes in the liver after a cumulative, sublethal exposure (Schoental and Head, 1955; Allen et al, 1967; Peckham et al, 1974). Clinical signs include a progressive decline in body weight and appetite and the development of an unkempt appearance (Schoental and Head, 1955; Peckham et al, 1974). Abdominal distention is not uncommon in humans and some animal species, often representing the accumulation of extravascular fluid (Stuart and Bras, 1957). Other physical findings may include jaundice and peripheral edema. The time course leading clinical symptoms may be weeks to years (Stuart and Bras, 1957; Kumana et al, 1985).

The gross and histologic liver lesions represent stages of injury and repair, and the extent of each component varies with time after injury. Early after PA exposure, hepatocellular necrosis may be the dominant lesion, although to a lesser extent than that seen with acute toxicity (Rosenfeld and Beath, 1945). With time, the appearance of the liver reflects scarring or fibrosis; the liver lobes are shrunken, firm and granular to knobby

(Mattocks, 1986; Epstein et al, 1992). Histologically, the distortion of the lobular architecture is often extensive (Allen et al, 1967). Hepatic lobules and clusters of hepatocytes may be encompassed by dense, fibrous connective tissue which can extend from the portal region to the central vein (Shulman et al, 1987). The lumen of the central vein may be obliterated by the hyperplasia of cells presumed to be of endothelial origin, or substantially reduced in size by encroaching connective tissue in the perivascular adventitia (Stuart and Bras, 1957; McGee et al, 1976; Shulman et al, 1987). The latter alteration is the basis for hepatic venoocclusive disease [VOD] frequently reported in humans after the ingestion of "bush teas" brewed from *Crotalaria* sp. plants (Stuart and Bras, 1957; Huxtable, 1980).

Extraordinary cellular enlargement or megalocytosis is a consistent finding in animals with chronic liver disease due to intoxication by MCT (Allen et al, 1970b; Chesney and Allen, 1973a) or other PAs (Davidson, 1935; Bull and Dick, 1959; Jago, 1970). The histologic presence of megalocytosis is almost uniformly synonymous with PA poisoning. Megalocytic cells often have more and larger intracellular organelles, enlarged nuclei and large and/or multiple nucleoli (Afzelius and Schoental, 1967; Samuel and Jago, 1975; Mattocks and Legg, 1980). Megalocytosis associated with PA intoxication is thought to represent mitotic inhibition (Bull, 1955; Allen et al, 1970a; Mattocks and Legg, 1980; Cheeke, 1988). Cell loss is not a prerequisite for megalocytosis

to occur, but concurrent cell death exacerbates the extent of cell enlargement (Schoental and Magee, 1954). Interestingly, megalocytosis occurs more often in the periportal regions of the hepatic lobule, whereas hepatocellular necrosis affects the centrilobular hepatocytes (Schoental and Magee, 1957; Downing and Peterson, 1968; Rogers and Newberne, 1971).

2. Cardiopulmonary Toxicity after MCT

PA-induced lung injury is somewhat unique to the predominantly hepatotoxic alkaloids (Kay and Heath, 1966; Allen et al, 1967; Kay et al, 1967; Wagenvoort et al, 1974; Smith and Heath, 1978; Meyrick and Reid, 1979; Meyrick et al, 1980). In the rat, the *Crotalaria*-derived PAs MCT and fulvine cause acute hepatocellular necrosis and death only when administered at a high dose, but when given at a sublethal dose, are almost uniformly pneumotoxic, producing pulmonary hypertension with minimal hepatocellular injury (Lalich and Merkow, 1961; Allen and Carstens, 1970a; Kay et al, 1971; Huxtable et al, 1978). Unlike the rapid development of clinical signs and lesions seen with acute hepatotoxicity, the onset of pneumotoxicity is delayed several days after MCT administration (Kay et al, 1971; Meyrick and Reid, 1979). Biologically relavent metabolism of MCT does not appear to occur in the lungs

(Mattocks, 1968; Hilliker et al, 1983; Lafranconi and Huxtable, 1984; Lafranconi et al, 1985; Pan et al, 1991).

MCT-induced pneumotoxicity is characteristically chronic; a dose of MCT large enough to be acutely pneumotoxic would likely cause death from massive liver necrosis (Hilliker et al, 1982). Acute pulmonary toxicity can be produced by the intravenous administration of a large dose of chemically-synthesized MCTP directly upstream of the lung (Hurley and Jago, 1975; Bruner et al, 1983). Cardiopulmonary toxicity after MCT(P) administration to the rat has been studied as a model of several human pulmonary vascular diseases.

a. Clinical Effects/Necropsy Results

A cumulative MCT dose of 20-100mg/kg by any route causes predominantly lung injury in the rat (Kay and Heath, 1966; Meyrick and Reid, 1979; Sugita et al, 1983). Clinical indications of toxicity are nonspecific and initially recognized as reduced body weight gain, hypothermia and the development of an unkempt appearance (Hayashi and Lalich, 1967; Wagenvoort et al, 1974b; Meyrick and Reid, 1979). Within 3-4 weeks, rats exposed to MCT are lethargic and anorexic (Wagenvoort et al, 1974b). Physical signs consistent with pneumotoxicity may not be evident for 28-35 days and consist of dyspnea and cyanosis (Meyrick and Reid, 1979). Sporadic deaths occur over the first 21

days, but the rate of mortality increases dramatically in the late stages of this 4-6 week time course. Interestingly, the severity of clinical signs and the rate of mortality are reduced significantly by dietary restriction during the first 2-4 weeks after MCT administration (Hayashi et al, 1979).

MCT-induced pneumotoxicity occurs in a delayed and progressive manner (Roth et al, 1989). The reduction in body weight gain associated with anorexia is accompanied by loss of body fat and dehydration (Hayashi and Lalich, 1967). Gross lesions are usually confined to the thoracic cavity, but evidence of hepatic necrosis preceeding the development of pulmonary lesions has been reported in some rats treated with a pneumotoxic dose of MCT or fulvine (Kay et al, 1971; Barnes et al, 1964; Wagenvoort et al, 1974b). MCT-treated rats may have pleural effusion (Hayashi and Lalich, 1967) and occasionally have subcutaneous and peritoneal fluid accumulation (Allen and Carstens, 1970b). Lung lesions consist of patchy to generalized consolidation with hemorrhage and are present 2-3 weeks after MCT (Hayashi and Lalich, 1967). Enlargement of the heart, suggested by rounding of the cardiac shape, becomes evident by 4 weeks after MCT (Allen and Carstens, 1970b).

b. Pulmonary Pathophysiology

During the 4-5 week time course of events which follow the administration of MCT to rats, sequential changes occur in the pulmonary vasculature, parenchyma and heart (Allen and Carstens, 1970; Meyrick et al, 1980). Although these changes occur as a continuum, they can be catagorized into three components (Kay and Heath, 1967; Meyrick and Reid, 1979). *Early events* [injury to the endothelium and associated vascular leak] occur within the first 7-10 days after MCT. The second group of changes can be described as *delayed events* which comprise the vascular remodeling and the apparent repair response to injury, and occur within 2-3 weeks of MCT. *Late events* represent the hemodynamic and cardiophysiological response to lung vascular injury and repair and may take up to 6 weeks to become evident. Although the reported times of initiation and duration of MCT-associated events vary, the order in which changes occur is consistent and predictable.

1. Early Events

Metabolic pyrroles of MCT which escape the liver parenchyma gain access to the systemic circulation and encounter the lung as the first downstream microvascular bed. The pulmonary vascular

endothelium is the primary target of blood-borne MCTP (Allen and Carstens, 1970; Butler, 1970; Meyrick et al, 1980; Wilson et al, 1992). Affected pulmonary vascular endothelial cells (ECs) exhibit vesiculation, pallor, swelling and a reduction of microfilaments within the first 4-96 hours of MCT administration (Valdivia et al, 1967b; Miller et al, 1978; Rosenberg and Rabinovitch, 1988). ECs death and loss is limited in distribution and confined to individual or small groups of cells; overt necrosis and sloughing of ECs does not occur (Valdivia et al, 1967a; Miller et al, 1978; Rosenberg and Rabinovitch, 1988; Wilson et al, 1989; Wilson and Segall, 1990).

Injury to pulmonary vascular endothelial cells is reflected not only as a change in cell morphology, but also by the disruption of normal cellular functions. Serotonin (5-hydroxytryptamine or 5-HT) is a vasoactive agent present in platelets and mast cells and is actively removed from the blood by pulmonary endothelium (Gillis, 1973). Serotonin uptake by the lung vasculature is markedly decreased within the first 7 days after MCT (Huxtable et al, 1978; Hilliker et al, 1983; Hayashi et al, 1984; Molteni et al, 1986), a measurement that has been used as a marker of endothelial cell injury.

Concurrent with endothelial cell injury induced by MCT is the development of pulmonary vascular leak (Valdivia et al, 1967b; Allen and Carstens, 1970b; Meyrick et al, 1980; Molteni et al, 1984). Pulmonary vascular leak after MCT is caused by an increase in pulmonary microvascular

permeability (Kido et al, 1981; Molteni et al, 1984). The pulmonary arterial pressure is not involved in the initiation of vascular leak and remains normal until vascular structural remodeling is well established [14-21 days] (Kay et al, 1967; Meyrick et al, 1980). Evidence of vascular leak has been reported as early as 2 hours in a canine pulmonary hypertension model (Miller et al, 1978) but more typically occurs 2-3 days after MCT administration to the rat (Kido et al, 1981; Sugita et al, 1983). Vascular leak after MCT is progressive (Valdivia et al, 1967b; Sugita et al, 1983) and ultimately results in distention of the perivascular space, dilation of lymphatic channels within the perivascular adventitia (Plestina and Stoner, 1972) and pulmonary edema (Valdivia et al, 1967b).

Other changes which occur in the first 10 days after MCT administration include a decrease in the number of circulating platelets and platelet sequestration in the lung (Hilliker et al, 1982), pulmonary vascular thrombosis (Allen and Carsten, 1970b; Chesney and Allen, 1973a; Lalich et al, 1977; Hayashi et al, 1984) and pulmonary inflammation (Valdivia et al, 1967b; Hayashi et al, 1984; Wilson et al, 1989). The reduction in the number of circulating platelets after MCT corresponds to the accumulation of platelet and fibrin thrombi in the lung (Valdivia et al, 1967b; Kay et al, 1971; Hayashi et al, 1984). In addition, messenger RNAs for several components of the basement membrane produced by endothelial cells are increased by 4 days and elevated for up to 14 days after MCT administration (Lipke et al, 1993).

Mononuclear cells and mast cells accumulate in the perivascular adventitia of pulmonary vessels after the administration of MCT to rats (Valdivia et al, 1967b; Wilson et al, 1989). Mononuclear cells may act as purveyors of cytokines involved in lung injury and vascular leak. For example, the activity of interleukin-1 is elevated in lungs affected by MCT (Gillispie et al, 1988; Gillispie et al, 1989a). Mast cells have also been identified in increased numbers in the perivascular adventitia (Kay et al, 1967; Wagenvoort et al, 1974b) and, although hypothesized to be contributors of vasoactive mediators which could induce vasoconstriction, have not been shown to be involved causally in MCT-induced pneumotoxicity or vascular remodeling (Valdivia et al, 1967a; Kay et al, 1969).

2. Delayed Events

On the heels of pulmonary endothelial cell injury and vascular leak are a series of structural changes in the pulmonary arterial microvasculature which constitute vascular remodeling (Hislop and Reid, 1974). Endothelial cell swelling immediately after MCT administration contributes to a reduction of the pulmonary microvascular surface area (Meyrick and Reid, 1979). Pulmonary vascular compliance is decreased and arterial resistance increased in conjunction with an increase in the arterial medial

thickness and muscularization of precapillary arteries (Meyrick and Reid, 1979). An increase in pulmonary arterial pressure, first significant at 14-21 days after MCT, closely follows the increase in arterial medial thickness and reduction in vascular compliance (Kay and Heath, 1966; Wagenvoort et al, 1974b; Arcot et al, 1993).

Thickening of the medial layer of pulmonary arteries after MCT comprises an increase in smooth muscle cell mass and the production of collagen (Wagenvoort et al, 1974b; Meyrick et al, 1980; Ghodsi and Will, 1981). The enlargement of smooth muscle cells [hypertrophy] or smooth muscle cell proliferation [hyperplasia] may contribute to the increase in medial cell mass (Owens, 1989). Vascular smooth muscle cells (VSMCs) revert from contractile cells to a synthetic phenotypic capable of cell division (Thyberg et al, 1983), presumedly in response to a mitogenic stimulus after MCT (Wagenvoort et al, 1974a; Chesney and Allen, 1973a). Rats fed *C. spectabilis* seeds have an increase in radiolabeled thymidine incorporation in pulmonary VSMCs, a process consistent with increased DNA synthesis and presumed to lead to an increase in artery medial mass through cell proliferation (Meyrick and Reid, 1982). In addition to an increase in muscle cell mass after MCT, arterial wall cells contribute acellular components the medial layer of pulmonary arteries through the production of collagen (Kameji et al, 1980).

Muscularization of nonmuscular arteries is thought to represent the migration of smooth muscle cells from adjacent muscular arteries or the differentiation of smooth muscle cell precursors present in the subintimal layer of precapillary vessels (Meyrick and Reid, 1979; Meyrick et al, 1980; Rosenberg and Rabinovitch, 1988). Factors generated by cellular injury or the increase in vascular premeability could induce either change (Bobik and Campbell, 1993); abnormal muscularization decreases the cross-sectional area of the smallest pulmonary arteries resulting in increased vascular resistance (Meyrick et al, 1980).

Additional changes in the lung within 2 weeks of MCT administration include neutrophilic arteritis, perivascular neutrophil accumulation (Kay et al, 1971; Molteni et al, 1984) and hyaline thrombi in the alveolar capillaries (Hayashi et al, 1984). Megalocytosis of type II pneumocytes and interstitial cells, and to a lesser extent, endothelial cells and VSMCs is evident (Merkow and Kleinerman, 1966; Valdivia et al, 1967a; Chesney and Allen 1973a; Wilson and Segall, 1990); enlarged type II pneumocytes have more prominent synthetic organelles and VSMCs contain fewer contractile elements (Wagenvoort et al, 1974a).

3. Late Events

The increase in pulmonary arterial pressure which follows vascular medial thickening and muscularization of small precapillary arteries has been reported as early as 8 days (Ghodsi and Will, 1981), or as long as 6 weeks (Kay et al, 1969; Meyrick et al, 1980; Lipke et al, 1993) after MCT, but more typically becomes evident after 3 weeks (Kido et al, 1981; Huxtable et al, 1978; Arcot et al, 1993). The most striking gross physical change that occurs during this interval is the increase in right ventricular weight, corresponding to an increase in the right ventricular muscle mass (Kay et al, 1971; Meyrick and Reid, 1979). The right heart weight changes in response to the progressively increasing pulmonary arterial pressure which accompanies vascular remodeling (Huxtable et al, 1978; Gillespie et al, 1985b; Wilson et al, 1989). Impaired gas exchange and decreased lung compliance and capacity (Gillespie et al, 1985b), as well as increased pulmonary vascular resistance (Meyrick et al, 1980) also characterize this stage.

Late stage vascular inflammation accompanies crenation of the arterial elastic laminae and vascular necrosis (Merkow and Kleinerman, 1966; Kay and Heath, 1966; Wagenvoort et al, 1974a). Persistant arterial contracture has been proposed as a cause of the vascular necrosis (Merkow and Kleinerman, 1966; Smith and Heath, 1978). Pulmonary vascular

thrombosis has been reported but with lower frequency than earlier after MCT administration (Allen and Carstens, 1970b; Lalich et al, 1977; Meyrick et al, 1980). MCT-induced perivascular edema persists (Hayashi and Lalich, 1967), and megalocytosis of epithelial and intersititial cells is more evident in a greater number of cells (Kay et al, 1969). In addition, alveolar septal or perivascular fibrosis (Lalich et al, 1977; Wilson et al, 1989), fragmentation of the elastic laminae of pulmonary arteries (Allen and Carstens, 1970b; Todorovich-Hunter et al, 1992; Zhu et al, 1994) and pleural surface neovascularization (Schraufnagel, 1990) have been described.

C. MCTP-induced Pneumotoxicity

Chemically synthesized MCTP causes liver and/or lung injury similar to that attributed to MCT (Butler et al, 1970). Compared to MCT, the timecourse over which MCTP-induced injury develops is reduced, perhaps because further metabolism of pyrrole is not required for toxicity (Mattocks, 1970; Bruner et al, 1986). The instability of MCTP requires that it be given by an intravascular route immediately upstream of the target organ [ie, lung] to maximize its delivery and to minimize inactivation in blood (Mattocks, 1968; Butler et al, 1970; Hooson and Grasso, 1976; Mattocks 1986).

1. Low Dose MCTP

MCTP administered at a dose of 3-5mg/kg via the tail vein of the rat causes lung injury leading to pulmonary hypertension, a process which requires approximately 2 weeks for full expression (Butler, 1970; Bruner et al, 1983; Reindel et al, 1990). Within 2-4 hours of the administration of MCTP, there is a transient increase in lung weight followed by a slow, but steady rise in bronchoalveolar fluid protein and inflammatory cells over 3-4 days (Plestina and Stoner, 1972; Kido et al, 1981; Schultze et al, 1991b). Similar to MCT, the first measurable change in lung structure is endothelial cell swelling and blebbing of the cell membrane, noted 2-3 days after MCTP exposure (Kido et al, 1981; Reindel et al, 1990). Endothelial cell injury is minimal but may be reflected in the release of an endothelial isoform of lactate dehydrogenase (Schultze et al, 1994), which accumulates in bronchoalveolar fluid within 2-4 days of MCTP administration (Roth, 1981; Bruner et al, 1983). A progressive increase in lung weight reflects the increase in pulmonary vascular permeability and the accumulation of extravascular water (Bruner et al, 1983; Reindel et al, 1990).

Pulmonary arterial remodeling is first evident by 5-7 days after MCTP and consists of muscularization of normally nonmuscular, precapillary arteries and medial thickening of larger, muscular arteries (Reindel et al, 1990). At that time, the increase in pulmonary vascular permeabilty is

evident histologically as widening of the perivascular space and dilation of adventitial lymphatic channels. Ultrastructurally, there is mild hypertrophy of endothelial cells of both small pulmonary arteries and lymphatic vessels (Reindel et al, 1990). By day 7, the pulmonary arterial pressure is elevated (Bruner et al, 1983) and by day 8-10, there is patchy alveolar edema (Reindel et al, 1990). The right ventricular weight increases by day 10-12 in response to the persistant increase in pulmonary arterial pressure (Chesney et al, 1974a; Reindel et al, 1990). Pulmonary vascular leak, increased pulmonary arterial pressure, vascular remodeling and right ventricular mass continue to increase through days 14-21. Terminally, the increase in pulmonary vascular permeability may be manifest as pleural, pericardial or peritoneal effusion (Butler et al, 1970). Enlargement of endothelial, interstitial and type II epithelial cell profiles, first evident by 5-7 days after MCTP, becomes more prominent by day 14 and beyond (Reindel et al, 1990).

Several changes ascribed to MCT-induced pneumotoxicity do not occur with regularity following MCTP. Vasculitis, perivasculitis and vascular necrosis, a presumed response to acute vascular injury, are rare with MCTP-induced pneumotoxicity suggesting that overt damage to the subintimal layer of pulmonary arteries is not necessary for vascular remodeling. Both MCTP and MCT cause platelet sequestration in the lung (White and Roth, 1988); unlike MCT, however, there is no concurrent reduction in the number of

circulating platelets with MCTP, a change which may reflect more severe pulmonary vascular injury after MCT (Bruner et al, 1983; White and Roth, 1988). MCTP-associated pulmonary vascular thrombosis, associated with decreased blood and lung fibrinolytic activity (Schultze and Roth, 1993), occurs less often than with MCT (Chesney et al, 1974; Lalich et al, 1977). In addition, the synthesis and deposition of extracellular matrix components in the vascular media and adventitia, a component of arterial wall remodeling after MCT, is not reported with MCTP-induced pulmonary vascular remodeling. An increase in cellular fibronectin has been identified in the plasma of MCTP-treated rats (Schultze et al, 1996); the role of cFN in vascular remodeling, however, is unclear.

2. High Dose MCTP

When administered to rats at a dose of 15-30mg/kg, MCTP causes more acute and severe pulmonary vascular leak which often culminates in death within 24-48 hours (Butler et al, 1970; Plestina and Stoner, 1972; Hurley and Jago, 1975). MCTP at this dose causes extensive interstitial and alveolar edema and pleural effusion within 24 hours (Hurley and Jago, 1975). Although pulmonary vascular permeability is increased at this elevated MCTP dose, the degree of overt endothelial injury may not be different from that reported after

MCTP at a lower dose (Hurley and Jago, 1975). Pulmonary hypertension and right ventricular hypertrophy do not develop over this short time course.

D. Factors Contributing to PH after MCT/MCTP

An increase in vascular pressure can occur either by changes in vascular tone or by structural alteration of vessels. Generally speaking, an increase in the sensitivity of arteries to contractile stimuli or the attenuation of the pathways which cause vasodilation can result in vascular hypertension (Rubin et al, 1996). Altered vasoreactivity leading to hypertension may also be manifest as a response to the increased release or decreased degradation of endogenous contractile mediators (Vita et al, 1996). Structurally, an increase in vascular medial thickness due to smooth muscle cell growth and/or proliferation can contribute to the elevation of arterial pressure and vascular resistance. Smooth muscle cell growth and proliferation initiated by vascular injury can be accentuated by mitogenic proteins (Bobik and Campbell, 1993). Alterations in vasoreactivity and/or the expression of vasoactive agents, and upregulation of cell growth or proliferation, perhaps via the release of mitogenic growth factors have been hypothesized to be involved in the development of pulmonary hypertension in rats after MCT or MCTP administration. Each of these

possibilities is discussed in the following sections. Where similar results are described for MCT and MCTP, the acronym MCT[P] is used.

1. Vasoreactivity after MCT/MCTP

The increase in pulmonary arterial pressure after the administration of MCT[P] to rats follows changes in the vascular medial layer leading to decreased compliance and increased resistance (Gillespie et al, 1985b; Meyrick et al, 1980). Structural remodeling has been proposed to follow the persistent increase in vascular tone due to altered vasoreactivity (Gillespie et al, 1985b; Rosenberg and Rabinovitch, 1988; Huxtable, 1990). The role of vasoreactivity in MCT[P]-induced pulmonary hypertension, however, is unclear and reports describing the response of vessels to MCT[P] are contradictory.

An early and transient increase [within 4-7 days] in the response of arteries from MCT-treated rats to vasoconstrictors such as angiotensin II and hypoxia has been reported (Gillespie et al, 1986; Shubat et al, 1987). That transient change is followed by inconsistent responses in pulmonary arteries or perfused lungs from MCT-treated rats to a number of exogenously applied mediators including angiotensin I, isoproterenol, hypoxia and potassium chloride (Altiere et al, 1986; Gillespie et al, 1986; Rosenberg and Rabinovitch, 1988). The cumulative results weigh more heavily in favor of increased vascular

responsiveness after MCT, but only after arterial medial thickening and increased arterial pressure have been established (Rosenberg and Rabinovich, 1988; Huxtable, 1990). Alterations in the vasoreactivity after MCTP have been less thoroughly examined, but also suggest that pulmonary arterial responsiveness is increased after vascular remodeling has been established (Hilliker and Roth, 1985a; Shubat et al, 1987; Langleben et al, 1988; Madden et al, 1994).

2. Vasoactive Agents and MCT[P]

a. EC-associated Mediators

Pulmonary vascular endothelial cell injury after MCT[P] is characterized by changes in cell morphology and the reduction in serotonin uptake by the lungs (Huxtable et al, 1978; Gillis et al, 1978; Lafranconi and Huxtable, 1984; Hilliker and Roth, 1985). A decrease in the uptake or metabolism or an increase in the synthesis and release of a number of endogenous vasoactive agents may induce critical functional disturbances in endothelial cells exposed to MCT[P]. The persistance of vasoactive agents in the blood might contribute to vascular remodeling and pulmonary hypertension after MCT[P].

Serotonin [5-hydroxytryptamine] is released from activated platelets, causes pulmonary vasoconstriction and is taken up and metabolized by the endothelial cells of the liver and lung (Gillis, 1973; Ryan, 1990). In rats exposed to MCT[P] and in perfused lungs isolated from MCT[P]-treated rats, serotonin uptake is decreased (Gillis et al, 1978; Hilliker et al, 1984). The administration of serotonin to blood-perfused lungs from MCTP-treated rats causes an increase in perfusion pressure (Hilliker and Roth, 1985a). The inhibition of serotonin synthesis reduces the severity of pulmonary hypertension induced by MCT (Kay et al, 1985). However, the concurrent use of serotonin receptor antagonists provides only partial protection (Kanai et al, 1993) or fails to protect (Ganey et al, 1986) against the development of pulmonary hypertension.

The endothelium also produces angiotensin converting enzyme (ACE) responsible for the conversion of angiotensin I to the vasoconstrictor angiotensin II (Ryan, 1990). ACE activity in lung tissue is either increased (Molteni et al, 1984), decreased (Hayashi et al, 1984) or unaffected (Huxtable et al, 1978; Lafranconi and Huxtable, 1983) by MCT and decreased in cultured endothelial cell exposed to MCTP (Hoorn and Roth, 1993). The discrepancies reported have been attributed to differences in the amount of reactive metabolite, degree of endothelial cell injury and the lack of endothelial cell metabolism of MCT by isolated lung preparations or cultured cells (Huxtable et al, 1978). The activity of ACE in the plasma (Hayashi et al, 1984) or perfusate

from the isolated lung (Lafranconi and Huxtable, 1984) from MCT-treated rats is not altered by this toxicant. Inhibitors of ACE synthesis provide partial protection against MCT-induced pulmonary hypertension and right ventricular hypertrophy (Molteni et al, 1986). The protective effect of ACE inhibitors, however, may be due to interference with collagen synthesis and prevention of perivascular fibrosis (Molteni et al, 1985).

The role of other endothelium-associated vasoactive agents or their enzymatic activators has been examined. The vasodilator prostaglandin I_2 [PGI_2] is synthesized by endothelial cells (Ryan, 1990). Inconsistent patterns of release of PGI_2 after MCT[P] exposure are reported (Stenmark et al, 1985; Ganey and Roth, 1988a; Ganey and Roth, 1988b). Inhibition of prostaglandin synthesis either protects (Kato et al, 1989) or does not affect the severity of pulmonary hypertension after MCT (Stenmark et al, 1985; Ganey and Roth, 1987). The infusion of a stable PGI_2 analog protects against MCT-induced pulmonary hypertension (Miyata er al, 1996).

Additional mediators with vasoconstrictive or vasorelaxant properties may contribute to MCT-induced vascular remodeling. The endothelium-derived vasoactive mediator, platelet activating factor [PAF], is increased in the blood 1-3 weeks after MCT; PAF receptor antagonists reduce the severity of vascular leak and pulmonary hypertension associated with PAF (Ono and Voelkel, 1991; Ono and Voelkel, 1992). Endothelium-derived relaxing

factor [EDRF] is decreased (Ito et al, 1988) and endothelin-1 [ET-1], a potent vasoconstrictor released from endothelial cells, is increased (Miyauchi et al, 1993; Okada et al, 1995b; Mathew et al, 1995) after MCT[P] exposure. Although specific modulators of EDRF or ET-1 activity have not been tested, the continuous inhalation of nitric oxide, intended to induce vasodilation after toxicant exposure, does not alter the course of pulmonary hypertension (Katayama et al, 1994; Maruyama et al, 1997).

b. Platelet-derived Mediators

Platelets become sequestered in the lungs in association with MCT[P], and thrombi composed of platelets have been identified in injured pulmonary microvessels (Chesney and Allen, 1973a; Hilliker et al, 1982). Platelets contain a number of vasoactive and mitogenic factors (Bobik and Campbell, 1993). Platelet depletion during the genesis of pulmonary hypertension provides protection against increased pulmonary arterial pressure after the administration of MCTP (White et al, 1989). The protective effect requires moderate platelet depletion [10-20% of normal] (Ganey et al, 1988) and occurs only when depletion is targeted to 3-5 or 6-8 days after MCTP administration (Hilliker et al, 1984). Interestingly, platelet depletion does not

interfere with lung injury after MCTP [characterized by lung vascular leak] (Hilliker et al, 1984).

Although the depletion of platelets results in protection against pulmonary hypertension and right ventricular hypertrophy after MCTP, the specific role of vasoactive mediators produced or released by activated platelets is unclear. Thromboxane A_2, a platelet-derived vasoconstrictor, is increased in the perfusate of lungs isolated from MCTP-treated rats (Ganey and Roth, 1988b). Antagonism of thromboxane activity, synthesis or receptor binding, however, does not interfere with the development of pulmonary hypertension after MCT[P] (Langleben et al, 1986; Ganey and Roth, 1987).

3. Pathways of Cell Growth/Metabolism

The upregulation of pathways involved in cell growth and/or proliferation contribute to an increase in the thickness of the media of pulmonary arteries after MCT[P]. Polyamines are important in cell proliferation and differentiation (Heby, 1981); an increase in the synthesis of polyamines may play a role in abnormal cell growth/proliferation or repair of injury (Orlinska et al, 1988; Olson et al, 1989). The polyamine content of the lungs and the activity of enzymes responsible for the synthesis of polyamines increase after MCT but

prior to the development of pulmonary hypertension (Olson et al, 1984a). A polyamine synthesis inhibitor, α-difluoromethylornithine [DFMO], reduces the degree of vascular remodeling and pulmonary hypertension after MCT (Olson et al, 1984), even when administered as late as 10 days after MCT (Olson et al, 1989b). Pulmonary vascular leak after MCT is also prevented by the administration of DFMO (Olson et al, 1985). MCT-associated polyamine synthesis has been linked with early airway bronchoconstriction (Zhou and Lai, 1992), the increase in vascular responsiveness to a contractile stimulus (Gillespie et al, 1985a) and the upregulation of DNA synthesis in lungs from MCT-treated rats (Hacker, 1992). All of these effects can be reduced or abolished by the administration of DMFO prior to or near the time of MCT exposure.

Other pathways involved in the regulation of cell growth may contribute to MCT[P]-induced vascular remodeling. The inhibition of farnesyltransferase activity, responsible for the synthesis of cholesterol precursors, protects against MCT-induced pulmonary hypertension (Touvay et al, 1995). General dietary restriction sufficient to inhibit weight gain [growth] delays the onset of pulmonary arterial hypertension and right ventricular hypertrophy in young rats subsequently treated with MCT[P] (Hayashi et al, 1979; Ganey et al, 1985). Dietary restriction sufficient to inhibit MCT-induced pulmonary hypertension also suppresses DNA and polyamine synthesis (Hacker,

1993). These results suggest that one or more growth stimuli may be required for the expression of MCT[P] pneumotoxicity and that polyamines may be one such stimulus.

4. Mitogenic Growth Factors

Smooth muscle cell mitogens are present in the blood and in cells and acellular components of the vascular wall (Bobik and Campbell, 1993). VSMC growth/proliferation may be influenced by factors released from activated or injured cells (Grotendorst et al, 1982; Reidy, 1992) or from storage sites in the extracellular matrix of vessels (Molteni et al, 1989; Bobik and Campbell, 1993; Zhu et al, 1994). Growth factors have been proposed to participate in the structural remodeling in pulmonary arteries seen after MCT[P] exposure of rats (Gillespie et al, 1989b; Arcot et al, 1993).

Platelets contain smooth muscle cell mitogens (Bobik and Campbell, 1993). The depletion of platelets from 3-5 or 6-8 days after MCTP administration results in a significant reduction in pulmonary hypertension and right ventricular hypertrophy (Hilliker et al, 1984; Ganey et al, 1988; White et al, 1989). Platelets and other cells of the blood and vascular wall contain and/or synthesize and release growth factors [eg. platelet-derived growth factor or PDGF] which can induce smooth muscle cell migration (Grotendorst et al, 1992; Jawien et al, 1992), a process which may be involved in vascular remodeling

after MCT[P] (Meyrick and Reid, 1979a). Epidermal growth factor [EGF] is released from activated platelets and other cells is present in blood plasma (Bagby et al, 1992; Bobik and Campbell, 1993) and accumulates in the lungs after the administration of MCT (Gillespie et al, 1989b). Rats infused with human recombinant EGF develop pulmonary arterial medial thickening and increased pulmonary arterial pressure, an increase in lung polyamine content as well as an increase in the activity of a polyamine synthesis-associated enzyme, ornithine decarboxylase [ODC] (Gillespie et al, 1989b). The expression of the gene for transforming growth factor-β [TGF- β] is increased after MCT (Arcot et al, 1993); TGF- β synthesis and release has been associated with collagen synthesis and deposition in pulmonary hypertension (Botney et al, 1994).

The activity of elastase produced by cells of the pulmonary arterial wall increases after MCT administration (Todorovich-Hunter et al, 1992), an action which may contribute to the release of matrix bound smooth muscle cell mitogens (Molteni et al, 1989; Zhu et al, 1994). The inhibition of elastase activity reduces MCT-induced right ventricular hypertrophy and vascular remodeling (Ilkiw et al, 1989; Ye and Rabinovitch, 1991).

5. Pharmacological Intervention Studies: Interpretation

As is evident in the section above, inconsistencies are widespread in the response of vessels and/or cells to agents intended to modulate the hypertensive effect of MCT[P]. As such, solid conclusions as to the mechanism of MCT[P]-induced pulmonary vascular injury leading to pulmonary hypertension have not been described, and the credibility of this model as representative of human pulmonary hypertension has been questioned (Heath, 1992).

Bioactivation is required for toxicity and, as previously described, compounds which reduce the activity of enzymes responsible for dehydrogenation [ie, pyrrole production] or increase the level of N-oxidation reduce the toxicity of MCT and other PAs [see section II.A.2]. Modulators used to affect MCT-induced toxicity may alter these enzymes; reports cited above typically lack any characterization of ancillary effects of these modulators on hepatic enzymes. Similarly, pathways of detoxification may be influenced by these pharmacologic agents. In addition, the reduction of body weight gain through dietary restriction provides a protective effect against MCT[P]-induced pulmonary vascular injury and hypertension (Hayashi et al, 1979; Ganey et al, 1985). The effect of various pharmaceuticals on body weight and the indirect contribution of reduced body weight gain to any protective effect needs to be

identified. Additional work will be necessary to determine the involvement of these nonspecific influences for each modulator of MCT[P]-induced vascular toxicity.

E. Effects of MCTP on Cells *In Vitro*

A large number of complex and interrelated events connect the administration of MCT[P] to the development of pulmonary hypertension. Early cellular structural and functional alterations identified after MCT[P] is administered *in vivo* occur in the pulmonary microvascular endothelial cell treated with MCTP (Hoorn and Roth, 1993; Hoorn et al, 1993; Thomas et al, 1996). As such, cultured endothelial cells exposed to MCTP have been used to characterize some of the early events as they relate to vascular injury and the response to injury. Other types of vascular and nonvascular cells have been exposed to MCTP to determine the direct cellular effects of this toxicant.

1. Cell Viability and Morphology

In vivo, MCTP causes limited, yet progressive pulmonary vascular endothelial cell injury manifest as cell swelling and membrane blebbing and the leakage of the cytosolic enzyme, lactate dehydrogenase [LDH] [see

II.C.1. above]. *In vitro*, endothelial cells derived from the rat pulmonary microvasculature exhibit a similar change upon exposure to MCTP (Hoorn et al, 1993). Cultured bovine pulmonary artery endothelial cells [BECs] respond to MCTP in a manner similar to rat vascular endothelial cells *in vitro* and have been used for much of the characterization of cell injury and alterations in structure (Reindel and Roth, 1991; Hoorn et al, 1993). Porcine pulmonary artery endothelial cells [PECs] are less sensitive to the cytotoxic effect of MCTP, but have provided evidence of the ability of MCTP to alter cell function without causing overt cell injury (Reindel et al, 1991).

A limited evaluation of the direct effects of MCT[P] on the viability and morphology of other cell types has also been done. Bovine vascular smooth muscle cells from the pulmonary artery respond to MCTP in a manner similar to that of PECs (Reindel and Roth, 1991). Murine hepatic sinusoidal endothelial cells are more sensitive to MCT-induced toxicity than hepatocytes, a process which may reflect the inability to sinusoidal endothelial cells to generate cytoprotective thiols [ie, glutathione] in response to pyrrole exposure (Deleve et al, 1996).

In vitro, the response of endothelial cells to MCTP-induced injury is dose-dependent and varies with cells derived from different animal species (Reindel et al, 1991). In BECs and rat ECs [RECs], LDH release after MCTP is significantly increased by 48 hours and remains elevated for 7-14 days

(Reindel et al, 1991; Hoorn et al, 1993). Overt cell loss from the monolayer is limited in scope but persistent after MCTP exposure. Injured cells become swollen, develop irregular membrane protrusions and may detach from the monolayer. Cells which remain attached extend pseudopodia into gaps left by cell loss (Reindel and Roth, 1991). With time and continued cell loss, RECs and BECs exposed to MCTP enlarge but show no indication of proliferation in response to cell injury (Reindel et al, 1991; Hoorn et al, 1993). Despite the massive enlargement of some surviving endothelial cells, gaps may remain in the monolayer. By contrast, PECs which are resistant to the cytotoxic effect of MCTP [minimal LDH release even after exposure to a large concentration of MCTP] suffer minimal cell loss and show no overt megalocytosis unless exposed to MCTP while growing at a subconfluent density (Hoorn and Roth, 1992).

2. Cell Enlargement and Proliferation

In addition to the structural and functional effects of MCTP on cultured endothelial cells, the ability of cells to undergo clonal expansion is also impacted by this toxicant. Whereas injury after MCTP is dependent on the toxicant dose, the cell type exposed and animal origin of specific cells used for exposure, the effect of this toxicant on cell proliferation is uniform across cell types tested and apparent at a low concentration of MCTP (Reindel and Roth,

1991). MCTP causes a significant reduction in the colony forming efficiency of BECs. This inhibition of cell proliferation occurs at one-tenth the dose required to produce minimal cytotoxicity in these cells. At the same range of concentration, the inhibition of proliferation by MCTP occurs in PECs, bovine arterial smooth muscle cells, Madin-Darby canine kidney cells and undifferentiated human keratinocytes (Reindel et al, 1988; Reindel et al, 1991). MCTP causes the suppression of blastogenesis in splenic lymphocytes isolated from mice, an effect which may contribute to the suppression of immune response seen *in vivo* after treatment of mice with MCT (Deyo and Kerkvliet, 1990; Deyo et al, 1994). It has been hypothesized that DNA crosslinking associated with the administration of MCT and other PAs causes the inhibition of mitosis and contributes to the development of megalocytosis (McLean, 1970).

MCT metabolites crosslink DNA and protein in the liver (Petry et al, 1984; Petry and Sipes, 1989). Subconfluent, log phase growth endothelial cells exposed to MCTP *in vitro* also develop DNA and protein crosslinks (Wagner et al, 1993). Covalent binding of MCTP to DNA of cultured endothelial cells has been suggested as the cause for inhibition of cell proliferation (Wagner et al, 1993; Thomas et al, 1996). Crosslinking of DNA by other alkylating agents has been associated with the inhibition of mitosis (Takanari and Izutsu, 1983; Kharbanda et al, 1994; Hoorn et al, 1995).

Although the ability of cells to complete cell division is presumed to be disrupted by the DNA crosslinking ability of MCT[P], the synthesis of nucleic acids and protein continues (Hsu et al, 1973; Hoorn and Roth, 1992). PECs exposed to a concentration of MCTP which inhibits proliferation continue to synthesize DNA, RNA and protein at a rate comparable to vehicle-treated cells (Hoorn and Roth, 1992). Prolonged synthesis of cellular macromolecules in the presence of mitotic inhibition has been proposed as a cause of megalocytosis (Davidson, 1935; Bull, 1955; Jago, 1970; Cheeke, 1988).

F. Human Cardiopulmonary Disease

The administration of MCT[P] to experimental animals has been used to generate models of several human diseases which alter the pulmonary circulation. Primary pulmonary hypertension and acute respiratory distress syndrome both have components involving endothelial damage and vascular remodeling which can contribute to pulmonary hypertension.

1. Primary Pulmonary Hypertension [PPH]

Pulmonary hypertension occurs when the cardiac output increases beyond the limits of distensiblity of the pulmonary vasculature [ie, left to right cardiac shunts] or when the pulmonary vascular resistance increases (Rubin et al, 1996). In humans, pulmonary hypertension due to increased vascular resistance is most common and frequently accompanies chronic parenchymal disease with fibrosis, pulmonary thromboembolism, pulmonary veno-occlusive disease and collagen vascular disease (Mooi, 1987). Cor pulmonale denotes an increase in right ventricular wall mass and occurs with the above-listed forms of pulmonary hypertension as a response to a sustained increase in pulmonary arterial pressure.

Human PPH is a condition in which cor pulmonale occurs without underlying cardiac or pulmonary parenchymal disease (Fishman and Pietra, 1980; Pietra and Rüttner, 1987). Changes in the pulmonary vascular structure reported with PPH occur in arteries between 50-500μm in diameter and include an increase in pulmonary arterial medial thickness, intimal fibrosis, perivascular inflammation and, in some instances, the development of "plexiform pulmonary arteriopathy" (Heath and Smith, 1977; Fishman and Pietra, 1980), an occlusive lesion thought to be produced by the intimal proliferation of endothelial cells (Rich and Brundage, 1989). The increase in medial thickness seen with

many forms of PPH resembles that seen with MCT or MCTP (Anderson et al, 1973; Fishman and Pietra, 1980). The cause of PPH is unknown, but hypoxia, abnormal growth factor expression and the uncontrolled growth of cells in response to damage have been suggested.

PPH has been reported after the comsumption of aminorex fumarate [2-amino-5-phenyl 2-oxazoline] (reviewed in Heath and Smith, 1977) and dexfenfluramine (Cacoub et al, 1995), both used as appetite suppressants to aid in weight loss. Attempts to reproduce aminorex-induced PPH in experimental animals has been unfruitful (Smith et al, 1973; Heath and Smith, 1977). As such, the mechanism of action responsible for the induction of PPH after the use of these chemicals is not known with certainty.

The MCT[P] rat model of pulmonary hypertension has been criticized, being labeled as a poor model of human PPH because the vascular lesions which accompany the development of hypertension in each are dissimilar (Heath, 1992). Pulmonary hypertension associated with MCT[P] admininstration does not produce plexogenic lesions in the arteries nor intimal proliferation of smooth muscle cells, both of which are seen frequently with human PPH (Fishman and Pietra, 1980). As such, MCT[P]-induced pulmonary hypertension may better serve as a general model of mechanisms of pulmonary vascular remodeling leading to hypertension.

2. Acute Respiratory Distress Syndrome [ARDS]

ARDS is a clinical complication of serious pulmonary and extrapulmonary processes including sepsis, aspiration of gastric contents and trauma (Lamy et al, 1976; Cunningham, 1991). The diagnosis of ARDS is based on several criteria: decreased oxygenation of the blood, generalized pulmonary infiltrates [proteinaceous fluid and/or cells] and the absence of cardiac failure [based on a normal pulmonary arterial occlusion pressure of less than 18 mm Hg (Stevens, 1982; Cunningham, 1991). The causes of ARDS are not known, but speculation abounds that one or more infectious agents or their associated toxins are involved. The development of ARDS concurrent with injury, infection or chronic lung/heart disease is associated with increased mortality (Stevens, 1982).

The pathophysiology of ARDS is divided into 3 phases (Lamy et al, 1976; Cunningham, 1991). The *acute phase of ARDS* is characterized by the disruption of the alveolar-capillary membrane, resulting in an increase in lung vascular permeability and severe, and often fatal pulmonary edema (Lamy et al, 1976; Holter et al, 1986). The degree of endothelial cell injury reported with early ARDS is variable, while notable injury to type I pneumocytes occurs (Cunningham, 1991). Neutrophils are consistently present within pulmonary infiltrates and around pulmonary blood vessels, suggesting the

involvement of an infectious agent. The direct role of neutrophils is uncertain, however, as patients deficient in neutrophils but affected by ARDS have been reported (Maunder et al, 1986; Laufe et al, 1986).

Patients who survive the acute phase of ARDS may recover fully or continue to manifest progressive lesions. Occurring 5-7 days after the onset of vascular leak, the *subacute phase of ARDS* is marked by the organization of proteinaceous alveolar exudate, alveolar fibrosis and extensive hyperplasia of type II pneumocytes (Cunningham, 1991). There is considerable accumulation of fibrous connective tissue within the interstitium of the lung which results in a loss of lung compliance (Cunningham, 1991). The *chronic stage of ARDS* is a maturation process for the subacute phase and in which there is continued organization of fibrous connective tissue in the interstitium, as well as perivascular and alveolar regions. These can reduce pulmonary compliance (Jones and Reid, 1991). Vascular remodeling has also been described as a component of chronic ARDS. Perivascular fibrosis and remodeling with ARDS can reduce the pulmonary microvascular area, increase the pulmonary arterial resistance, and lead to the development of pulmonary hypertension (Lamy et al, 1976; Cunningham, 1991).

The time courses to development of chronic ARDS and pulmonary hypertension after MCT are similar as are the clinical changes and histologic lesions present during the acute, subacute and chronic phases

(Langleben and Reid, 1985; Jones and Reid, 1991). Both ARDS and MCT-induced pulmonary injury start as cellular injury and vascular leak. With both [when ARDS does not resolve after the acute phase], parenchymal and/or vascular remodeling follow. The end result of both syndromes is the development of chronic lung disease and pulmonary hypertension, neither of which resolve spontaneously in either condition. The cause of the pathophysiologic changes that occur in the early stages of ARDS are unknown. Endothelial cell injury and increased vascular permeability appear to play an early and important role in ARDS and may be responsible for the downstream effects.

G. Summary

MCT is metabolized in the liver to produce a number of intermediates; the reactive pyrrolic metabolite of MCT causes injury to the liver and lungs. The character of the injury produced is highly dose-dependent and influenced by the age, sex and species of animal exposed. Humans exposed to plant components containing MCT most often develop hepatic necrosis followed by fibrosis and cirrhosis. A large dose of MCT in most experimental animals causes a similar result. When a small dose of MCT[P] is administered to the rat, delayed and progressive cardiopulmonary injury occurs which is characterized

by vascular leak, arterial remodeling and pulmonary hypertension leading to right heart hypertrophy.

Pulmonary vascular endothelial cells are the primary target of MCT[P], and the structural and functional alterations produced in these cells precede changes in other components of the lungs. The smooth muscle medial layer of small pulmonary arteries increases in thickness, and normally nonmuscular precapillary arteries acquire a muscular layer. This transformation is followed by an increase in pulmonary arterial resistance and pressure. Efforts to understand how MCT[P] causes pulmonary hypertension have concentrated on the study of mechanisms which could induce an increase in the amount of subintimal smooth muscle and cause the sustained elevation of vascular resistance.

An increase in the reactivity to contractile agonists, the overexpression of endogenous vasoactive mediators and the upregulation of pathways involved in cell growth and proliferation all occur to some extent after MCT[P] administration to rats. Inhibitors of the synthesis of or the receptor binding of certain vasoactive chemicals impede the development of pulmonary vascular remodeling and hypertension. The interpretation of many of these findings is problematic, given the potential nonspecific actions of the drugs used. Disruption of specific cell growth pathways or general animal growth [ie, restriction of caloric intake] effectively halts the development of medial thickening

and right heart enlargement. Collectively, these studies indicate that multiple pathways may contribute to arterial medial hypertrophy after MCT[P]. How these diverse pathways are upregulated is not known.

Interestingly, the endothelial cell plays a role in the control of vasoreactivity, in the synthesis, release or metabolism of vasoactive mediators and in the induction of growth or proliferation of vascular smooth muscle cells. Pulmonary endothelial cell injury after MCT[P] *in vivo* is followed by vascular leak, which continues for several days before pulmonary arterial pressure becomes elevated. *In vitro*, limited injury and loss of endothelial cells precedes the protracted reformation of a confluent monolayer. Monolayer repair is hampered by an inability of cells to proliferate in spite of continued cell enlargement. The result is megalocytosis with the persistence of gaps in the monolayer. A similar delay in repair after MCT[P] *in vivo* could result in the exposure of subintimal cells [ie, smooth muscle cells] to growth factors from plasma, the expression of vasoactive or mitogenic substances released by activated endothelial cells or platelets, and the induction of growth factor synthesis or release in medial smooth muscle cells. An understanding of normal vascular repair, and repair deficiencies which can result in chronic disease, may provide mechanistic clues to the progression of initial pulmonary artery injury after MCT[P] that leads to vascular remodeling and pulmonary hypertension.

II. Cell Injury, Repair, and Altered Repair Responses

A. Response to a Growth Stimulus

1. Permanent, Labile and Stable Cells

In higher mammals, the compensatory response of a tissue or organ to an increase in workload or the repair of injury occurs through the dynamic growth and/or proliferation of cells (Cotran et al, 1994). The pattern of response is dictated by the type of stimulus and the ability of the stimulated cell to undergo growth or cell division. All of the cells which make up an organism are described as permanent, labile or stable, a classification which defines their ability to respond to growth or mitogenic stimuli. Permanent cells [ie, neurons] are terminally differentiated and typically unresponsive to growth stimuli. If permanent cells are lost due to senescence or injury, they are not replaced. Labile cell populations [ie, gastrointestinal epithelium or circulating blood cells] are the product of the proliferation of undifferentiated precursor or stem cells. Labile cells have a relatively short half-life and require continuous production to provide for rapid turnover. A third group of cells [stable cells] are terminally differentiated but have retained the capacity to dedifferentiate and undergo hypertrophy [growth in cell size and the duplication of structural and functional

components without cell division] or hyperplasia [cell proliferation] in response to a mitogenic stimulus.

Endothelial cells, smooth muscle cells [and their precursors] and fibroblasts comprise most of the cellular content of arteries, capillaries and veins (Wagenvoort and Wagenvoort, 1979). All three differentiated cell types are considered stable cells, each with a low turnover rate but capable of a growth or proliferative response after injury (Schwartz et al, 1980). Smooth muscle cell precursor cells are incompletely differentiated, have contractile properties and can be induced to grow or proliferate prior to terminal differentiation (Davies et al, 1986; Shepro and Morel, 1993).

2. Optimal Repair of Injury

The circulation of the respiratory tract comprises two separate vascular systems which carry blood derived from the right heart [ie, pulmonary arteries] and the left heart [ie, bronchial arteries] (Wagenvoort and Wagenvoort, 1979). The pulmonary arterial circulation is a high volume, low pressure system with the exchange of respiratory gases as its primary responsibility. The bronchial arterial compartment is part of the systemic circulation [ie, higher pressure system] and will not be considered further.

The pulmonary vasculature can be injured by mechanical forces, changes in oxygen tension, toxins and infectious agents and may undergo functional disruption without overt cell injury or loss (Wagenvoort and Wagenvoort, 1979). Limited, localized injury to the vascular cells may be of little consequence to the overall health of an individual because of the large functional reserve of the lung and the active mechanisms responsible for repair of injury (Bowden, 1983). In contrast, more severe and widespread injury to the arteries, capillaries or veins of the lungs can have devastating results, not only in the reduced ability to oxygenate the blood, but in the alteration of lung vasoreactivity and vascular pressure, altered production and removal of biologically active agents, activation of the coagulation system, and the increased permeability to blood fluid and proteins (Heath and Smith, 1979; Cotran, 1994). When mechanisms responsible for the repair of injured lung vascular tissue are incapable of rapid or complete regeneration of normal cell components, each of these effects may be exacerbated.

a. Vascular Intima

The intima consists of a single layer of endothelial cells resting on a circumferential elastic lamina and the intervening basement membrane (Wagenvoort and Wagenvoort, 1979; Reid and Meyrick, 1982). The

endothelium is the primary target for blood-borne pathogens or irritants and the repair response by endothelial cells is dictated by the size of the injury and the health of endothelial cells adjacent to the injury site (Ettenson and Gotlieb, 1992; Ettenson and Gotlieb, 1994). Minor injuries with limited cell loss *in vitro* are repaired by extentions of the endothelial cell membrane [lamellipodia] and migration by endothelial cells immediately adjacent to the site of injury [Figure 3] (Wong and Gotlieb, 1984). The lamellipodia fill gaps in the monolayer left by injured cells in an apparent attempt to restore monolayer confluence. When the injury is more extensive, cytoplasmic extension alone may be insufficient to reform the endothelial monolayer adequately (Schwartz et al, 1980; Ettenson and Gotlieb, 1992; Ettenson and Gotlieb, 1994). As such, cell spreading is usually followed by the proliferation of endothelial cells behind the row of advancing cells (Schwartz et al, 1980; Wong and Gotlieb, 1988; Ettenson and Gotlieb, 1992). The combination of cell spreading, migration and proliferation results in a rapid reformation of monolayer confluence.

Injury to the intimal monolayer initiates repair but can result in actions which impact other vascular cells [ie, smooth muscle cells, fibroblasts]. The loss of monolayer confluence can result in the leak of plasma from the affected blood vessel, resulting in subintimal fluid accumulation [Figure 3]. Blood plasma contains several protein growth factors capable of inducing migration, growth or proliferation of endothelial, smooth muscle and epithelial

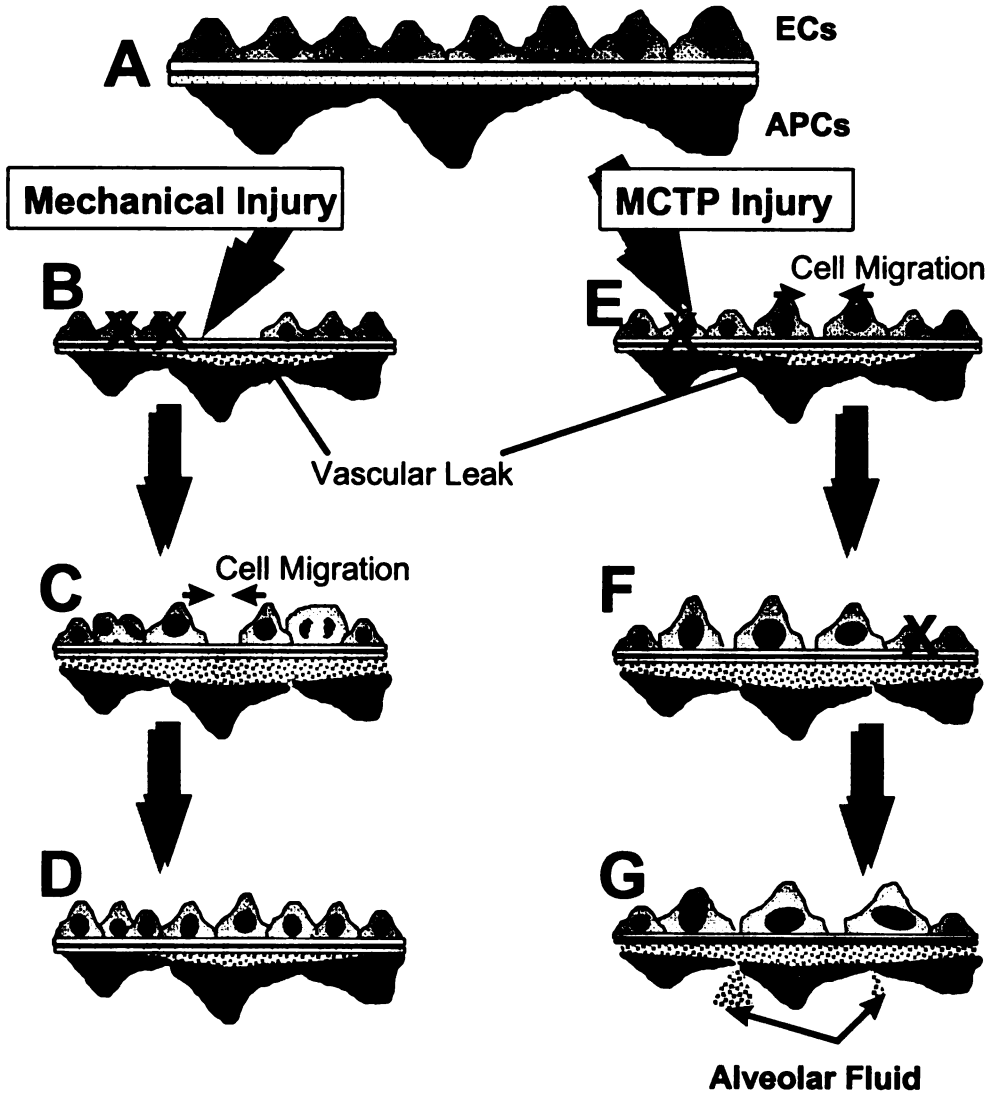

Figure 3. Vascular repair after endothelial cell injury.

Panel A depicts the normal morphology of a small blood vessel. Endothelial cells [ECs] and type I alveolar pneumocytes [APCs] are shown. With injury [B] and adequate repair [cell enlargement, migration and proliferation [C]] the monolayer is reformed and vascular leak resolved [D]. After MCTP-induced injury, continuous cell loss and defective replication impede repair, possibly resulting in persistant vascular leak [G]. X's denote concurrent or impending cell loss.

cells (Bagby et al, 1992; Bobik and Campbell, 1993). The endothelium can produce both mesenchymal and epithelial cell growth factors in response to injury (Collins et al, 1987), and platelets activated by endothelial injury can release mitogenic factors (Bobik and Campbell, 1993). Some vasoactive mediators produced or metabolized by the endothelium can have mitogenic effects on smooth muscle cells (Owens, 1991; Jackson and Schwartz, 1992). Rapid regrowth of the endothelium is necessary to reestablish vascular homeostasis, but it also serves to reduce smooth muscle cell migration and mitogenesis which can occur after intimal injury (Bjornsson et al, 1991). The endothelium produces heparan sulfate proteoglycan, an extracellular matrix component which binds protein growth factors produced by vascular cells and inhibits smooth muscle cell mitogenesis (Lindner et al, 1991; Campbell et al, 1992; Nugent et al, 1993).

b. Vascular Media

The vascular media comprises smooth muscle cells, collagen, elastic fibers and proteoglycan ground substance. These components vary in amount and orientation dependent on the size and type of vessel (Wagenvoort and Wagenvoort, 1979). Muscular pulmonary arteries contain one or more layers of smooth muscle within the media, whereas small precapillary

arteries have an incomplete or no differentiated muscle layer and smooth muscle cell precursor cells [intermediate cells or pericytes] (Reid and Meyrick, 1982; Shepro and Morel, 1993).

Smooth muscle cells *in vivo* are contractile with little capacity to divide; isolated smooth muscle cells retain their contractile phenotype for several days to weeks *in vitro* before converting to a synthetic conformation capable of proliferation (Thyberg et al, 1983). When the vessel wall sustains damage deep enough to affect the medial layer, smooth muscle cells in the region of the wound convert from a contractile form to a synthetic form which is highly responsive to mitogenic growth factors (Cuevas et al, 1991). After injury, DNA synthesis in smooth muscle cells is delayed 24 hours or longer, presumedly to accomodate the phenotypic conversion, and significant cell proliferation may not be seen for an additional 24-48 hours (Goldberg et al, 1979; Clowes et al, 1983). The complete regeneration of the medial layer of muscular arteries may take weeks to months (Clowes et al, 1983) and ideally results in a medial muscle mass comparable to that before injury [Figure 4].

Smooth muscle cells produce and release mitogens which can be involved in the reformation of the medial layer after injury (Jackson and Schwartz, 1992) or can induce endothelial cell proliferation (Lindner et al, 1990). Smooth muscle cells also contribute matrix proteins which, when excessive, can compromise the complete cellular regeneration of the vascular

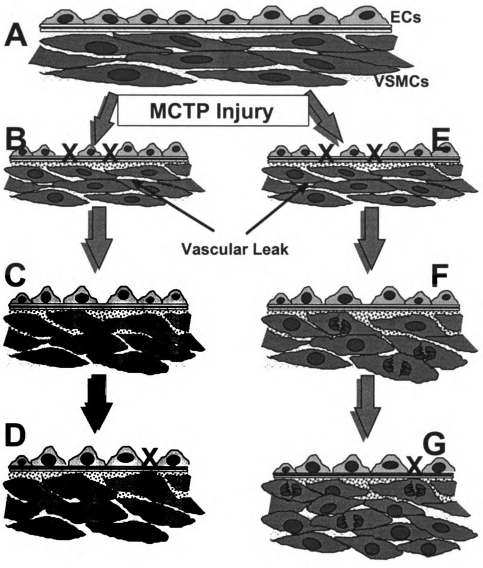

Figure 4. Potential VSMC responses to MCTP and endothelial cell injury.

Panel A represents the normal endothelial [EC]-smooth muscle cell [VSMC] relationship in pulmonary arteries. MCTP causes injury to endothelial cells resulting in vascular leak [B,E]. Vascular smooth muscle cells may undergo hypertrophy [B-D] or hyperplasia [E-G] in response to MCTP-induced proliferative stimuli, resulting in arterial medial thickening. X's denote concurrent or impending cell loss.

media (Jackson and Schwartz, 1992). With optimal repair of arterial medialinjury, cell regeneration must be balanced by cell loss to prevent the development of medial hypertrophy (Clowes et al, 1983).

c. Vascular Adventitia

The adventitia of pulmonary arteries and veins is composed of loosely arranged fibroblasts and collagen fibers which connect the vessel with the surrounding lung parenchyma. Fibroblasts respond to chronic injury by replication, but more importantly, by the production of connective tissue elements (Kameji et al, 1980; Reid and Meyrick, 1982). The adventitial response to injury is often late in the timecourse of vascular repair (Kameji et al, 1980; Cunningham, 1991). Vascular injury severe enough to involve the adventitia can result in complete obliteration of the vessel lumen.

After the administration of either MCT or MCTP to rats, pulmonary vascular leak is followed by distention of the perivascular adventitia [ie, fluid accumulation] (Meyrick et al, 1980; Bruner et al, 1983). As stated previously, factors present in plasma may induce subintimal cell proliferation or, in the case of fibroblasts, the production of extracellular matrix components. Adventitial fibrosis is significant only after MCT, possibly reflecting the longer time course required for maturation of vascular remodeling. Because the accumulation of

connective tissue in the perivascular adventitia of pulmonary arteries from MCTP-treated rats is insignificant or considered a minor contributor to vascular remodeling, adventitial fibrosis will not be considered further in this dissertation.

B. MCT[P]-Induced Vascular Injury

Ideal vascular repair after injury results in the restoration of the normal structure and function to all cell layers. Faulty repair can be associated with vascular occlusion, reduction in vascular distensibility or compliance, thrombosis, and, in the lungs, reduced gas exchange and pulmonary hypertension. Faulty repair is associated with incomplete tissue regeneration, excessive cell proliferation or repair by second intention [ie, scar tissue formation]. Each of these components are suggested by the effects of MCT[P] on the pulmonary vascular structure. Because MCTP-induced vascular injury does not result in excessive collagen deposition, repair by second intention will not be considered further.

1. Incomplete Repair

Limited endothelial cell injury and loss lead to an increase in pulmonary vascular permeability in the rat after MCT[P] administration (Meyrick

et al, 1980; Reindel et al, 1990). Increased vascular pressure is not involved in vascular leak initially as the pulmonary arterial pressure does not become significantly elevated until approximately 7 days after MCTP (Bruner et al, 1983) or longer after MCT (Meyrick and Reid, 1979a). MCT[P]-induced pulmonary vascular leak is progressive, leading to perivascular and alveolar edema (Valdivia et al, 1967b; Reindel et al, 1990).

The unrelenting nature of vascular leak after seemingly inconsequential endothelial structural damage and loss suggests that MCT[P] alters the mechanisms responsible for rapid regeneration of a confluent monolayer. As previously indicated, endothelial monolayer repair after injury occurs through a combination of cell spreading, migration and proliferation. The participation of each component is dependent on the severity of the injury (Schwartz et al, 1980; Wong and Gotlieb, 1984; Ettenson and Gotlieb, 1992; Ettenson and Gotlieb, 1994). Endothelial cells exposed to MCTP *in vitro* possess the ability to spread and enlarge in response to cell loss (Reindel and Roth, 1991; Hoorn et al, 1993); the progression of cell loss is not followed, however, by cell proliferation. It has been hypothesized that the inhibition of cell proliferation causes a delay in the repair of lung vascular injury after MCT[P], and that inadequate repair results in persistant vascular leak, possibly leading to pulmonary hypertension (Roth and Reindel, 1990; Hoorn et al, 1993). There are several lines of evidence to support the involvment of the inhibition of cell

proliferation in MCT-induced liver injury; a similar process could provide a mechanism by which MCT[P] causes progressive lung injury and pulmonary hypertension.

After the administration of a necrogenic, hepatotoxic PA, the observed repair does not correspond with the normal repair response. The liver has an extraordinary capacity to regenerate after acute necrosis or hepatectomy. For example, the administration of a single dose of carbon tetrachloride causes extensive hepatocellular necrosis which is rapidly repaired by hepatocellular proliferation, resulting in the reformation of the hepatic parenchyma (Herbst et al, 1991). By contrast, a single administration of a PA can cause a similar degree of hepatocellular necrosis, but the consequent regeneration is confined to scattered foci separated by thick connective tissue cords [ie, faulty repair with incomplete regeneration of normal tissue] (Allen et al, 1967; Butler et al, 1970).

Cell proliferation is critical to the development of fetal organs. Disruption of cell growth or proliferation during organ growth can result in organ malformation [eg. hydrocephalus of the cerebral hemispheres] or, in severe cases, the absence of an entire organ [eg. ancephaly] (Rogers and Kavlock, 1995). Arrest of cell development or the inhibition of cell proliferation necessary for organ maturation is thought to be responsible for incomplete lung development and fetal death after exposure of a pregnant rat to MCT (Todd et al, 1985) and for other nonfatal malformations in fetal rats exposed to PA

metabolites during intervals of critical tissue growth (Green and Christie, 1961). The inhibition of proliferation after lung injury by MCT[P] could delay repair.

Megalocytosis of hepatocytes and other cell types occurs after the administration of MCT[P] and other PAs, and is thought to represent the inhibition of cell proliferation in cells induced to undergo replication (Allen et al, 1970b; Jago, 1970). Megalocytosis in the liver is most prevalent in the periportal regions of the lobule while regenerative foci [see above] are localized to areas most affected by necrosis (Davidson, 1935; Allen et al, 1970b). In the lung, overt injury to type II pneumocytes is not evident after exposure of rats to MCT[P], yet these cells become megalocytic; other cells [endothelial, smooth muscle and interstitial cells] enlarge and there is a distinct absence of mitotic figures in each population (Reindel et al, 1990; Wilson and Segall, 1990).

In vitro studies showning the antiproliferative effect of MCTP on endothelial and other cultured cells have provided support for the role of disrupted repair in PA-induced injury (Reindel and Roth, 1991; Hoorn and Roth, 1992). Similar effects appear to occur *in vivo*, evident by the prolonged incorporation of ^{3}H-labeled thymidine [ie, a marker of DNA synthesis] (Meyrick and Reid, 1982) absence of mitotic figures in injured pulmonary arteries [ie, inhibition of proliferation], the increase in endothelial cell size and the persistence of vascular leak after MCT[P] (Butler, 1970; Chesney et al, 1974; Hurley and

Jago, 1975; Reindel et al, 1990). Both *in vitro* and *in vivo* effects have been described [see above].

2. Vascular Medial Hypertrophy

Exactly how the increase in thickness of the medial layer of pulmonary arteries is initiated after MCT[P] and how medial smooth muscle cells growth processes are involved in medial hypertrophy are not known. A number of mitogenic stimuli have been studied for their potential role in this model; the participation of some has been supported by the protective effect of various inhibitors or blocking agents [see above]. The induction of smooth muscle cell proliferation after MCT[P] by the direct activation of intracellular proliferation pathways by the toxicant has also been proposed and defended by the modulating effect of pathway inhibition. Some clues may be gleaned from the characterization of vascular remodeling in the systemic circulation.

In systemic arteries, hypertension is associated with vascular smooth muscle cell hypertrophy or hyperplasia (Owens and Schwartz, 1983; Owens and Reidy, 1985; Owens et al, 1988b). The existence or preponderence of hypertrophy or hyperplasia is determined by the type of injury, the acuteness and severity of the injury, and the size and location of the artery involved in that injury. The character of that injury may also be influenced by

injury to other cell layers [ie, endothelium] and/or the presence of vascular leak (Owens and Reidy, 1985). Vascular smooth muscle cells in large conduit vessels become hypertrophic and synthesize additional DNA in response to sustained elevation of the intravascular pressure (Owens and Schwartz, 1983), whereas persistent hypertension in small mesenteric arterial branches causes hyperplasia with little hypertrophy (Owens et al, 1988b). By contrast, acute systemic hypertension with endothelial denudation and vascular leak following aortic coarctation causes smooth muscle cell hyperplasia in the thoracic aorta (Owens and Reidy, 1985). Endothelial cell injury may contribute through the generation of growth factors or the exposure of subintimal cells to blood-borne mitogens via increased vascular permeability (Owens and Reidy, 1985).

The administration of MCT[P] to rats causes endothelial cell injury, pulmonary vascular leak and arterial remodeling which culminates in pulmonary hypertension. The administration of MCT to rats causes an increased number of medial smooth muscle cells to incorporate ^{3}H-thymidine within 3 days, consistent with increased DNA synthesis (Meyrick and Reid, 1982). In that study, increased incorporation continued for 14 days, several days beyond the establishment of a thickened arterial media. The sustained increase in VSMC DNA synthesis preceded an increase in medial thickness, but it was not accompanied by an obvious increase in muscle cell numbers consistent with proliferation (Meyrick and Reid, 1982). A detailed morphologic study of the

pulmonary vasculature after MCTP has not demonstrated overt cell proliferation [ie, lack of vascular wall cell mitotic figures]; however, vascular and nonvascular lung cells do undergo enlargement after exposure to MCT[P] (Reindel et al, 1990; Wilson and Segall, 1990). These results suggested that proliferation was not essential for some of the vascular changes associated with MCT[P] administration. The role of incomplete proliferative stimuli [ie, growth factors unable to induce cell actions necessary for mitosis] (Owens, 1991; Bagby et al, 1992; Reidy, 1992; Rothman et al, 1994) and the inhibition of mitosis by a toxic effect of MCT[P] (Raczniak et al, 1979; Mattocks, 1986; Wilson and Segall, 1990; Reindel and Roth, 1991) were considered in the design of experiments described in this dissertation. The ability of MCT[P] to inhibit cell proliferation became the focus of the work described herein.

C. Inhibition of the Cell Proliferation

The process of cell proliferation requires the activation of a complex series of interrelated events, resulting in the complete duplication of all cell components and the generation of two daughter cells (Alberts et al, 1989). The events which constitute the interval between mitogenic stimulation and cell division define the cell cycle. Noxious agents can interfere with cell cycle progression by creating structural damage or inactivating critical enzymes

(Takanari and Izutsu, 1983; Usui et al, 1991; Kharbanda et al, 1994). MCT[P] may cause the inhibition of cell proliferation through cell cycle arrest.

1. The Cell Cycle

Stable cells which grow in a monolayer and are exposed to a proliferative stimulus can proceed through several rounds of cell division before replication is inhibited by confluence. The interval of time between mitoses is one cell cycle and the component parts of that cycle are often depicted as fractions of a circle [Figure 5] (Alberts et al, 1989). The cell cycle is composed of 4 phases. Each cell cycle phase is identified by its duration relative to the entire cycle; the length of each phase and of the entire cell cycle can vary considerably among cell types (O'Farrell and Dealtry,1992).

Phases of the cell cycle consists of one or more processes including the synthesis, assembly and/or destruction of proteins, lipids and nucleic acids. The interaction of each component results in a cell functions necessary for mitosis. G_1, S, G_2 and M phases characterize actively cycling cells, whereas those in G_0 are metabolically active but noncycling cells which can reenter the cycle after the appropriate stimulus (Hartwell and Weinert, 1989). Each phase has a single major function related to cell proliferation.

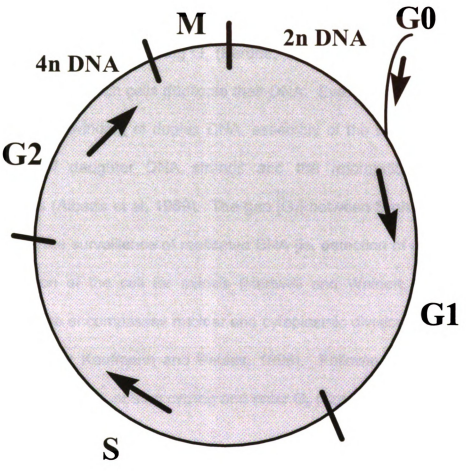

Figure 5. Stages of the cell cycle.

G0 - Noncycling, proliferation competent cells
G1 - Cells preparing for DNA synthesis
S - Cells undergoing DNA synthesis
G2 - Cells preparing for mitosis
M - Cells undergoing mitosis

Cells in G0-G1 contain a diploid DNA complement [**2nDNA**] while cells in G2-M contain a replicated diploid DNA complement [**4nDNA**].

G_1 phase constitutes those activities necessary to prepare cells for the replication of DNA. Proteins necessary for the synthesis of DNA are snythesized and activated during G_1 (Pardee, 1989; Reddy, 1994). S phase is the interval during which cells duplicate their DNA. Events which occur during S phase include unwinding of duplex DNA, assembly of the replication forks, the construction of daughter DNA strands and the reformation of duplicated chromosomes (Alberts et al, 1989). The gap [G_2] between S phase and mitosis is involved in the surveillence of replicated DNA [ie, detection of damage] and in the preparation of the cell for mitosis (Hartwell and Weinert, 1989; Elledge, 1996). M phase encompasses nuclear and cytoplasmic division [mitosis] (Dorèe and Galas, 1994; Kaufmann and Paules, 1996). Following mitosis, cells can reenter the cycle at G_1, or stop cycling and enter G_0 (Cotran et al, 1994).

2. Control of the Cell Cycle

The initiation of events in each phase requires the orderly completion of events in the previous phase (Hartwell and Weinert, 1989). The fidelity of cell cycle progression is controlled by regulatory 'checkpoints' [Figure 6] (Elledge, 1996). Checkpoint functions serve to ensure that the cells have acquired all of the necessary structural modifications and have undergone the phase-related functional changes required to proceed into the next cell cycle

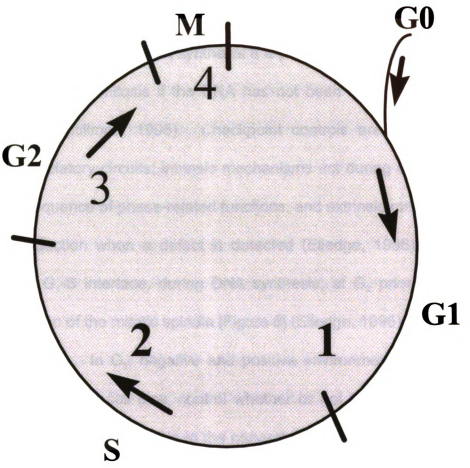

Figure 6. Cell cycle checkpoints.

1. G1 - Prior to DNA synthesis
2. S - During DNA synthesis
3. G2/M - Prior to mitosis
4. M - During mitosis [proposed]

Checkpoints responsible for the initiation of cell cycle delays for DNA damage repair, completion of DNA replication and assembly of mitotic spindle [proposed].

phase (Stillman, 1996). Checkpoint activity can upregulate DNA repair processes or cause cell death (Elledge, 1996). Checkpoint controls also regulate entry of cells into DNA synthesis if a previous mitosis has not occurred and the inhibition of mitosis if the DNA has not been replicated (Hartwell and Weinert, 1989; Stillman, 1996). Checkpoint controls are composed of two classes of regulatory circuits; intrinsic mechanisms act during each cell cycle to control the sequence of phase-related functions, and extrinsic mechanisms occur only after induction when a defect is detected (Elledge, 1996). Checkpoints occur at the G_1-S interface, during DNA synthesis, at G_2 prior to mitosis and during formation of the mitotic spindle [Figure 6] (Elledge, 1996).

In G_1, negative and positive environmental signals, as well as attaining a critical cell size, control whether or not the cell enters S phase (Peeper et al, 1994). In addition to the general production of proteins necessary for DNA synthesis (Hamilton et al, 1992), specific enzymes and their protein substrates must be present and of sufficient activity to initiate S phase (Pardee, 1989; Dorée and Galas, 1994).

The G_1 checkpoint consists of both intrinsic and extrinsic components. Specific cyclin-dependent kinase [Cdk] subtypes and cyclins, the activating subunits for the Cdks, dimerize during G_1, are phosphorylated, and promote the transition to S phase (Elledge, 1996). Insufficient amounts of either Cdk or cyclin, inhibition of Cdk-cyclin binding or a

lack of posphorylation of the Cdk-cyclin complex prevent G_1 cells from entering S phase (Dorée and Galas, 1994). The major extrinsic control of G_1-S transition is a protein transcription factor derived from the anti-oncogene, p53 (Dorée and Galas, 1994; Kaufmann and Paules, 1996) which acts by inhibiting Cdk activity (Reddy, 1994; Kaufmann and Paules, 1996; Elledge, 1996). The inhibition of G_1-S transition can be induced by certain types of DNA damage which upregulate p53 expression (Kaufmann and Paules, 1996).

An S phase checkpoint is involved in the regulation of DNA synthesis through the control of replicon initiation (Kaufmann and Paules, 1996). The replicon is a cluster of enzymes necessary for the unwinding, separation and replication of the DNA duplex (Alberts et al, 1989). DNA damage in the form of strand breaks or mismatches initiates S phase-dependent repair mechanisms which inhibit replicon activity and delay transit through S phase (Elledge, 1996). The S phase checkpoint may actually comprise a series checkpoints spread through the interval of DNA replication (Kaufmann and Paules, 1996).

The transition of cells from S phase through mitosis is controlled by a third checkpoint which resides at the G_2 gap phase. Cell cycle arrest prior to mitosis occurs by the activation of an intrinsic checkpoint mechanism involving inhibition of Cdk-1 activity or the reduction of its respective subunit, cyclin B (Nurse, 1990; Elledge, 1996). The increase in cyclin B, its

binding to Cdk-1, phosphorylation of the complex and subsequent degradation are strictly ordered events necessary for the initiation and completion of mitosis (Dorée and Galas, 1994; Kaufmann and Paules, 1996). The Cdk-1/cyclin complex plays a role in unwinding and relaxation of DNA, assembly of the mitotic spindle and cytoskeletal alterations needed for shape change during cell division (Hartwell and Weinert, 1989; Nurse, 1990). Interestingly, antibodies to the homologous enzyme in yeast inhibits mitosis but does not affect DNA synthesis (Riabowol et al, 1989).

A specific extrinsic checkpoint factor associated with G_2 arrest has not been characterized. DNA damage and incomplete DNA replication can activate the G_2 checkpoint, possibly through mechanism similar to those described for the G_1 checkpoint above (Hartwell and Weinert, 1989). Activation of the G_2 checkpoint provides additional time for repair of DNA damage prior to cells undergoing mitosis (Hawn et al, 1995). Insufficient activity of the G_2 checkpoint allows chromosomal aberrations to become fixed in proliferating cells and is a common initiating step in cell transformation (Elledge, 1996).

An additional checkpoint in mammalian cells may be active during M phase to regulate the proper formation of the mitotic spindle (Elledge, 1996). This assembly checkpoint has been proposed to prevent the onset of anaphase and the segregation of chromosomes until the spindle has formed, the

chromosomes have attached to the spindle and the chromosomes are properly aligned on the metaphase plate.

The events comprising the cell cycle constitute a means by which tissue damage can be repaired in a timely fashion, yet provide mechanisms which halt cell division and prevent the clonal expansion of defective or abnormal cells. Disruption of the orderly progression of cell cycle events or defects in the signalling mechanisms which trigger checkpoint activity can markedly delay tissue repair or result in attempted repair by abnormal cells.

3. The Cell Cycle and MCTP-induced Injury

MCTP inhibits cell proliferation in all cultured cells tested and causes megalocytosis *in vitro* when exposed cells are stimulated to proliferate. Hepatocytes and, to a limited extent, cells in the lungs undergo changes suggesting that a similar effect of PAs occurs *in vivo*. A limited evaluation of the effect of MCTP on cell cycle progression in cultured endothelial cells indicates that cells are arrested prior to mitosis, the pattern of which is dose-dependent (Thomas et al, 1996). The ability of MCT[P] to bind covalently and to crosslink DNA (Petry et al, 1984; Wagner et al, 1993; Thomas et al, 1996) suggests that DNA damage may induce cell cycle arrest.

Whether MCT[P]-induced cell cycle arrest occurs in pulmonary vascular cells *in vivo* is not known. Cell cycle arrest has been identified in hepatocytes *in vivo* following the administration of the PA, lasiocarpine to rats; similar to the effect of MCTP on cultured endothelial cells, affected hepatocytes were arrested at G_2-M (Samuel and Jago, 1975).

D. Summary

After injury, cellular repair is initiated by stimuli which promote cell enlargement, migration and/or proliferation. The extent of involvement of each is dictated by the severity of injury and capacity of the cell to participate in the repair response.

Several terminally differentiated cell types comprise pulmonary arteries and veins. In response to injury or other mitogenic stimuli, each cell type is able to undergo cell division. The rapid repair of lung vascular injury encompasses the regeneration of vascular wall cells and matrix components. When the repair of injury is incomplete or delayed, chronic processes such as scarring and tissue hypertrophy can impede normal lung vascular function.

A single administration of MCT[P] to the rat causes limited injury to endothelial cells in small pulmonary arteries. This injury proceeds to persistant pulmonary vascular leak, arterial remodeling and hypertension leading to right

ventricular hypertrophy, which can take several weeks to develop. The extent of vascular remodeling which occurs after endothelial cell injury seems excessive relative to the degree of endothelial cell injury caused by MCT[P]. This toxicant may cause excessive vascular remodeling in response to its long-lasting effect on tissue repair and not so much to its ability to induce cytotoxicity. The alteration in the ability to undergo repair may occur in one or more individual cell types.

Tissue repair requires cell enlargement or proliferation, possibly through the successful coupling of a mitogenic stimulus to a series of functional and structural events leading to the replacement of tissue mass by hypertrophy or hyperplasia. The cell cycle consists of many interrelated and complex events, all of which must occur in the proper sequence and at the appropriate level to result in growth and proliferation. The disruption of any one of these events can result in cell cycle arrest and the inhibition of mitosis. Cell cycle progression is regulated through biochemical pathways [checkpoints] which work to insure that cell division results in the production of normal daughter cells. Cell cycle arrest provides delays for the repair of damage or the correction of other intracellular deficiencies. The pattern of cell cycle arrest [ie, checkpoint initiation] is determined by the cellular abnormality and the phase in which that abnormality occurred [eg, DNA damage during late S phase results in G_2 arrest].

The exposure of cultured endothelial cells to MCTP causes cell cycle arrest prior to mitosis. The pattern of cell cycle arrest has been correlated with the degree of covalent DNA binding and crosslinking by MCTP. DNA damage can activate one of several cycle phase checkpoints resulting in cell cycle delay or arrest. MCTP inhibits cell proliferation *in vitro* at a dose comparable to that which produces cell cycle arrest. Although mitosis is impeded by MCTP, DNA synthesis continues at a normal or above normal rate, suggesting that cell cycle arrest induced by MCTP may occur through a mechanism not involving extensive DNA damage.

Clarification of the cause of mitotic arrest with continued DNA synthesis *in vitro* after MCT[P] requires the dissection of complex events which occur during the cell cycle. Determining the importance of cell cycle arrest and the inhibition of cell proliferation to the development of MCTP-induced pulmonary hypertension will require the identification of similar patterns of mitotic arrest and DNA synthesis *in vivo*. A hypothetical pathway of MCTP-induced cell cycle arrest, inhibition of cell proliferation and the development of vascular changes which leads to pulmonary hypertension is shown in Figure 7.

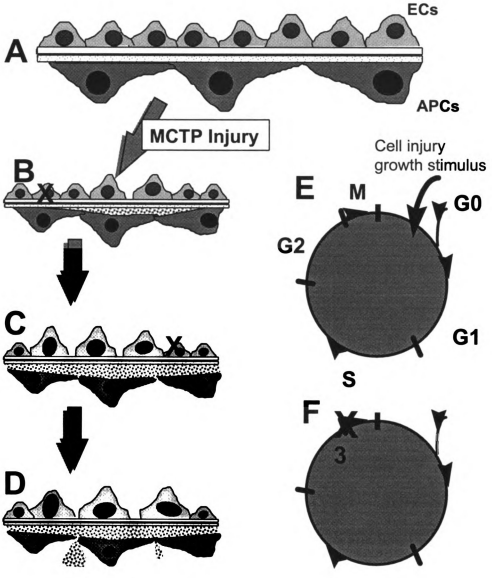

Figure 7. MCTP-induced endothelial cell injury and hypothetical cell cycle effect.

Panels A-D are described in Figure 3 [panels A,E-G].
The proposed effect of MCTP on the progression of the cell cycle is depicted in panel F, showing inhibition of the cell cycle at the G2 checkpoint [3] [see Figure 6]. Continued DNA synthesis could contribute to the increase in endothelial cell size and may result in polyploidy.

IV. Research Goals

MCTP targets the pulmonary vascular endothelium, resulting in a finite structural injury to a small fraction of cells, but an apparent functional disruption in many cells which reduces the ability of cells to proliferate after injury. The inability to proliferate in response to injury and loss of endothelial cells may result directly in delayed and progressive vascular leak and indirectly in vascular remodeling and pulmonary hypertension. Therefore, understanding the characteristics of mitotic inhibition is crucial to determining its role in MCTP-induced vascular disease.

The first objective of this dissertation was to test the hypothesis that MCTP inhibits mitosis by interrupting cell cycle progression. Previously defined DNA crosslinking after MCT[P] prompted the expectation that the most striking alteration in cell cycle activity would occur during S phase. Thus, cycle phase-specific effects of MCTP were considered. In previous studies, MCTP had been applied to the culture medium of cells for periods of 24 hours or longer. To mimic more closely the endothelial exposure interval presumed to occur *in vivo* after MCTP administration [instability of MCTP and redistribution of the original bolus dose by the circulation] and to limit MCTP exposure of cells to specific cell cycle phases, cultured endothelial cells were treated with MCTP for only 4 hours. Cell cycle analysis was done using fluorescence-activated cell sorting [FACS].

This method allows the definition of cell cycle stages at specific points in time based on the determination of DNA content in individual cells of a population. Chemically synchronized BECs undergoing log phase growth were exposed to MCTP during different cell cycle phases and examined for differences in DNA distribution patterns at 24 hours.

A second component of this dissertation research was to characterize the effect of MCTP on endothelial cell proliferation and DNA synthesis *in vivo* and to determine the presence of effects *in vivo* similar to those reported *in vitro* and anticipated from the experiments comprising the first research goal [see above]. It was expected that the results generated would further support the hypothesis that mitotic inhibition and the disruption of repair play a role in the prolonged course of events leading to vascular remodeling and pulmonary hypertension after MCTP. Unfortunately, the technology necessary for cell cycle analysis in specific populations of cells from the microvasculature *in vivo* does not yet exist and alternative, less direct methods to identify the effect of MCTP on cell growth and replication had to be used. Two specific hypotheses were proposed: 1] MCTP causes the upregulation of DNA synthesis in endothelial cells, and this synthesis corresponds chronologically to the earliest damage recognized in pulmonary vascular endothelial cells, and 2] endothelial cell proliferation, as an important component of vascular repair, does not follow that injury. Rats were treated with MCTP or vehicle and the level of DNA synthesis in endothelial cells

of small pulmonary arteries was quantified by the measurement of bromodeoxyuridine incorporation. In addition, the endothelial cell density of those same arteries was determined over 8 days to determine if cell proliferation occurred in response to endothelial cell injury. The results were compared to the data generated *in vitro* and to previous reports showing the effects of MCT on DNA synthesis and cell proliferation *in vivo*.

Although changes in the endothelium constitute the first readily observable alteration in the pulmonary microvasculature after MCT[P], an increase in the medial thickness of small pulmonary arteries is instrumental in the development of pulmonary hypertension. It has been suggested that medial thickening after MCT administration is associated with increased DNA synthesis, but the subsequent proliferation of smooth muscle cells has not been clearly identified (Meyrick and Reid, 1982). The antiproliferative action of MCTP may extend to subintimal cells as is suggested by the enlargement of type II pneumocytes in MCT-treated rats (Wilson and Segall, 1990). Experiments were done to test the hypotheses that [1] MCTP causes an increase in vascular smooth muscle cell DNA synthesis prior to evident medial hypertrophy, and [2] medial thickening is the result of smooth muscle cell proliferation. An alternative hypothesis [2b] is that MCTP causes an increased arterial medial thickness through cellular enlargement or hypertrophy in the absence of smooth muscle cell proliferation. Rats exposed to MCTP were examined for DNA synthesis and

cell proliferation in smooth muscle cells of small precapillary arteries; the method of measurement was similar to that defined above for endothelial cells *in vivo*. The results were to be correlated with those generated by *in vitro* and *in vivo* studies with endothelial cells [see above].

Overall, the data generated and presented in this dissertation has extended the body of knowledge concerning the antiproliferative effect of MCTP *in vitro*. In addition, the reported effect of MCTP on cellular DNA synthetic and proliferative patterns *in vivo* correlate with the pattern identified *in vitro*, suggesting that similar mechanisms may be involved in both systems. This work has established the framework for additional studies to characterize the role of inhibition of cell proliferation in MCTP-induced pulmonary hypertension and to study mechanisms necessary for the induction, completion and regulation of cell proliferation present during specific cell cycle phases.

Chapter II

THE RESPONSE OF PULMONARY ENDOTHELIAL CELLS TO MONOCROTALINE PYRROLE: CELL PROLIFERATION AND DNA SYNTHESIS *IN VITRO*

Summary of Chapter II

Monocrotaline pyrrole (MCTP) causes pulmonary vascular endothelial cell (EC) injury followed by progressive pulmonary vascular leak *in vivo*. When MCTP is applied to ECs *in vitro*, cell injury is associated with the inhibition of proliferation. The inhibition of proliferation *in vivo* after MCTP could postpone monolayer repair and contribute to progressive pulmonary vascular leak. To determine the effect of MCTP on cell cycle progression as it relates to the inhibition of proliferation, fluorescence-activated cell sorting [FACS] was used to measure alterations in the distribution of DNA within a cell population and to identify differences in DNA synthesis related to altered cell cycle patterns. Subconfluent cultures of BECs were allowed to cycle randomly or were synchronized with aphidicolin [APH], a reversible G_1-S phase inhibitor. Upon removal of APH, BECs were exposed to MCTP [5µg/ml] or its vehicle for a 4 hour interval corresponding to either the G_1-S, S-G_2 or G_2 through mitosis (M) phases of the cell cycle. Unsynchronized cells were treated with a single administration of MCTP or vehicle for 4 hours. The transit of S phase cells through the cycle was characterized using the thymidine analog, bromodeoxyuridine (BrdU). During the 24 hours after release from APH, cells exposed to MCTP between mid S-G_2 or G_2 through M were briefly delayed in G_2-M at 12 hours, but underwent cell division by 24 hours. Likewise, unsynchronized cells exposed to MCTP for 4

hours were delayed in late S but proceeded through mitosis. In contrast, BECs treated with MCTP immediately after release from APH block became arrested in G_2-M at 24 hours and showed evidence of hypertetraploidy, but they did not divide. In summary, MCTP inhibits mitosis in a cycle phase-dependent manner in BECs *in vitro*, but DNA synthesis continues. These data suggest that MCTP inhibits monolayer repair by blocking mitosis and causing the disconnection of DNA synthesis from cell division. This cell cycle arrest and consequent failure of replicative repair may contribute to the persistent pulmonary vascular leak characteristic of MCTP-induced lung injury in the rat.

Introduction

Pyrrolizidine alkaloids [PAs] cause limited, direct cell injury which progresses to chronic and severe hepato- or pneumotoxicity (Kay et al, 1967; Allen and Carstens, 1970a; Culvenor et al, 1976; Meyrick et al, 1980; Reindel et al, 1990). The apparent discrepancy between the severity of initial injury and the long-term results of intoxication suggests that PAs induce functional alterations in cells which may impede their ability to repair damage.

In vitro, the alkaloid metabolite monocrotaline pyrrole [MCTP] inhibits the proliferation of endothelial cells [ECs] (Reindel et al, 1991; Hoorn and Roth, 1992) and inhibits cell cycle progression in cultured BECs, with cells arresting at

late S to G_2-M after a 24 hour exposure (Thomas et al, 1996). Porcine ECs exposed to MCTP continue to produce DNA, RNA and protein but are unable to divide (Hoorn and Roth, 1992). Accordingly, the antiproliferative effect of pyrrolizidine alkaloids appears to result from the arrest of nuclear and cellular division, while other cell functions, such as macromolecule synthesis, continue. The inhibition of cell proliferation by MCTP and other PAs may, in turn, be responsible for the long term and progressive effects of these toxicants.

The cell cycle comprises a series of events which result in DNA replication and mitosis after a proliferative stimulus (Nurse, 1990; Dorée and Galas, 1994). It has been hypothesized that PAs inhibit cell proliferation by interfering with the progression of the cell cycle (Mattocks, 1969). Previous studies (Hsu et al, 1973; Samuel and Jago, 1975) showed that hepatocytes, from PA-treated rats which were subsequently exposed to a mitogenic stimulus, became arrested in the late S or G_2 phase of the cell cycle and did not divide. Likewise, subconfluent, cultured hepatocytes are unable to progress through mitosis after exposure to MCT (Skilleter et al, 1988).

The inhibition of mitosis may be initiated at one or more points in the cell cycle (Hartwell and Weinert, 1989). Cycle progression in somatic cells requires the completion of early events (ie, DNA synthesis) prior to the initiation of late events (ie, mitosis) and is regulated by a series of checkpoints (Hartwell and Weinert, 1989; Kaufmann and Paules, 1996). Major checkpoints allow cells to

enter S phase from G_1 and undergo DNA replication (Peeper et al, 1994), to continue DNA synthesis (Hartwell and Weinert, 1989) and to divide after the completion of DNA synthesis (Nurse, 1990; Laskey et al, 1989). Flow cytometry can be used for the analysis of cell cycle dynamics allowing the identification and characterization of disruptions of cycle progression, including the loss of checkpoints (Dolbeare et al, 1983; Gray et al, 1986).

This study was designed to characterize further the antiproliferative action of MCTP on ECs *in vitro*. Heretofore, in most studies done to examine the effect of MCTP on cell replication, the exposure intervals have encompassed one or more complete cell cycles and all of the functions which occur therein. Given the number and complexity of early cell cycle events and the potential for mitotic inhibition with disruption of one or more of these events, short [4 hours] MCTP exposures were used in this study to determine how MCTP influences progression through the cell cycle. Using synchronized cells, we tested the hypotheses that [1] a limited time of exposure of BECs to MCTP would cause disruption of the cell cycle and [2] the pattern of inhibition varies in a cell cycle phase-dependent manner.

Materials and Methods

Preparation of MCTP: Monocrotaline pyrrole was synthesized from monocrotaline [Trans World Chemical, Rockville, MD] using the method described by Mattocks et al (Mattocks et al, 1989). Briefly, monocrotaline was converted directly to MCTP using o-chloranil, a quinone which readily dehydrogenates pyrrolizidine alkaloids to pyrrolic compounds. MCTP generated by this method has Ehrlich activity (Mattocks and White, 1971) and a structure consistent with MCTP as determined by mass spectrometry and nuclear magnetic resonance (Bruner et al, 1986). MCTP was maintained in N, N'-dimethylformamide [DMF; Sigma Chemical Co., St. Louis, MO] under nitrogen at -20°C and was diluted to working concentrations with DMF immediately before use. Unless otherwise indicated, the concentration of MCTP used for each experimental application in medium was 5µg/ml of medium.

Preparation of Endothelial Cells: Bovine endothelial cell lines [BECs] were isolated from segments of the pulmonary artery removed from freshly killed young cattle, as described by Reindel et al (1991). Arteries were collected aseptically, rinsed gently in sterile Hank's balanced salt solution [HBSS; Sigma] containing calcium and magnesium, and place into cold, sterile Puck's saline [HBSS with calcium and magnesium, bicarbonate and glucose] containing 3%

antibiotic/antimycotic solution [300 units/ml penicillin, 300 µg/ml streptomycin, 0.75µg/ml Fungizone; GIBCO, Grand Island, NY] on ice for transport. In a laminar flow hood using sterile instruments, the adventitia and external lamina were removed by blunt dissection. The artery was cut into 2 cm squares and placed endothelium side down into 100 mm culture plates containing collagenase [Type 1A-S, 0.1%, Sigma]. After incubation at room temperature for 3-5 minutes, the endothelial surface was gently scraped with a rubber policeman and the scrapings were resuspended in fresh calcium/magnesium-free HBSS. Using an inverted phase contrast microscope [Nikon TMS-F, Tokyo, Japan], clusters of endothelial cells were isolated with a micropipettor and removed to individual 23mm wells of a multi-well culture plate [Becton Dickinson, Franklin Lakes, NJ] containing 0.5 ml Dulbeco's Modified Eagles Medium [DMEM] or Medium 199 [M199] [GIBCO, Grand Island, NJ], containing 10% fetal bovine serum [FBS, Intergen, Purchase, NY] and 1% antibiotic/antimycotic [PSF containing penicillin {100 units/ml}, streptomycin {100 µg/ml}, fungizone {0.75µg/ml}; GIBCO, Grand Island, NJ]. Plates were incubated for 5-9 days at 37° C in 5% CO_2. At that time, uniform colonies of cells exhibiting a cobblestone morphology and free spindle cells were passed into larger wells. For cell passage, individual colonies were isolated with sterile, plastic O-rings, exposed to 0.025% trypsin/0.01M EDTA [GIBCO] for 5 minutes, removed by gentle aspiration and placed into a new culture well. These cells were then grown to

confluence and were subsequently passed if they remained a uniform population of cells with a cobblestone morphology. Cultures were split at a ratio of 1:5 at weekly intervals by dissociation with trypsin/EDTA. BECs used in this study were from 3 different cell lines between passages 3 and 20. Culture medium was changed every second day, unless otherwise noted.

The presence and purity of each endothelial cell line derivation was confirmed by their ability to take up acetylated low-density lipoprotein labeled with the fluorescent marker 1,1'-dioctadecyl-1-3,3,3',3'-tetramethyl-indo-carbocyanine perchlorate [Biomedical Technologies, Inc., Stoughton, MA] and the positive staining with factor VIII-related antigen:fluorescein isothiocyanate [FITC] conjugate [Biogenix Laboratories, Dublin, CA]. Both markers were visualized using a fluorescence binocular microscope [Olympus BX50, Olympus Optical Co., Ltd., Tokyo, Japan] equipped with an FITC detection system.

Cell Cycle Progression of Unsynchronized Subconfluent BECs: To obtain subconfluent log phase growth cultures, confluent monolayers of BECs were dissociated enzymically with trypsin/EDTA and plated into 35mm wells in plastic, multiwell plates [Becton Dickinson, Franklin Lakes, NJ] at a concentration of 2-3 X 10^5 cells/2 ml medium. To determine the interval required for the resumption of cell cycling after passage, BECs were collected from individual, subconfluent wells at 4-6 hour intervals through 24 hours after passage. In a later study,

BECs exposed to ethanol [final concentration, 0.2%; vehicle for the synchronizing agent aphidicolin] were collected at 3 hour intervals for 40 hours, starting 24 hours after passage [corresponding to the point of removal of aphidicolin from synchronized cells] to determine the pattern of cell cycle progression once cycling resumed. The cells were fixed and stained for quantitation of DNA content by flow cytometry, as described below.

Cell Synchronization and MCTP Exposure: BECs were synchronized chemically with, aphidicolin [APH; Sigma], a reversible DNA polymerase-α inhibitor (Huberman, 1981). Cells were passed from confluent plates as described above. Two hours after passage (for cell attachment), APH [2 µM] was added to the medium and cells were incubated at 37° C in 5% CO_2 for 24 hours to allow cells to synchronize at the G1-S interface [ie, prior to DNA synthesis]. To initiate cell cycling, the medium containing APH was removed, and the monolayers were washed twice with warm calcium/magnesium-free HBSS followed by application of warm APH-free medium. This technique initiates cell cycling within 30-60 minutes [see Results]. Synchronized BEC samples were collected every 3 hours over a 40 hour interval to determine the time course of cell cycle progression.

The exposure of synchronized BECs to MCTP [5µg/ml] or vehicle was limited to 4-hour intervals corresponding to discrete phases of the cell cycle [see

Results]. Unsynchronized BECs treated for 24 hours with APH vehicle [ethanol - 0.2% final concentration] were washed and exposed to MCTP or its vehicle for 4-hour intervals commencing approximately 26, 30 or 34 hours after cells were passed from confluence.

Cell Viability: Lactate dehydrogenase [LDH] release, an indicator of cellular injury, was measured up to 24 hours after MCTP or vehicle, and up to 72 hours after APH removal using the method of Bergmeyer and Brent (1974). Briefly, medium from above monolayers was removed and conserved, and the cells were washed twice with HBSS. Triton-X 100 [0.01%, Sigma] in HBSS was used to lyse the cells. The percent LDH release was determined by the following formula:

$$\% \text{ LDH release} = \frac{\text{LDH in medium above the monolayer}}{\text{LDH from lysed cells} + \text{LDH in medium above the monolayer}}$$

BrdU Labeling of BECs: The kinetics of the cell cycle were studied by exposing synchronized BECs to 2-bromo-5-deoxyuridine [BrdU, Sigma] to label cells actively synthesizing DNA. Briefly, medium containing APH was removed, and cells were washed twice with warm medium. BrdU was added to the medium 1 hour after APH was removed, to achieve a BrdU concentration of

20μM. The one hour delay allowed synchronized cells to resume cycling. After a thirty minute BrdU exposure, the medium was removed and the cells were washed twice with fresh medium containing no BrdU. BECs exposed to BrdU were collected at 1.5, 4, 8, 12, and 24 hours after APH removal to examine cell cycle progression. MCTP or vehicle applied to BECs from 0-4 hours was removed with BrdU-containing medium after the 30 minute pulse, but was replaced in fresh medium that was subsequently applied to the cells. The second application of MCTP at 1.5 hours did not change the pattern of cell cycle progression by BECs through 24 hours compared to cells exposed to MCTP continuously for the 0-4 hour interval [data not shown]. Cells which had incorporated BrdU were identified with an antiBrdU immunoglobulin [Becton Dickinson, San Jose, CA] [see below].

Cell Preparation for Flow Cytometry: At specified times after the removal of aphidicolin or vehicle [1.5, 4, 8, 12, and 24 hours], medium was removed from wells and cells were washed twice with HBSS. Trypsin/EDTA [see above] was applied, and cells were incubated at 37° C for 5-7 minutes to detach them from the plate. The cells were resuspended in 2 ml DMEM [0.5-1 X 10^6 cells] and spun at 500 X G at 10° C. The cell pellet was fixed by resuspension in fetal bovine serum [FBS] to reduce cell clumping followed by the addition of HBSS

and 70% ethanol [final concentration - 20% FBS and 40% ethanol]. The cell pellet was stored in FBS/HBSS/ethanol at 4°C for a minimum of 1 hour. Fixed BECs to be analyzed only for DNA distribution were spun at 500 X G at 10° C for 10 minutes. The supernatant fluid was decanted, and the cell pellet was resuspended in propidium iodide [PI] stain (Telford et al, 1991) in phosphate-buffered saline [PBS] containing EDTA and RNAse A. Triton X-100, a cell permeant, was eliminated from the original stain mixture (Telford et al, 1991) as it caused excessive clumping of cells. Cells were incubated for a minimum of 30 minutes at room temperature in the dark prior to analysis. Unfixed chicken red blood cells [cRBCs] were lysed to isolate cell nuclei (Pollock, 1990) and stained with propidium iodide as above. Labeled cRBC nuclei, used to standardize the measurement of DNA content, were added to stained BEC samples (Vindelφv and Christensen, 1990). Additional steps required for the preparation of BECs exposed to BrdU for kinetic analysis are described [see below].

Flow Cytometric Analysis: Fluoroscein isothiocyanate-conjugated antibromodeoxyuridine [FITC-antiBrdU]- and/or PI-fixed and stained cells were analyzed using a Becton Dickinson FACS Vantage [Becton Dickinson Immunocytometry Systems, San Jose, CA] equipped with an argon laser, pulse processing circuitry and a Consort 32 computer system with Lysis II software.

FITC and PI were excited at 488 nm, and their fluorescent emissions were quantified at 530±15 and 630±11 nm, respectively. Electronic color compensation was used to correct for spectral overlap of PI in the FITC detection channel using single color-stained controls. PI fluorescence data, a measure of DNA content, were collected from 5,000-10,000 single cells through a doublet discrimination DNA fluorescence gate. Negative controls used to calibrate the FACS included BECs not exposed to BrdU but stained with FITC-conjugated antiBrdU [FITC negative] and unstained BECs [PI negative]. Additional treatment groups were analyzed for FITC-antiBrdU, indicative of BrdU incorporation, and PI, both used to identify cells labeled during S-phase as these cells progressed through the cell cycle. In selected experiments, BECs from gated populations were sorted onto microscope slides and examined for the presence of cell aggregates that might be detected as a single event by FACS analysis. Doublets or higher order aggregates were not apparent in any of the gated regions examined.

Measurement of Total DNA and Analysis of Cell Cycle Data: From DNA histograms of PI fluorescence in untreated, cycling BECs spiked with PI-stained cRBCs, the peaks corresponding to cRBC nuclei [approximately 0.3n mammalian DNA; Vindelφv and Christensen, 1990], G_0-G_1 [diploid or 2n DNA] and G_2-M [tetraploid or 4n DNA] populations of cells were identified. The median

fluorescence intensity of each of these three peaks was defined as the channel containing the greatest number of events. The width of each peak measured in channels was determined at the baseline [X-axis]. The channel positions of the G_0-G_1 and G_2-M peaks were normalized to the cRBC nuclei by calculating the ratios of G_0-G_1/cRBC and G_2-M/cRBC. The average width of the G_0-G_1 and of the G_2-M peaks was normalized in a similar manner. S phase was defined by the area under the curve between the G_0-G_1 and G_2-M distributions, which were assumed to be Gaussian. The resulting ratios between G_0-G_1/cRBC and G_2-M/cRBC and the calculated range comprising S-phase were applied subsequently to treated BEC samples containing cRBC nuclei and analyzed by computer using the Modfit software program [version 5.2, Verity Software House, Inc., Topsham, ME]. The assignment to specific cycle phases was accomplished by applying a "best fit" mathematical model [non-linear, least-squares analysis] to each data set, incorporating defined ratios [see above]. Each data set consisted of 3-4 replicates, each of which comprised cells from different passages or from different cell lines.

Correctness of fit to the model was defined by a Chi-square value for each data set. Data that fit appropriately to the model had a Chi-square value of 1-3 [Modfit Operations Manual], and values greater than 3 were excluded from the comparison.

Identification of BrdU-Containing Cells: Synchronized BECs to be evaluated for cycle kinetic changes were collected and fixed as described above. An FITC-conjugated anti-BrdU immunoglobulin [Becton Dickinson, San Jose, CA] was used to identify cells which had incorporated the thymidine analog, and the manufacturer's protocol for labeling cells was followed with minor modifications. Cells were pelleted by centrifugation [500 X G at 10°C for 10 minutes] between treatment steps. Briefly, fixed cells were denatured with hydrochloric acid [2N for 30 minutes, room temperature] followed by neutralization with a 0.1M sodium borate solution. An additional wash was added after neutralization to assure neutral pH conditions for the binding of immunofluorescent antibody. After incubation with FITC-antiBrdU for 30 minutes in HBSS containing 1% BSA [Bayer Corp., Kankakee, IL] and 0.5% Tween-20 [Sigma], cells were pelleted by centrifugation, resuspended in propidium iodide stain mixture and incubated at room temperature, protected from light, for 30-60 minutes.

Evaluation of Cell Cycle Kinetics: BECs pulse-loaded with BrdU were collected, fixed and labeled as described above. DNA histograms of the relative PI fluorescence [DNA content] and contour plots of PI vs FITC fluorescence [ie, BrdU positive and negative cells] were generated simultaneously to define G_0-G_1,

S and G_2-M phases in each plot, as well as to identify the progressive movement of BECs after pulse-labeling. The collection of serial samples over 24 hours after the removal of APH allowed the identification of cycle transition by cells containing BrdU.

Statistical Analysis: Qualitative data which were normally distributed were analyzed by one way analysis of variance [ANOVA] (Steel and Torrie, 1980). All data expressed as percentages were arcsin square root transformed and analyzed by ANOVA. Multiple comparisons were made using Student-Newman-Keuls method (Steel and Torrie, 1980). When the homogeneity of variance test failed, data were analyzed by the Kruskal-Wallis One Way ANOVA and comparisons between groups made by Dunn's method. Statistical significance was defined as a $p < 0.05$.

Results

Data Presentation: For orientation purposes, representative plots of cell cycle and kinetics data are shown. Cell cycle data are represented as histograms with the DNA content of cells on the X-axis [PI fluorescence] and cell number on the Y-axis [Figure 8]. The X-axis labels indicating G_1, S, and G_2-M phases are derived from the analysis of populations of untreated, cycling BECs

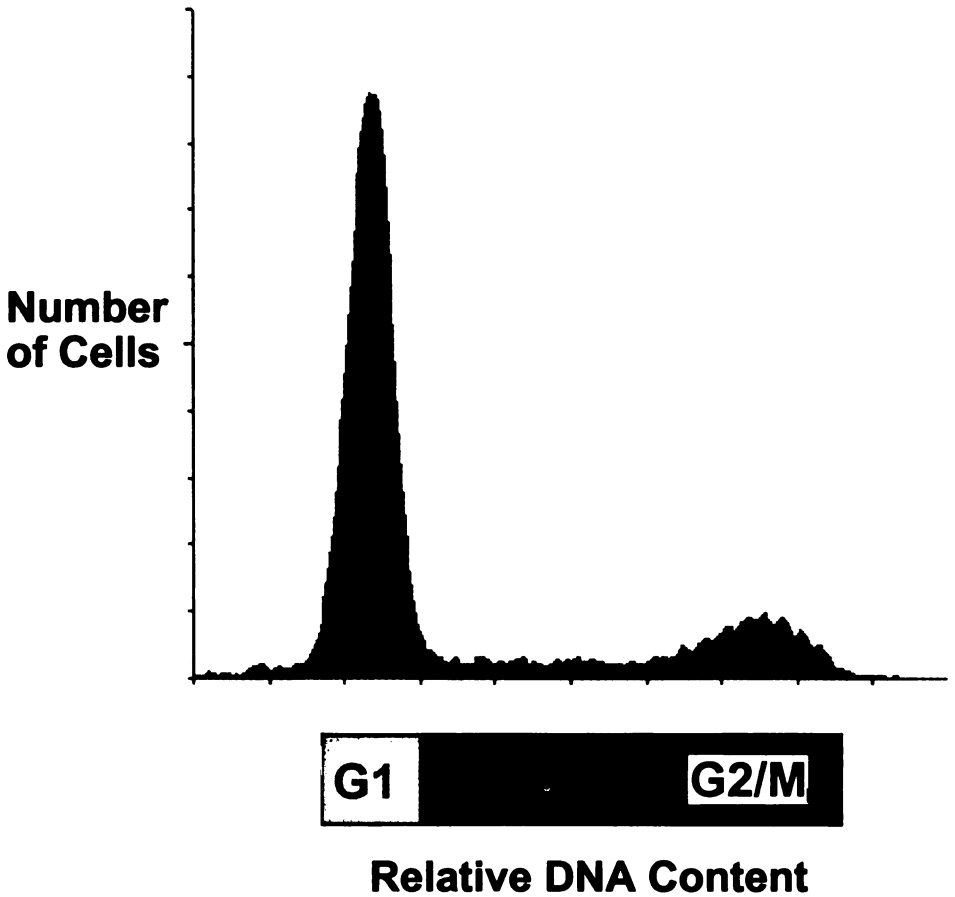

Figure 8. Cell cycle phase distributions.

The X-axis delfines the cell cycle phases determined by the propidium iodide [PI] fluorescence. The intensity of PI fluorescence corresponds directly to the DNA content of the nucleus. The Y-axis is the number of cells counted.

as described in the Materials and Methods. Data showing the cell cycle kinetic patterns by the distribution of cells which had synthesized DNA [cycled through S phase] during the BrdU pulse [at 1-1.5 hours after APH removal] are plotted as contours with the X-axis indicating DNA content [PI fluorescence] and the Y-axis representing the relative incorporation of BrdU [Figure 9]. The Y-axis labels indicating BrdU positive cells delimit that proportion of the population containing BrdU:FITC fluorescence at levels above background.

Unsynchronized BECs: Cell Cycle Pattern: The progression of the cell cycle for the initial 24 hours after BECs were passed from a confluent state is shown in Figure 10. Cells retained a confluent pattern for approximately 16 hours after passage. By 24 hours, a contingent of cells began to move into S phase, indicating the resumption of cell cycling. The DNA distribution patterns of cells collected at 26, 30, 34 and 38 hours after passage represent the distribution of BECs present at 0, 4, 8 and 12 hours of treatment with MCTP or vehicle.

Cell Synchronization with Aphidicolin: [Figure 11] BECs in log phase growth that were exposed to APH for 24 hours arrested at the G_1-S interface, which was maintained for at least 1 hour after APH removal. Replacement with APH-free medium resulted in the progression of cells into S phase at 1.5 hours, to mid S by 4 hours, G_2-M by 8 hours and through M to G_0-G_1 by 12 hours. By

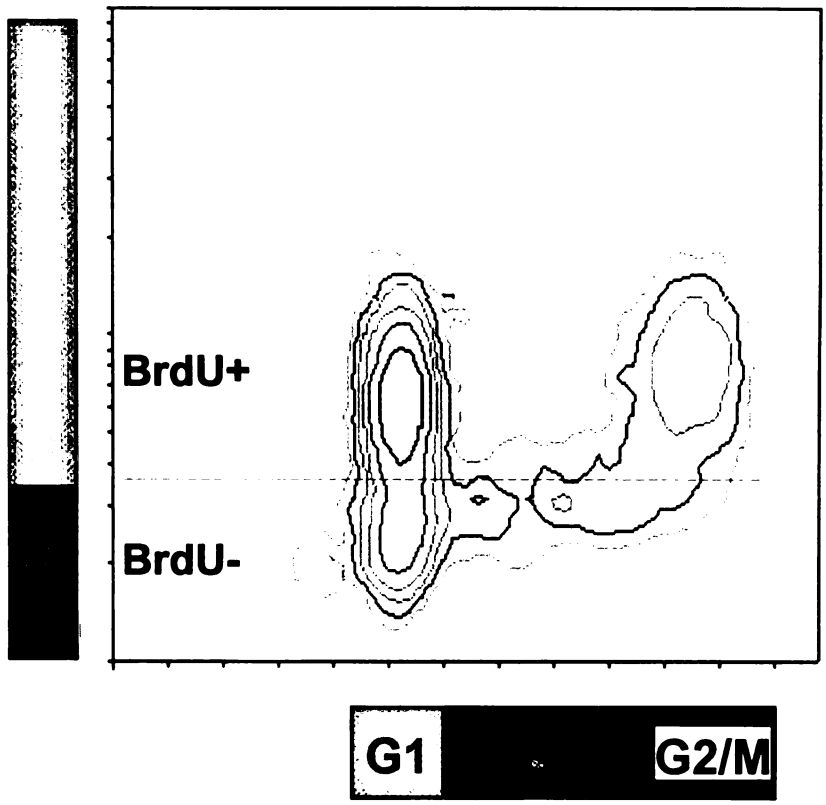

Figure 9. BrdU Incorporation.

The X-axis constitutes the cell cycle phases [see Figure 8] based on the relative intensity of PI fluorescence. The Y-axis differentiates the proportion of cells within the population which have incorporated BrdU during S phase [DNA synthesis].

Figure 10. Cell cycle progression of unsynchronized BECs.

Confluent BECs were disassociated with trypsin/EDTA and replated at a subconfluent density. Cell samples were collected at the intervals indicated, fixed, stained with propidium iodide [PI] and the DNA quantified by fluorescence activated cell sorting [FACS] analysis. DNA histograms collected at 26, 30, 34, and 38 hours show the pattern of DNA distribution during each treatment interval [see Materials and Methods]. The X-axis is the PI fluorescent intensity [DNA content] which defines the cell cycle phases. The Y-axis is the number of cells counted.

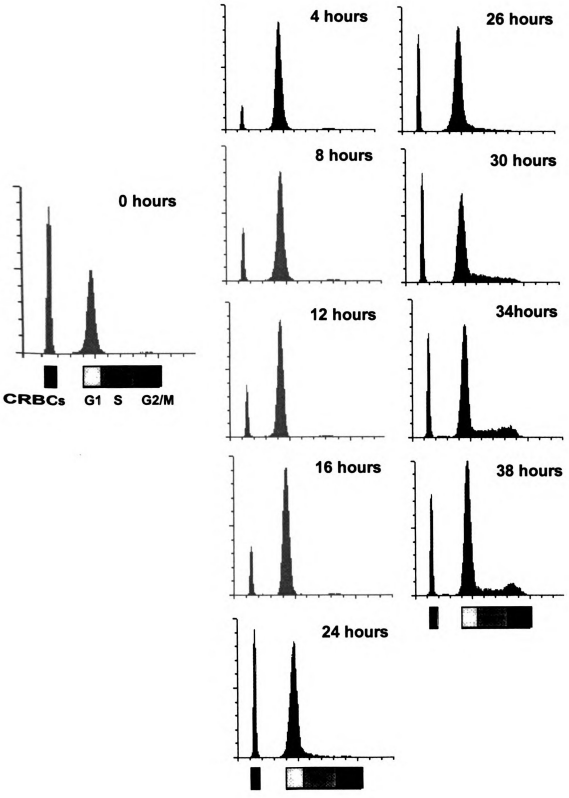
0 hours
4 hours
26 hours
8 hours
30 hours
12 hours
34hours
16 hours
38 hours
24 hours
CRBCs
G1
S
G2/M

Figure 10.

Figure 11. Cell cycle progression of synchronized BECs.

BECs were exposed to APH for 24 hours to synchronize cells at the G_1-S interface. Cells were collected at the times indicated after APH removal, fixed [see Materials and Methods] and stained with PI. The X-axis is the DNA content based on the PI fluorescence. The shaded boxes reflect the cell cycle phases. The Y-axis is the number of cells counted.

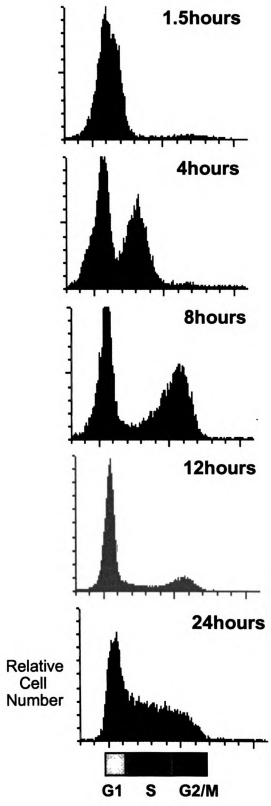
1.5hours
4hours
8hours
12hours
24hours
Relative
Cell
Number
G1
S
G2/M

Figure 11.

24 hours, cells had become asynchronous with many cells in G_1 through late S phases. The predominant cell phases present in synchronized BECs between 0-4 hours, 4-8 hours, and 8-12 hours after release from APH block were G_1-mid S, mid S-G_2, and G_2-through mitosis, respectively [Figure 11].

The time required for completion of a single cell cycle after release from APH block was approximately 21 hours. Cell cycle progression was not affected by APH vehicle [0.2% ethanol - final concentration].

Cytotoxicity: Exposure of BECs to vehicle or to MCTP at 5 µg/ml for 4 hours caused no significant LDH release by 24 hours [data not shown]. This result confirmed data previously reported (Reindel and Roth, 1991). Cells exposed to APH at doses sufficient to induce synchronization caused no increase in LDH release compared to controls at 24, 48 or 72 hours [data not shown].

MCTP-Induced Cell Cycle Arrest: BECs were exposed to MCTP or vehicle from 0-4, 4-8 or 8-12 hours after the removal of APH or its vehicle. These 4 hour exposure intervals were chosen based on the APH studies described above as representing cells predominantly in G1-early S, mid S-G_2 and G_2 through mitosis, respectively.

Unsynchronized BECs treated with vehicle [DMF] for 4 hour intervals corresponding to the preparation and treatment schedule for APH synchronized BECs [see Materials and Methods] continued to cycle and had DNA distribution in all cycle phases [Figure 12A, C or E]. The cell cycle pattern of unsynchronized cells exposed to MCTP for corresponding 4 hour increments consisted of a greater percent of cells in S phase and fewer cells in G_1 [Figure 12B, D or F] compared to their respective controls. There was no difference in the cycle phase distribution pattern of unsynchronized, vehicle-treated BECs across the three exposure intervals, nor was there a difference in MCTP-treated cells similarly analyzed [Figure 13].

Synchronized cells treated with vehicle from 0-4 hours, 4-8 hours or 8-12 hours after APH removal, and evaluated at 24 hours had an asynchronous cell cycle pattern [Figure 14A, C, or E]. By 24 hours after APH removal, synchronized cells treated with MCTP for the initial 4 hour interval [0-4 hours] became inhibited at G2-M [Figure 14B]. A proportion of the cells had greater fluorescence than that predicted for G2-M cells [ie, > G2-M], consistent with a hypertetraploid DNA content [Figure 14B]. Conversely, synchronized cells treated with MCTP for 4 hours starting at 4 or 8 hours after release from APH accumulated in late S phase at 24 hours [Figure 14D and F, respectively].

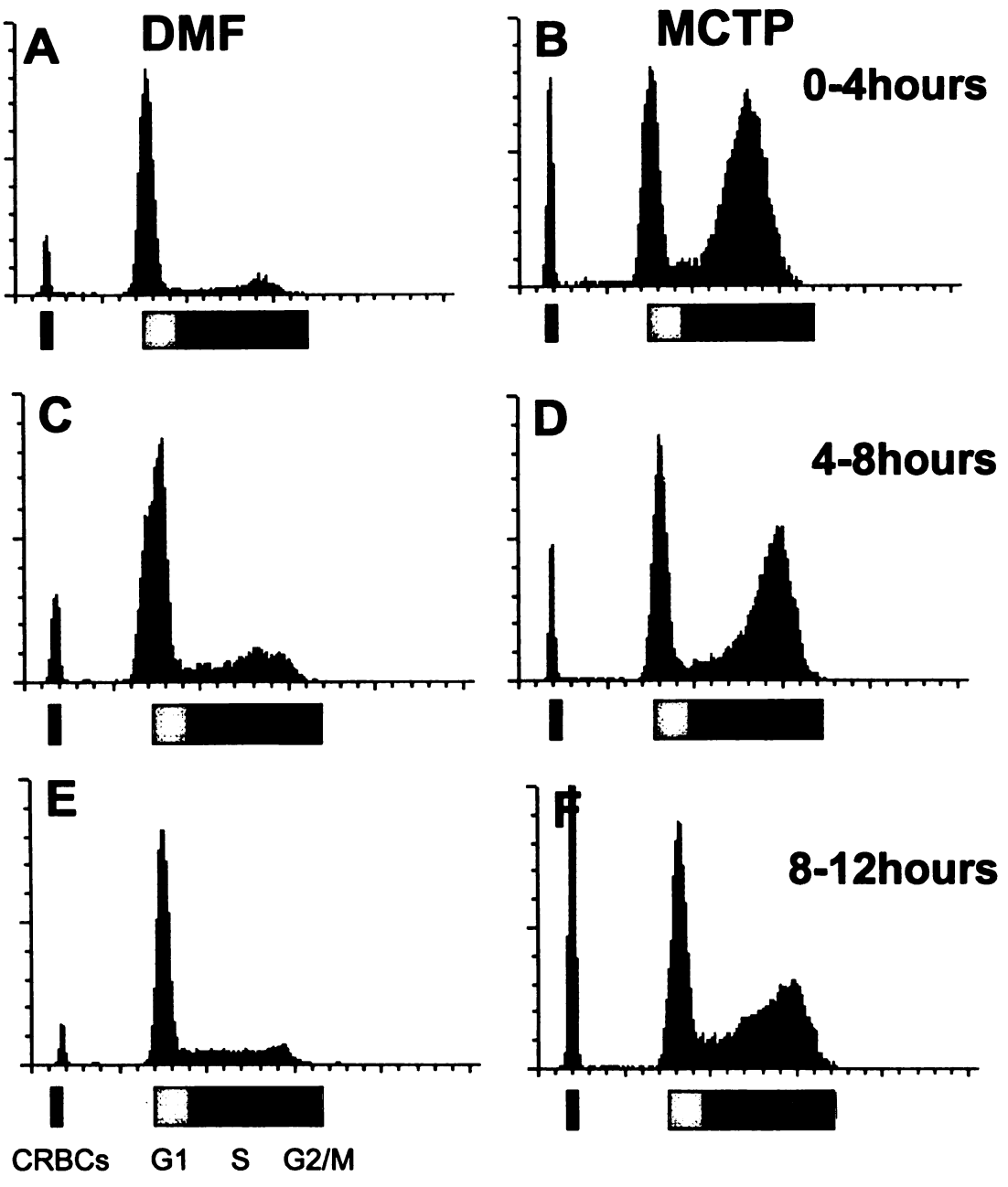

Figure 12. Cell cycle pattern in unsynchronized BECs exposed to vehicle or MCTP.

BECs were treated with vehicle [A, C, or E] or MCTP [B, D, or F]. The exposure intervals corresponded to those used for synchronized cells [see Materials and Methods]. The X-axis is the measure of DNA content based on propidium iodide [PI] fluorescence [see Figure 8]. Chicken red blood cells [cRBCs] were added to each sample as a DNA standard [see Materials and Methods]. The Y-axis represents the number of cells counted.

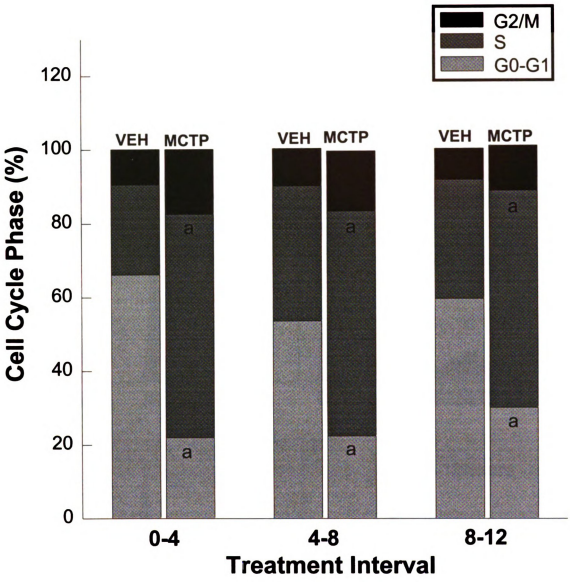

Figure 13. Cell cycle phase distribution in unsynchronized BECs. treated with vehicle or MCTP.

Confluent BECs were disassociated and passed into wells at a subconfluent density. For 4 hour intervals starting 26, 30 or 34 hours after passage, the cells were exposed to MCTP or its vehicle. Cells were collected 24 hours after the start of the initial exposure interval [0-4 hours - see Materials and Methods]. The results represent the of three replicates using cells of different lineage.

The error mean square = 0.01

a = different from respective vehicle control; $p < 0.05$.

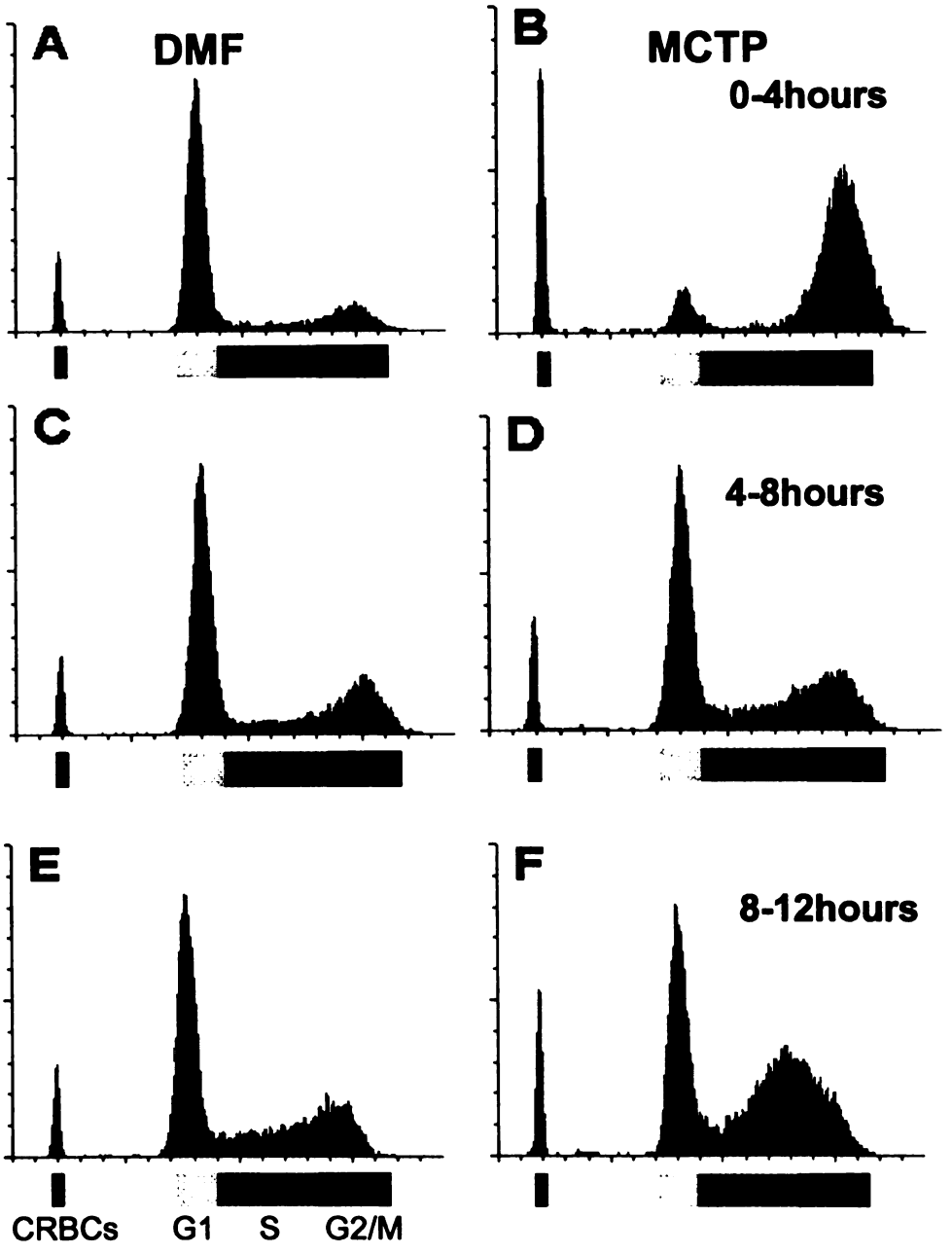

Figure 14. Cell cycle pattern in synchronized BECs exposed to vehicle or MCTP.

The plots represent BECs 24 hours after removal of APH and the subsequent exposure to vehicle [A, C, or E] or MCTP [B, D, or F]. The exposure intervals were from 0-4 hours [A and B], 4-8 hours [C and D] or 8-12 hours [E and F] after the removal of APH. The X-axis delimits the DNA content of cRBCs [a DNA standard] or the cell cycle phases [G1, S, or G2/M]. The Y-axis is the number of cells counted.

MCTP-Induced Changes in Cell Cycle Phase Distribution: Twenty four hours after release from APH, the cell cycle phase distribution of vehicle-treated BECs consisted of a predominence of G_1 and S cells, similar to that of synchronized, untreated cells. Compared to vehicle-treated cells, synchronized BECs exposed to MCTP from 0-4 hours after removal of APH had a large increase in the fraction of cells in G_2-M and a corresponding decrease in G_0-G_1 cells with no significant change in S phase cells [Figure 15]. In contrast, BECs treated with MCTP at 4-8 or 8-12 hours after the resumption of cell cycling had an increase in the proportion of cells in S phase with a corresponding decrease in G_0-G_1 phase cells [Figure 15].

Cell Cycle Kinetics after Aphidicolin: One hour after the removal of APH, untreated BECs were exposed to BrdU in the medium for 30 minutes, allowing incorporation of BrdU into cells synthesizing DNA during that period. Cells were subsequently collected and processed for FACS identification of BrdU-positive BECs within a cycling cell population. Results are presented in Figure 16; the DNA histograms from samples collected over 24 hours were shown previously in Figure 11 and are included in Figure 16 [A] for orientation. During the 24 hours after APH was removed, synchronized cells which had incorporated BrdU [BrdU+] [Figure 16 B] proceded from the G_1-S interface [ie, the APH arrest site] to mid S phase by 4 hours, to G_2-M by 8 hours, into and partially through cell

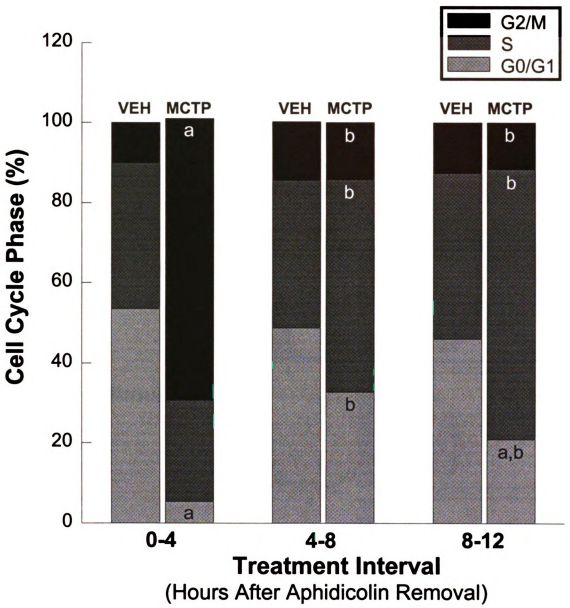

Figure 15. Cell cycle phase distribution in synchronized BECs treated with vehicle or MCTP.

Synchronized BECs were exposed to MCTP or its vehicle from 0-4 hours, 4-8 hours or 8-12 hours after APH removal. Cells were collected 24 hours after APH removal for analysis of the cell cycle pattern. The results represent the mean of three replicates using cells of different lineage.

The error mean square = 0.01

a = different from respective vehicle control; $p < 0.05$.
b = different from MCTP 0-4 hour treatment group; $p < 0.05$.

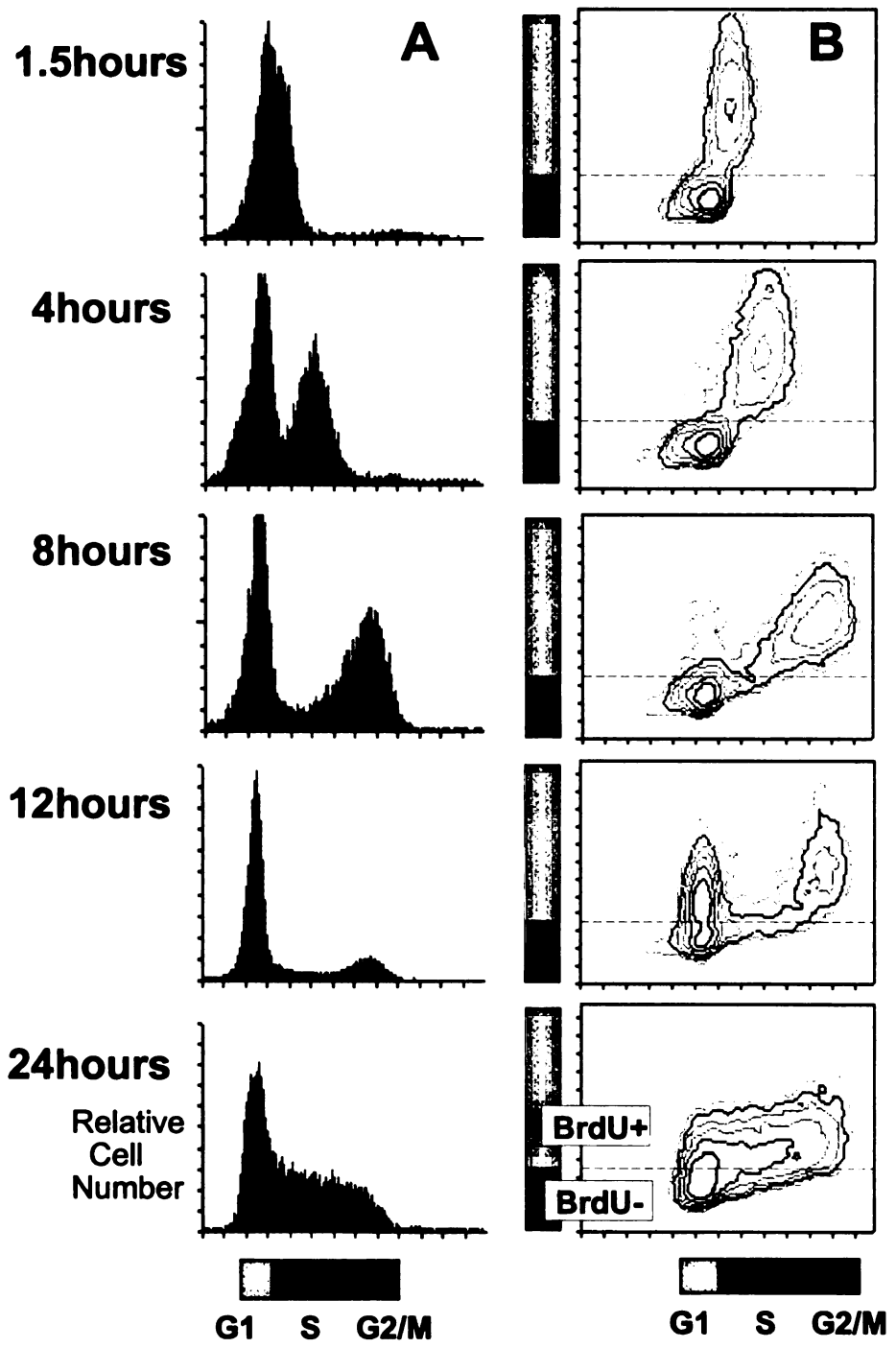

Figure 16. Cell cycle kinetic pattern in untreated, synchronized BECs.

Column A represents DNA distribution histograms of BECs collected at times over 24 hours after the removal of APH. The cell cycle phases are defined by the relative propidium iodide fluorescence as an indicator of DNA content [X-axis]. Column B shows the cycle location of BECs at times over 24 hours which had incorporated bromodeoxyuridine [BrdU+] between 1 and 1.5 hours after APH removal.

division by 12 hours [note at this time the appearance of cells with reduced FITC fluorescence {due to cell division} at the G_1-S interface; Figure 16. 12hours] and well into a subsequent S phase by 24 hours. The changes in percentage of BrdU-labeled cells in G_0-G_1 and G_2-M from 8 to 24 hours [Figure 17] reflect cell division.

In a separate experiment, the percentage of noncycling cells in each treatment group was identified by continuous exposure to BrdU through 24 hours after APH removal. A representative series of contour plots shows the progressive incorporation of BrdU as cells resumed cycling over 24 hours [Figure 18]. The fraction of cells that failed to incorporate BrdU during this 24 hour period ranged from 5-10% for all treatment and control groups.

MCTP-Induced Changes in Cell Cycle Kinetics: Synchronized BECs treated with vehicle [Figure 19A] had a cycle progression pattern similar to that of untreated, synchronized cells [Figure 16]. Synchronized BECs treated with MCTP from 0-4 or 4-8 hours after APH removal [Figure 19B or C, respectively] progressed from G_1-S to G_2-M over a timecourse similar to untreated, synchronized cells [Figure 16] until 12 hours. At 12 hours, BrdU-labeled BECs from both MCTP-treated groups were delayed in G_2-M [ie, fewer cells of reduced FITC fluorescence at the G_1-S interface {Figure 19B, C} compared to vehicle-treated cells {Figure 19A}]. By 24 hours, BrdU-labeled BECs exposed to MCTP

Figure 17. Progression of BrdU+ BECs after removal of APH.

One hour after APH was removed from the medium, cells were pulse labeled with BrdU for 30 minutes. The X-axis is the DNA content of BECs based on the PI fluorescence, reflected by the limits of each cell cycle phase [**G_1, S, G_2/M**]. The Y-axis depicts the incorporation of BrdU. The number values in parentheses represent the percent of cells within G_1 or G_2/M and show the progression of cells to G_2/M by 8 hours * and cell division by 12 hours **.

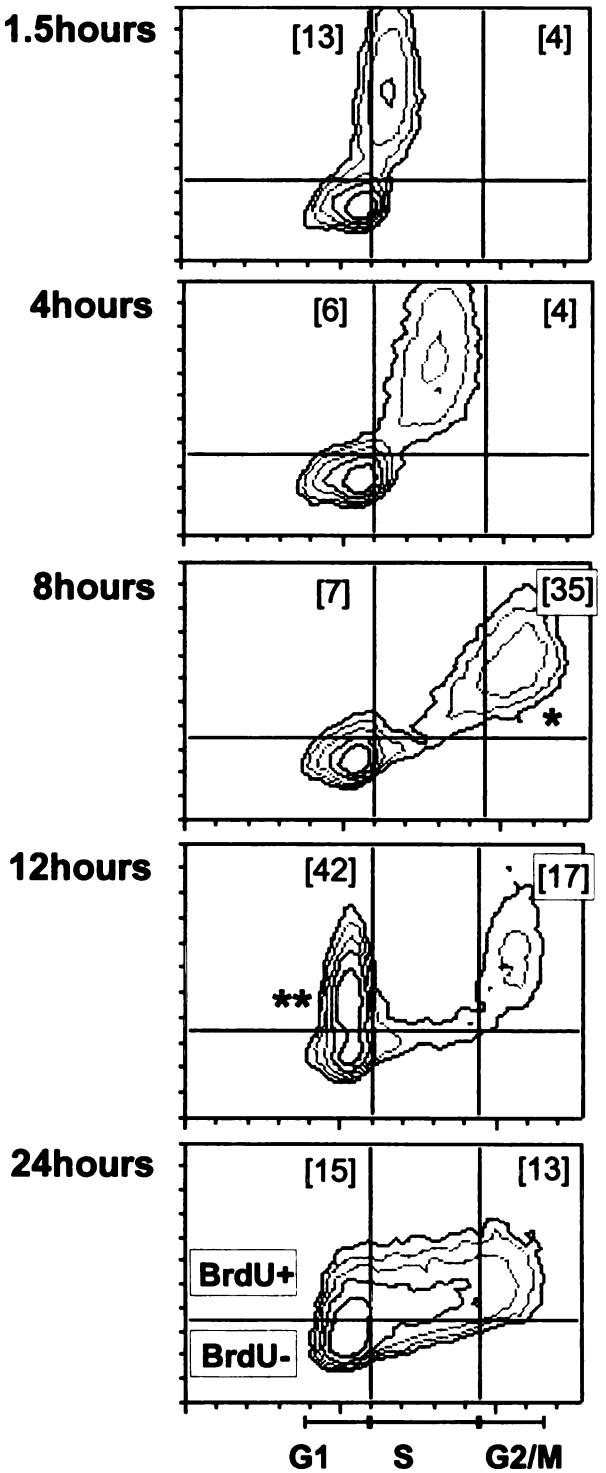
1.5hours
[13]
[4]
4hours
[6]
[4]
8hours
[7]
[35]
*
12hours
[42]
[17]
**
24hours
[15]
[13]
BrdU+
BrdU-
G1
S
G2/M

Figure 17.

Figure 18. Progressive entry of untreated, synchronized BECs into the cell cycle.

BECs were exposed to BrdU for 24 hours starting immediately after removal of APH. Cells were collected at the indicated intervals after APH removal, fixed and labeled with a FITC-labeled antiBrdU to delineate cells which had incorporated BrdU. The numbers in parentheses represent the percent of BrdU+ and BrdU- cells in **G_1, S and G_2/M** at each time point. The data presented were representative of vehicle- and MCTP-treated cell groups.

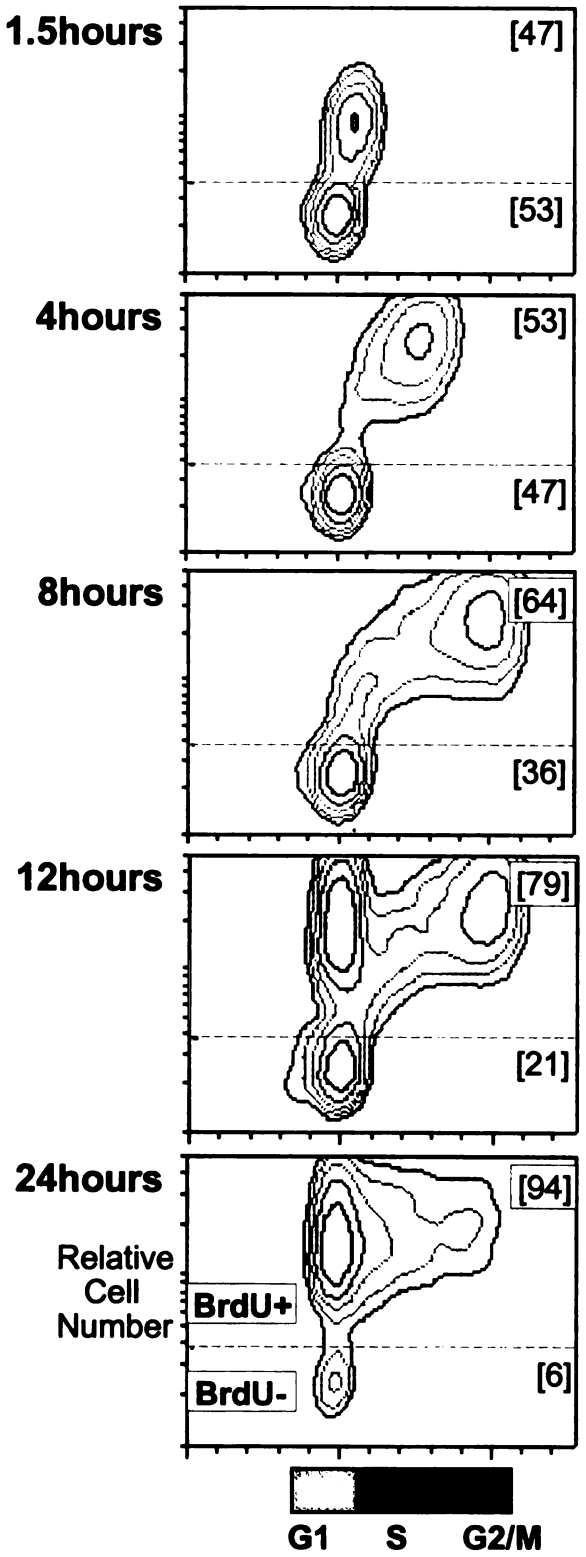
1.5hours
[47]
[53]
4hours
[53]
[47]
8hours
[64]
[36]
12hours
[79]
[21]
24hours
[94]
Relative
Cell
Number
BrdU+
BrdU-
[6]
G1
S
G2/M

Figure 18.

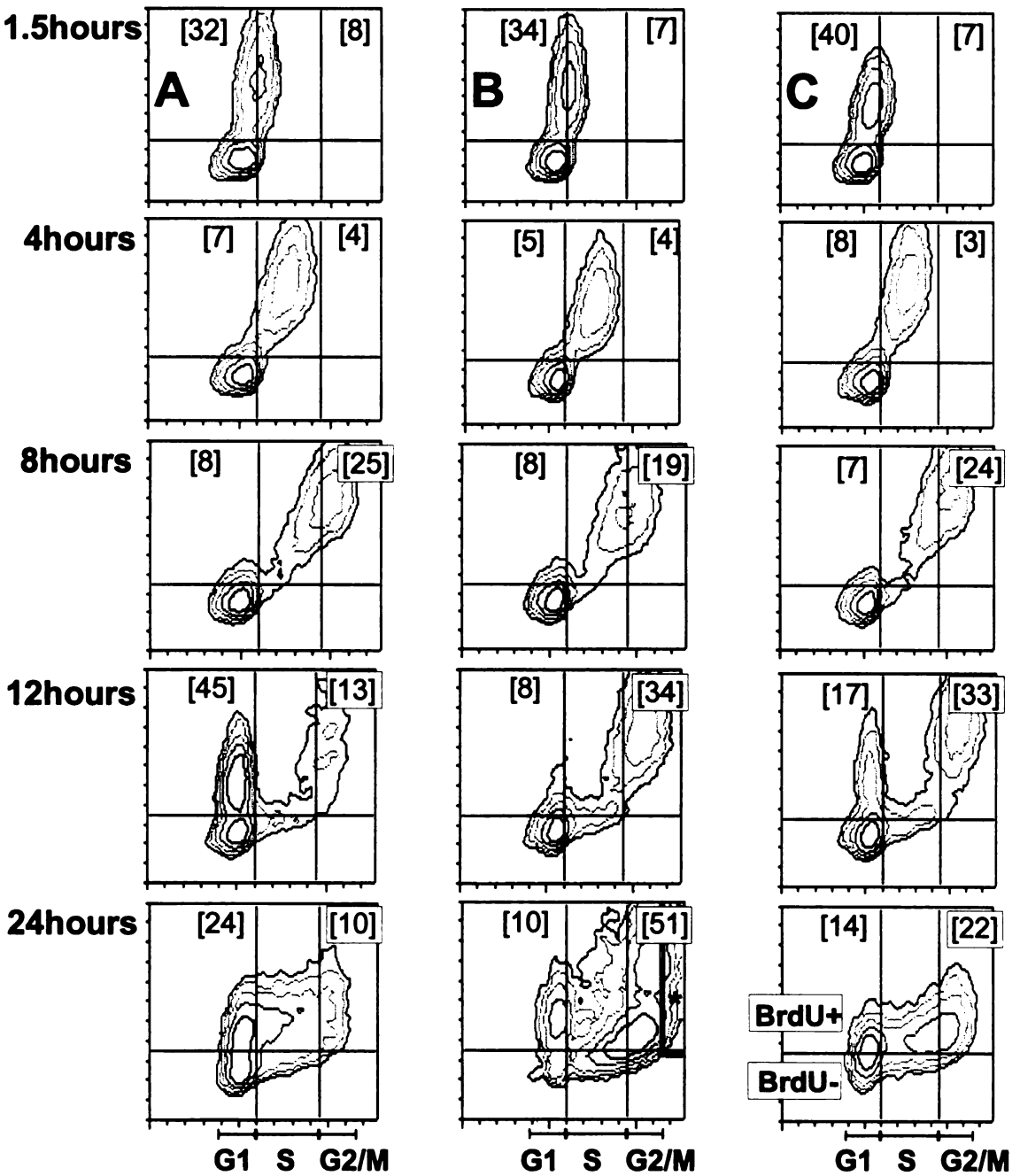

Figure 19. Cell cycle kinetic pattern after exposure of synchronized BECs to vehicle or MCTP.

BECs were treated with [A] vehicle from 0-4 hours, [B] MCTP from 0-4 hours or [C] MCTP from 4-8 hours after APH removal. The axes labels are as described in Figure 9. Column B [24 hours] - [*] Cells emitting PI fluorescence greater than that expected from normal G2/M cells, suggesting hypertetraploid cells. *Number values in parentheses* indicate the percent of cells within a specific cycle phase labeled with BrdU [BrdU+].

from 0-4 hours after APH removal accumulated in G_2-M with very few undergoing cell division through 24 hours [Figure 19B], whereas cells exposed to MCTP from 4-8 hours [Figure 19C] entered and completed mitosis between 12 and 24 hours. The change in the relative percent of cells in G_0-G_1 and G_2-M between 1.5 and 24 hours in vehicle- and MCTP-treated BECs are noted [%] [Figure 19]. In BECs exposed to MCTP from 0-4 hours after APH removal, 5-11% of the cells registered a PI fluorescence emission greater than the predicted range for G_2-M cells [Figure 19B, 24 hours], suggesting a population of BECs with a DNA content greater than 4n. At 24 hours, both MCTP treatment groups had cell fractions of low BrdU content at the junction of S and G_2-M [# in Figures 20B and 21B, 24 hours]. Synchronized BECs treated with MCTP from 8-12 hours had a cycle progression pattern similar to that of cells treated from 4-8 hours.

Discussion

MCTP administered intravenously to rats causes a limited, but continuous loss of endothelial cells which is accompanied by progressive pulmonary vascular leak (Reindel et al, 1990). The mechanism of increased vascular permeability is not fully understood, but it is thought to reflect the protracted loss of or damage to cells from the endothelial monolayer. *In vitro*, BEC cultures treated with MCTP have a similar degree of cell loss, but subsequent reformation

Figure 20. Effect of MCTP exposure [0-4 hours after APH removal] on the cell cycle kinetic pattern.

BECs were synchronized for 24 hours with APH. Upon removal of APH, cells were exposed to MCTP. BrdU was added to the medium for 30 minutes [1 hour after APH removal]. Column A represents the change in DNA distribution over time and column B shows the cycle progression of BECs which had incorporated BrdU. Comparable DNA histograms [column A] and contour plots [column B] of untreated, synchronized BECs are shown in Figures 11 and 17, respectively.

= BECs arrested in G2/M which had incorporated little or no BrdU.

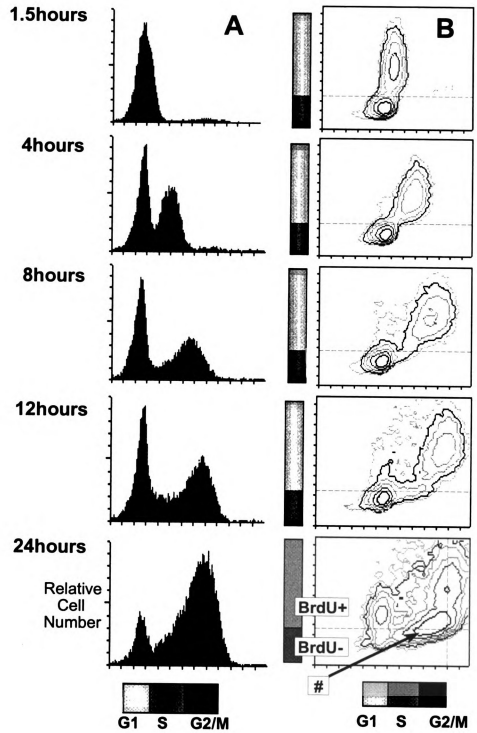
1.5hours
4hours
8hours
12hours
24hours
A
B
Relative
Cell
Number
BrdU+
BrdU-
#
G1 S G2/M
G1 S G2/M

Figure 20.

Figure 21. Effect of MCTP exposure [4-8 hours after APH removal] on the cell cycle kinetic pattern.

BECs were synchronized for 24 hours with APH. Four hours after removal of APH, cells were exposed to MCTP. BrdU was added to the medium for 30 minutes [1 hour after APH removal]. Column A represents the change in DNA distribution over time and column B shows the cycle progression of BECs which had incorporated BrdU. Comparable DNA histograms [column A] and contour plots [column B] of untreated, synchronized BECs are shown in Figures 11 and 17, respectively.

= BECs arrested in G2/M which had incorporated little or no BrdU.

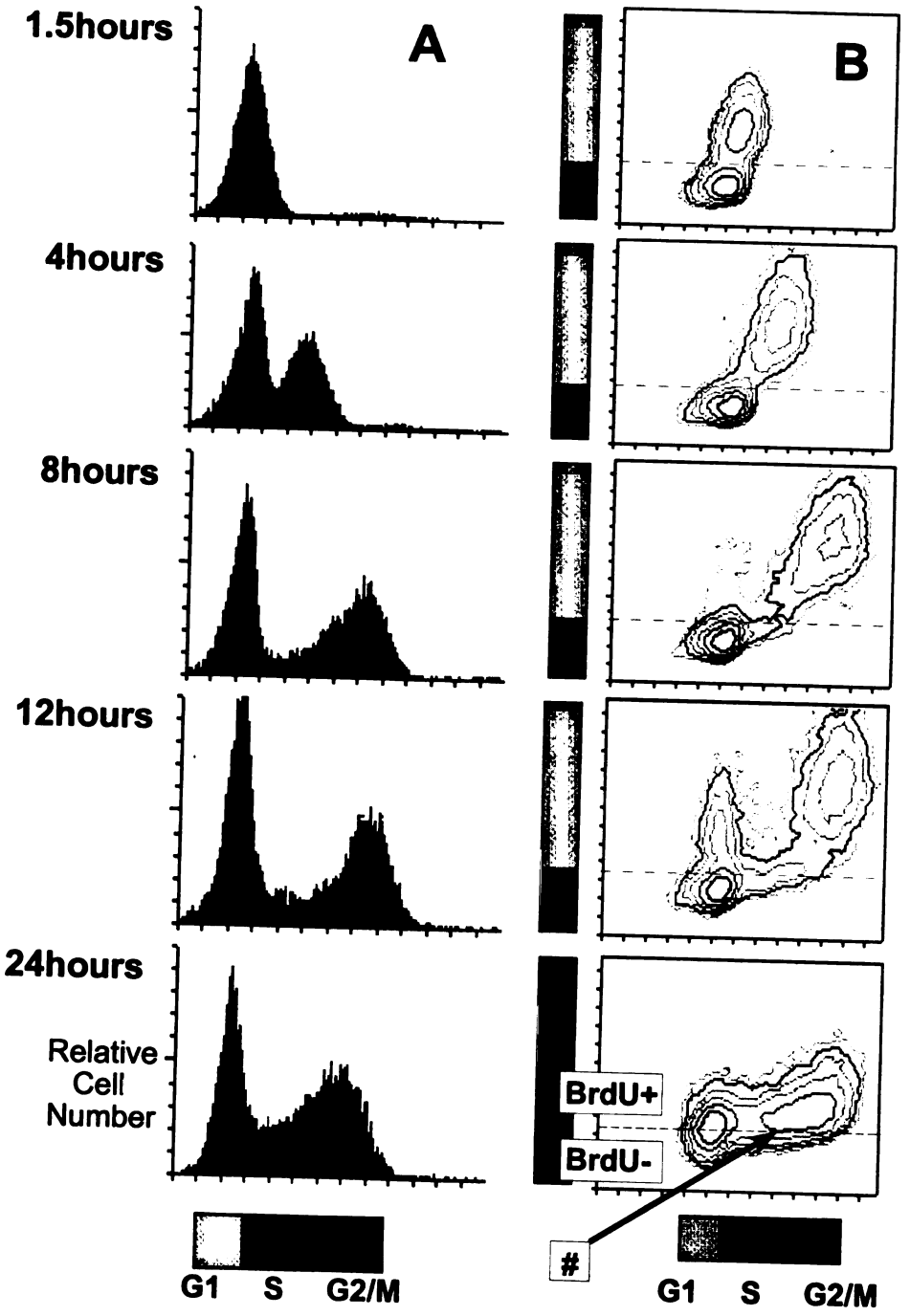
1.5hours
A
B
4hours
8hours
12hours
24hours
Relative Cell Number
BrdU+
BrdU-
#
G1
S
G2/M
G1
S
G2/M

Figure 21.

of a confluent monolayer does not occur at nominal MCTP concentrations greater than 1.5μM due to inhibition of cell proliferation (Reindel et al, 1991). Others have shown that MCTP causes cell cycle inhibition in a pattern which varies as the concentration of MCTP applied to the cells changes (Thomas et al, 1996). The pulmonary vascular endothelial cell injury seen after the administration of MCTP to rats may be compounded by cell cycle arrest and inhibition of proliferation, resulting in a deficient repair response and vascular leak that is protracted and progressive.

Exactly how MCTP causes inhibition of mitosis is unclear, but its ability to bind to cellular macromolecules suggests that its interference with an essential cellular function or structure may be involved. MCTP is a bifunctional alkylating agent, capable of crosslinking DNA and protein (Petry et al, 1984; Wagner et al, 1993), an attribute which suggests that it may arrest cell cycle progression by interfering nonspecifically with a process common to more than one cycle phase [eg, protein or DNA synthesis]. Previous studies have used extended exposure intervals [24 hours or longer], potentially involving and interfering with all cycle phases (Reindel and Roth, 1991; Reindel et al, 1991; Thomas et al, 1996). We proposed that cell cycle inhibition was due to a phase-specific event and tested this hypothesis by limiting the exposure of BECs to MCTP to 4-hour intervals corresponding to different parts of the cell cycle and therefore to different phase-specific events. Cell cycle inhibition due to a phase-independent event should

occur irrespective of the timing of the MCTP exposure. In contrast, the interaction of MCTP with a phase-specific process should result in a unique pattern of cell cycle progression or inhibition depending on the phase of the cycle during which cells were exposed.

Preliminary studies characterized the transition of synchronized cells through the cell cycle during the 24 hours after APH removal [Figures 11 and 16]. This allowed the delineation of cell cycle phases which would be impacted during each of three, 4-hour MCTP exposure intervals. Although APH uniformly inhibited cycle progression at the G_1-S interface, not all of the cells moved synchronously into and through S, G_2 and M phases after APH removal [Figures 11 and 16]. The lack of 100% synchronous cycling after APH removal suggested a noncycling cell fraction or incomplete synchronization. The true fraction of cycling BECs after APH was determined by continous 24 hour exposure to BrdU after APH removal. Over that 24 hour period, the proportion of BrdU negative cells remaining in G_0-G_1 gradually decreased; 90-95% of BECs had traversed at least a portion of S phase by 24 hours [Figure 18], consistent with passage out of G_1 and incomplete synchronization. Although the method of reversible cell cycle arrest used in the present work failed to synchronize 100% of exposed BECs, it provided a synchronous, cycling population of BECs [50%] to allow the evaluation of the phase-specific effects of MCTP.

Unsynchronized BECs treated with MCTP accumulated in S and G2/M at the time of examination [see Materials and Methods] regardless of the exposure intervals [Figure 12B,D, and F]. Synchronized BECs treated with MCTP during late G_1 to mid S phase were arrested at G_2-M by 24 hours and exhibited mitotic inhibition [Figure 19B]. In addition, a fraction of cells [6-10%] in that group were hypertetraploid. In contrast, synchronized cells treated from mid S through mid G_2, or mid G_2 through mitosis were transiently delayed in G_2-M at 12 hours but proceeded through mitosis to G_1 by 24 hours [Figure 19C represents the pattern seen with MCTP exposure from 4-8 or 8-12 hours after APH removal]. A portion of synchronized BECs exposed to MCTP from 0-4 hours or 4-8 hours after APH removal were located near the level of detection of FITC-BrdU positivity at the S-G_2 interface at 24 hours [# in Figure 20B and 21B]. The incomplete synchronization of BECs with APH and gradual entry of remaining nonsynchronous G_1 cells into S phase suggests that these cells at the S-G_2 interface are ones which incorporated a small amount of BrdU in early S phase but were delayed in their transit through S phase to G_2-M. In addition, G_1 cells which resumed cycling during MCTP exposure [either 0-4 hours or 4-8 hours] but after the BrdU pulse could contribute to this fraction.

These results confirmed that the exposure of BECs to MCTP for 4 hours results in cell cycle inhibition, and that the pattern of inhibition was phase-specific. In all MCTP exposure groups there was cell cycle delay as cells

entered G_2-M, but arrest and inhibition of mitosis only occurred when BECs were exposed from late G_1 to mid S phase. Furthermore, this arrest of BECs prior to mitosis did not halt DNA synthesis, suggesting a disconnection of these two events, possibly through the disruption of the G_2-M checkpoint (Hartwell and Weinert, 1989; Kaufmann and Paules, 1996).

The pattern of cell cycle inhibition and mitotic arrest described above suggests that MCTP disrupts a cell process initiated during G_1-mid S but not expressed until G_2-M. By contrast, cells exposed to MCTP after G_1-mid S did not demonstrate inhibition of mitosis [Figure 15C]. The G_1-S phases of the cell cycle include steps required in the preparation for and initiation of DNA replication (reviewed in Alberts et al, 1989; Pardee, 1989). Phosphorylation events late in G_1 result in the production or activation of enzymes necessary for DNA synthesis [ie, thymidine kinase, ribonucleotide reductase; (Pardee, 1989)], as well as proteins which are required later in the cell cycle [ie, cyclins; (Reddy, 1994)]. Protein synthesis is markedly reduced in cells deprived of isoleucine and affected cells arrest in G_1 (Bhuyan and Groppi, 1989). Likewise, the absence of a specific protein[s] required for DNA synthesis can cause G_1 or S phase arrest (Bhuyan and Groppi, 1989). Previous work has shown that MCTP-treated pulmonary artery endothelial cells maintain normal to elevated protein and DNA synthesis for up to 7 days after exposure (Hoorn and Roth, 1992). In the present study, the exposure of BECs to MCTP during G_1-S did not cause G_1 arrest,

suggesting that the protein requirements for DNA synthesis were met. It is possible, however, that MCTP exposure at this time affects the production of a protein or the replication/transcription of a gene required for the transition from G_2 to M.

Cell cycle arrest at G_2-M may result from preexisting DNA damage or from the interruption of serial processes necessary to prepare the chromatin for separation (Reddy, 1994). The transition from G_2 into M phase is regulated by $p34^{cdc2}$ kinase, the purported 'master control enzyme' (Nurse, 1990; Norbury et al, 1991). This enzyme controls DNA condensation, chromatin cutting and unwinding (decatenation), nuclear membrane dissolution and actions of the mitotic spindle (Datta et al, 1996; Andreassen and Margolis, 1994). The complex scheme of $p34^{cdc2}$ phosphorylation and dephosphorylation, and subsequent binding to cyclin are necessary for the initiation of mitosis and must be completed before the next round of DNA synthesis (Hartwell and Weinert, 1989; Kaufmann and Paules, 1996). A number of diverse agents cause G_2-M arrest with continued DNA synthesis concurrent with the inhibition of $p34^{cdc2}$ kinase. These agents include protein kinase inhibitors (Usui et al, 1991; Matsukawa et al, 1993), topoisomerase II inhibitors (Ishida et al, 1994) and antitumor antibiotics (Takanari and Izutsu, 1983; Nakamura et al, 1989; Kharbanda et al, 1994). The present study clearly identifies phase-dependent G_2-M arrest and inhibition of

mitosis, and the results suggest that continued DNA synthesis leads to hypertetraploidy in BECs treated with MTCP.

Examination of another bifunctional alkylating agent, mitomycin C (MMC), has provided information which may help to direct subsequent studies. MMC is an antitumor antibiotic which is structurally similar to MCTP and is capable of inducing similar morphologic and functional responses in endothelial cells *in vitro* (Hoorn et al, 1995). MMC treatment results in DNA crosslinks and causes dose-dependent inhibition of cell proliferation (Hoorn et al, 1995; Coomber, 1992). It causes G2-M arrest in HL-60 cells by causing phosphorylation of $p34^{cdc2}$, thereby limiting the ability of that enzyme to participate in the induction and completion of mitosis (Kharbanda et al, 1994). As with MCTP, cells exposed to MMC *in vitro* become polyploid (Nakamura et al, 1989; Kharbanda et al, 1994). Additional work is required to determine if MCTP acts by a similar mechanism.

In conclusion, MCTP inhibits cell cycle progression and mitosis *in vitro* in a manner that depends on when during the cycle exposure to MCTP occurs. BECs exposed to MCTP after the middle of S phase continue to cycle and divide, whereas those treated prior to and early in DNA synthesis arrest in G_2-M and are unable to divide. In conjunction with cell cycle arrest at the G_2-M phase, BECs accumulate additional DNA to become hypertetraploid, consistent with the disconnection of DNA synthesis from mitosis. Mitotic arrest and continued DNA synthesis with polyploidy are actions commonly identified with DNA crosslinking

agents, which appear to produce those effects through interference with one or more functional components of the G_2-M checkpoint. The G_2-M effect of MCTP *in vitro* appears to be initiated in late G_1 or early S phase. It is noteworthy that a healthy arterial EC monolayer *in vivo* comprises predominantly G_0-G_1 cells, a distribution similar to that of cells synchronized with APH. Upon exposure to MCTP *in vitro*, cells in this condition were arrested in G_2-M and unable to divide. A similar process of inhibition of endothelial cell proliferation after injury *in vivo* would be expected to limit intimal repair and could underlie the persistent vascular leak that occurs after the administration of MCTP to rats.

Chapter III

PULMONARY VASCULAR ENDOTHELIAL CELL DNA SYNTHESIS AND CELL PROLIFERATION *IN VIVO* AFTER MONOCROTALINE PYRROLE EXPOSURE

Summary of Chapter III

Endothelial cell [EC] injury after monocrotaline pyrrole [MCTP] administration to rats precedes a cascade of events which result in pulmonary hypertension. The application of MCTP to cultured ECs inhibits cell proliferation; a similar process *in vivo* could delay the repair of EC injury and contribute to pulmonary vascular leak. To clarify a role for inhibition of proliferation in MCTP-induced pulmonary vascular disease, EC DNA synthesis and cell replication were examined *in vivo*. Male, Sprague-Dawley rats were treated with a single dose of MCTP [3.5 mg/kg, iv] or its vehicle. The rate of DNA synthesis in arterial ECs, identified by the incorporation of the thymidine analog bromodeoxyuridine [BrdU], as well as changes in EC density, were measured over the next 8 days. BrdU incorporation by arterial ECs increased between days 3-7 in MCTP-treated rats without a subsequent increase in EC density. These data show that MCTP initiates a proliferative stimulus [the upregulation of DNA synthesis], but the anticipated increase in EC number representing cell proliferation does not follow. The data suggest that the mitotic stimulus produced after MCTP administration is insufficient to cause cell proliferation, or conversely, that MCTP inhibits cell proliferation similar to the effect seen *in vitro*. The incomplete stimulation of mitosis or mitotic arrest may result in failure of replicative repair and could contribute to the persistent pulmonary vascular leak characteristic of MCTP-induced lung injury in the rat.

Introduction

When administered at a small doses to rats, the pyrrolizidine alkaloid monocrotaline [MCT], or its toxic metabolite monocrotaline pyrrole [MCTP], causes pulmonary vascular injury resulting in persistently increased microvessel permeability and pulmonary hypertension (Butler, 1970; Meyrick et al, 1980; Reindel et al, 1990). MCTP causes the inhibition of cell proliferation *in vitro* (Reindel and Roth, 1991; Reindel et al, 1991). In chapter II, it was shown that MCTP inhibits cell cycle progression *in vitro* in a phase-specific manner and that the application of this toxicant to BECs during late G_1 or early S phase resulted in mitotic inhibition with continued DNA synthesis. It has been hypothesized that the inhibition of mitosis may contribute to the chronic and progressive nature of liver injury *in vivo* after exposure toxic pyrrolizidine alkaloids (Jago, 1969; Hsu et al, 1973; Samuel and Jago, 1975; Mattocks and Legg, 1980). In the lung, the effect of MCT[P] on vascular endothelial cell replication, and the impact of altered replication on the repair of vascular injury have received little attention (Meyrick and Reid, 1982).

This study was designed to characterize further the antiproliferative action of MCTP on ECs by assessing the effect of this toxicant on DNA synthesis and subsequent cell proliferation by ECs of the pulmonary vasculature *in vivo*. Because quiescent endothelial cells which line pulmonary arteries or veins reside predominantly in G_0-G_1, it was expected that their response to MCTP *in vivo*

would be similar to that seen *in vitro* [exposure in G_1-early S phase results in inhibition of mitosis but continued DNA synthesis - see Chapter II]. Unfortunately, the direct measurement of changes in the cell cycle pattern [as was done in Chapter II] was not technologically possible in microvascular ECs *in situ*.

The correlation of *in vivo* results to those generated by *in vitro* studies is often problematic because isolated and purified cell systems may lack important comtributors necessary for a specific response to occur. The results presented here are interpreted in that light and provide additional support to the hypothesis that the inhibition of cell proliferation is involved in the progressive lesion produced in the rat lung by MCTP.

Materials and Methods

Animals: Male, Sprague-Dawley (CD-Crl:CD$^{(R)}$(SD)BR VAF/PLUS$^{(TM)}$) rats (Charles River Laboratories, Portage, MI) weighing 175-225g were housed 3 to a plastic cage on corncob bedding (The Andersons, Delphi, IN). The cages were contained in animal isolators supplied with HEPA-filtered air. Animals had free access to tap water and pelleted rodent diet (Harlan Teklad 22/5 Rodent Diet 8640, Harlan, Madison, WI) and were maintained in controlled temperature and humidity conditions with a 12 hour light/dark cycle. Animals were allowed 3-5

days minimum to acclimate to conditions in the isolator units before subjected to experimental manipulations.

Preparation of MCTP: Monocrotaline pyrrole was synthesized from monocrotaline as previously described in Chapter II. MCTP was maintained in N, N'-dimethylformamide [DMF] under nitrogen at -20°C and was diluted to working concentrations with DMF immediately before use. The concentration of MCTP used was adjusted to allow accurate dosing at volumes less than 0.2 ml.

Treatment Protocol: On day 0, rats received a single injection of either MCTP [3.5 mg/kg] or an equivalent volume of vehicle [DMF] via the tail vein. Three rats in each treatment group were killed on days 3, 5, 8, and 14 for the evaluation of markers of injury and pulmonary hypertension as previously described (Reindel et al, 1990) or on days 1-8 for histopathology and immunohistochemistry. Rats to be evaluated for DNA synthesis were given 2-bromo-5-deoxyuridine [100 mg/kg, ip BrdU, Sigma Chemical Co., St Louis, MO], to label cells actively synthesizing DNA, at 18, 5 and 2 hours before they were killed (Lanier et al, 1989; Wynford-Thomas and Williams, 1986). Three administrations were used to maximize the differences in DNA labeling between treated and control animals since the cell turnover for ECs is normally very slow (Schwartz and Benditt, 1976). Prior to necropsy, animals were anesthetized with sodium pentobarbital (50 mg/kg, ip) and exsanguinated by severing the

abdominal aorta. A tracheal cannula was secured in all animals (Roth, 1981), and an additional pulmonary arterial cannula was placed (Schultze et al, 1994) in animals used for histologic evaluation. Animals killed for the measurement of biochemical markers of injury were not used for histologic evaluation.

Evaluation of MCTP-Induced Injury: The heart, lungs and mediastinum were removed enbloc and, prior to lavage, blotted dry and weighed. The lungs were lavaged twice with 0.9% sodium chloride solution (23 ml/kg) as previously described (Roth, 1981), and the volumes of bronchoalveolar lavage fluid [BALF] were combined and placed on ice. After lavage, the lung lobes were excised from the trachea by severing the major bronchi. The remaining heart, trachea and mediastinum were then weighed. The lung weight was determined by subtracting the weight of the heart, trachea and mediastinum from the total weight of the original tissue block removed from the thoracic cavity (Schultze et al, 1991).

The lavage fluid was spun at 600 X G for 10 minutes to pellet the cells, and the supernatant fluid was used for quantitation of protein. BALF protein was measured by the method of Lowry et al (1951) using an EL 340 Microplate Bio Kinetics Reader [Bioteck Instruments, Winooski, VT].

Right ventricular hypertrophy was assessed as an increase in the ratio of the right ventricular weight to the weight of the left ventricle and interventricular

septum (RV/(LV+S)) and used as a marker of pulmonary hypertension (Fulton et al, 1952).

Histopatholgic Evaluation and Immunohistochemistry: A 0.5 cm length of duodenum was harvested from each rat, fixed in Histochoice [a noncrosslinking tissue fixative; Amresco, Solon, OH], and used as a positive control for BrdU immunohistochemistry. Rat lungs were removed from the thorax, and the pulmonary vasculature was perfused with 0.9% NaCl for 10 minutes to remove blood while the lungs were inflated and deflated gently with room air. After perfusion, the lungs were infused with Histochoice through both the tracheal and pulmonary arterial cannulae. Constant-pressure fixative perfusion of the vasculature was done to distend arteries uniformly. The infusion pressures of fixative were maintained at 28 and 40 cm of water through the tracheal and pulmonary arterial cannulae, respectively, modified from the technique previously described (Reindel et al, 1990). Infusion was continued for 2 hours, at which time the trachea was ligated, and the fixative-inflated lungs were immersed in Histochoice for an additional 24-36 hours. Sections of the midportion of each of 3 lobes [1 section of lung from each of the left, right anterior and right posterior lobes] from each rat were excised perpendicular to the mainstem bronchus and embedded in paraffin. Tissue sections were stained with hematoxylin and eosin for routine histologic evaluation and for elastin by the Verhoeff-Van Gieson method.

Additional sections of lung [from 3 lobes per rat] and duodenum were prepared for immunohistochemical examination with a mouse-derived monoclonal antibody to BrdU [Becton Dickenson, San Jose, CA] using an automated immunostainer [Leica Histostainer Ig, Leica, Inc., Deerfield, IL]. Briefly, paraffin sections were cleared with xylene, rehydrated, and treated to remove endogenous alkaline phosphatase. Sections were proteinase-digested and then denatured in 2N HCl. After rinsing with Tris-buffered saline [TBS] and drying, the sections were covered with normal horse serum [Vector Laboratories, Burlingame, CA], followed by application of the anti-BrdU antibody at a 1:150 dilution. The secondary antibody, biotinylated horse anti-mouse IgG [Vector Laboratories], was diluted in TBS, applied to tissue sections and subsequently reacted with avidin/biotin-conjugated alkaline phosphatase [ABC-AP, Vector Laboratories]. The sections were incubated with Vector Fast Red chromagenic substrate [Vector Substrate Kit 1, Vector Laboratories] and counterstained with hematoxylin.

Nuclei of ECs labeled red under halogen light were quantified in 51-75 arteries 60-250μm in diameter [3 lung lobes per rat] from each animal. Only arteries with clearly defined endothelial cells and vascular smooth muscle cells were evaluated. Nuclei were visualized using a Microstar IV microscope [Reichert Scientific Instruments, Buffalo, NY] and enumerated at 400X magnification. The labeling index was defined as the number of chromagen-labeled EC nuclei/total EC nuclei.

The density of EC nuclei for each artery was quantified in arteries 60-250μm intimal diameter as the number of EC nuclei per unit length of arterial intima. The density of EC nuclei was determined on days 1 and 8 to compare the differences in cell density prior to histologically-evident injury [day 1] and after development of vascular leak [day 8]. The circumference of the arterial wall was derived from the average of 2 perpendicular measurements of the arterial diameter calculated from the internal elastic membrane. The arterial circumference was determined using the following formulae:

$$\textbf{Average diameter } [\mu m] = \frac{\text{2 perpendicular measurements of diameter } [\mu m]}{2}$$

$$\textbf{Circumference } [\mu m] = \text{Average diameter } [\mu m] \times \pi.$$

The number of EC nuclei per length of arterial circumference was calculated for each artery. Observations for 27-78 arteries 60-250μm in diameter from each rat on days 1 and 8 [3 rats per treatment group] were used for statistical analysis.

Statistical Analysis: Qualitative data which were normally distributed were analyzed by one way analysis of variance [ANOVA] (Steel and Torrie, 1980). All data expressed as percentages were arcsin square root transformed and analyzed by ANOVA. Multiple comparisons were made using Student-Newman-

Keuls method (Steel and Torrie, 1980). When the homogeneity of variance test failed, data were analyzed by the Kruskal-Wallis One Way ANOVA and comparisons between groups made by Dunn's method. Statistical significance was defined as a $p < 0.05$.

Results

Markers of Lung Injury: Alterations in markers of lung injury after MCTP exposure followed a pattern similar to that previously described (Reindel et al, 1990). The lung weight/body weight ratio [LW/BW] increased by day 5 and continued to be elevated through day 14 [Figure 22A], consistent with an increase in lung interstitial and/or alveolar fluid and cellularity as revealed by morphologic examination [see below]. BALF protein concentration was significantly increased on days 5-14 [Figure 22B], consistent with increased pulmonary vascular permeability (36). RV/[LV+S] was increased over controls at both days 8 and 14 [Figure 22C]. These results confirm the delayed and progressive nature of MCTP-induced pulmonary effects as previously described (Reindel et al, 1990; Schultze et al, 1994).

Histopathology [Figure 23]: Lungs from untreated rats or rats receiving vehicle had no significant lesions. Changes in the lungs after MCTP administration were evident in 1 of 3 rats at day 4 and in 3 of 3 rats at days 6 and

Figure 22. Markers of lung injury after MCTP.

The effect of MCTP on [**A**] lung weight to body weight ratio [LW/BW], [**B**] the bronchoalveolar lavage fluid [BALF] protein and [**C**] right ventricular weight [RV/{LV+S}] are shown.

* = different from vehicle [DMF] control. $p < 0.05$.
n = 3 rats/treatment group/time point.

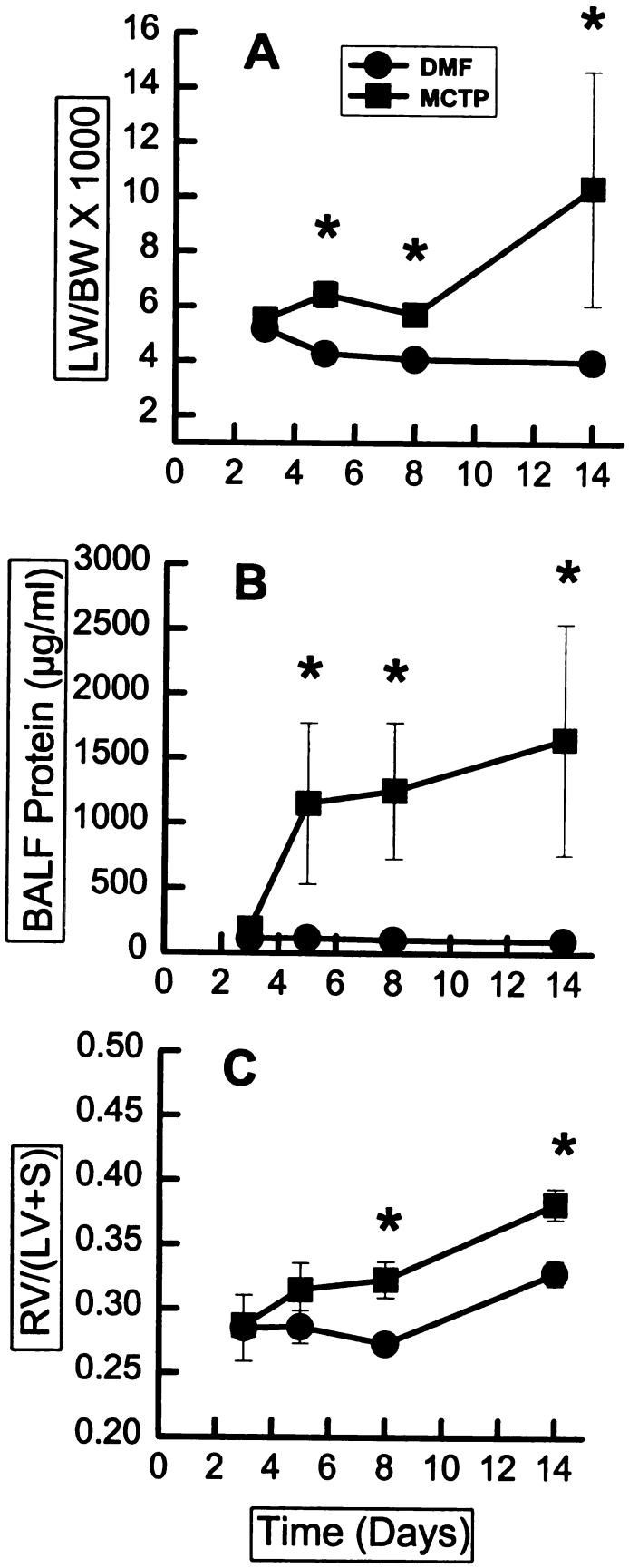
A
DMF
MCTP
LW/BW X 1000
16
14
12
10
8
6
4
2
0 2 4 6 8 10 12 14
B
BALF Protein (µg/ml)
3000
2500
2000
1500
1000
500
0
0 2 4 6 8 10 12 14
C
RV/(LV+S)
0.50
0.45
0.40
0.35
0.30
0.25
0.20
0 2 4 6 8 10 12 14
Time (Days)

Figure 22.

Figure 23. Photomicrographs of lung from vehicle- or MCTP-treated rats.

Histologic sections of lung from rats collected 8 days after exposure to vehicle [DMF - panel A] or MCTP [panel B and C]. Alterations present in MCTP-exposed lung include diffuse thickening of the alveolar wall [*], protein and fibrin within the alveoli [arrowhead] and enlargement of type II pneumocytes [solid arrow] and bronchiolar epithelial cells [open arrow].

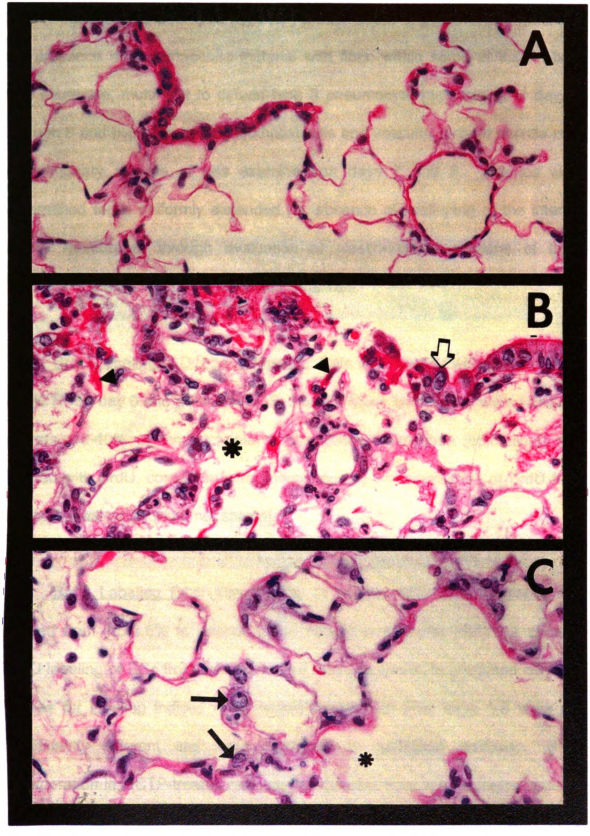

Figure 23.

8. Lesions included patchy to regionally diffuse thickening of alveolar walls and the presence of proteinaceous material with fibrin within some alveoli. There was moderate, multifocal to diffuse type II pneumocyte hypertrophy at days 4 through 8 and hypertrophy of endothelial cells and vascular smooth muscle cells in pulmonary arteries of rats examined on days 7 and 8. Arteries were determined to be uniformly distended [ie, absence of scalloping of the internal elastic membrane] through evaluation of elastin-stained sections of lung. Sections of the duodenum were normal in all rats.

BrdU Labeling of Duodenal Mucosa: Rats were treated with vehicle [DMF] or MCTP on day 0 and given BrdU 18, 5 and 2 hours before they were killed. In all rats, 33-40% of the thickness of the duodenal mucosa [epithelium] was labeled with BrdU, consistent with uniform dosing and absorption of BrdU from the peritoneal cavity [data not shown].

BrdU Labeling ECs: The fraction of labeled ECs from untreated rats ranged from 1.5-3.5% in arteries up to 250μm in diameter [data not shown]. BrdU labeling of ECs from vehicle-treated rats was similar to untreated controls. Values for labeling indices from vehicle-treated rats from days 1-8 were not significantly different and were combined for statistical analysis. BrdU incorporation in MCTP-treated rats was not different from vehicle-treated rats for the first 48 hours after MCTP [Figure 24]. However, MCTP-treated rats had a

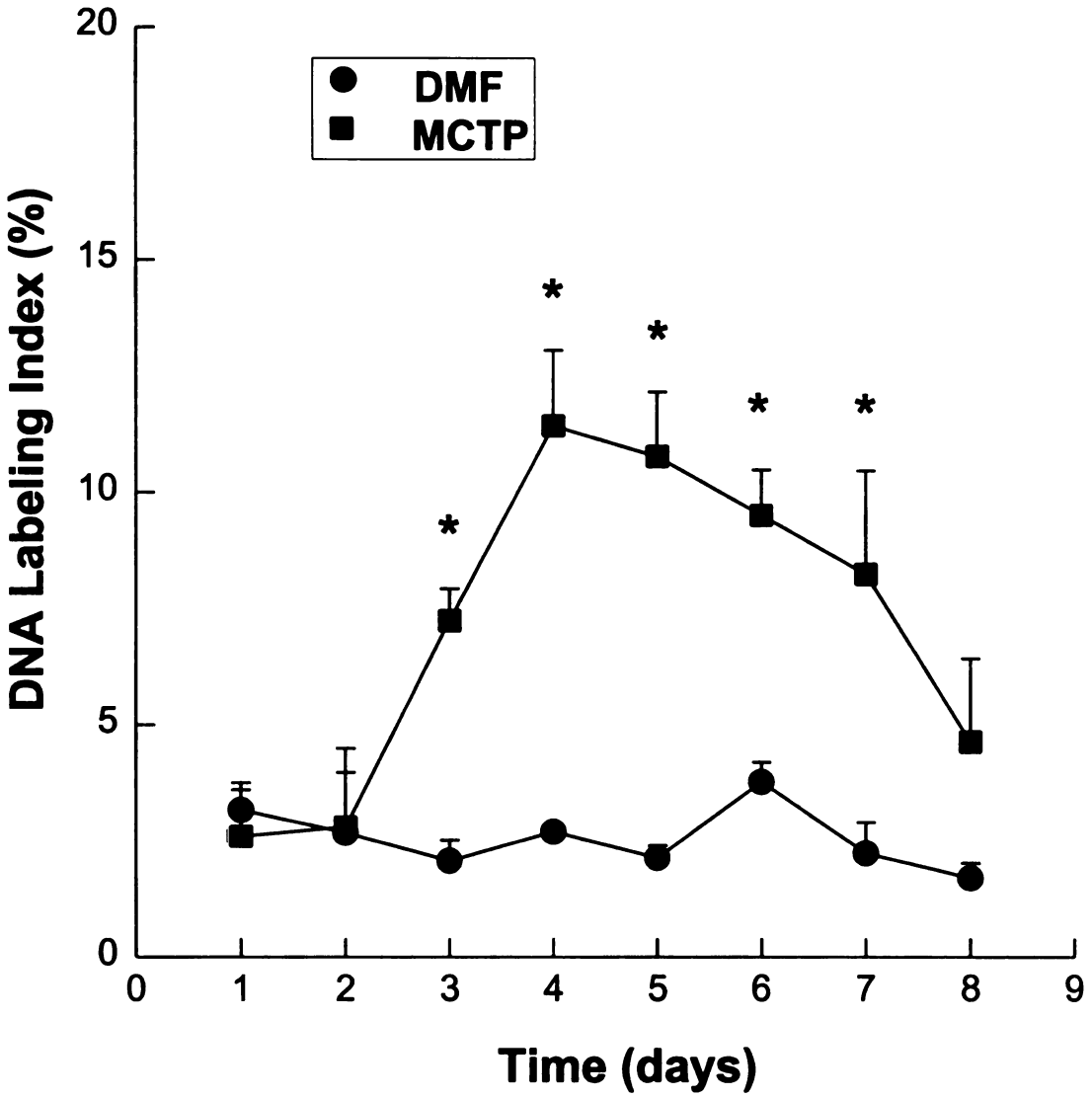

Figure 24. BrdU incorporation in pulmonary artery endothelial cells after vehicle or MCTP administration.

The endothelial cell labeling index was quantified as described in Materials and Methods. The labeling index was determined in arteries

* = different from respective vehicle control; $p < 0.05$.

n = 153-225 arteries/treatment group/timepoint.

significant increase in BrdU labeling of ECs in pulmonary arteries at 3 days, and this persisted through 7 days [Figure 24]. Maximum EC labeling in arteries from MCTP-treated rats was 6.5 fold greater than vehicle-treated rats. Representative examples of BrdU labeling of small pulmonary artery endothelial cells is shown in Figure 25.

EC Density: The mean numbers of EC nuclei per 100μm of arterial wall length are shown in Figure 26. There was no significant difference in EC density between MCTP- and vehicle-treated rats on day 1. The cell density was slightly but significantly decreased in arteries from MCTP-treated rats at 8 days compared to vehicle controls.

Discussion

Depending on the size and severity of the lesion, injury to the endothelium either *in vitro* or *in vivo* is normally followed by cell spreading, migration, and cell proliferation (Schwartz et al, 1980; Wong and Gotlieb, 1984; Ettenson and Gotlieb, 1992; Ettenson and Gotlieb, 1994). Physiologic reformation of an endothelial cell monolayer can occur within 24 hours after small wounds; the inhibition of endothelial cell migration or proliferation can severely impair the ability to recreate monolayer confluence in any size wound (Schwartz et al, 1980; Ettenson and Gotlieb, 1994). Inadequate or incomplete repair of endothelial

Figure 25. Representative photomicrographs showing the relative BrdU incorporation in pulmonary vascular endothelial cells.

Sections of lung from rats treated on day 0 with vehicle [DMF] or MCTP and exposed to BrdU during the 24 hours prior to euthanasia on day 5. BrdU+ cells are present in lung exposed to vehicle [A] or MCTP [B] [arrowheads]. Labeled endothelial cells lining arteries in the lung of rats treated with MCTP [B] are numerous [arrows].

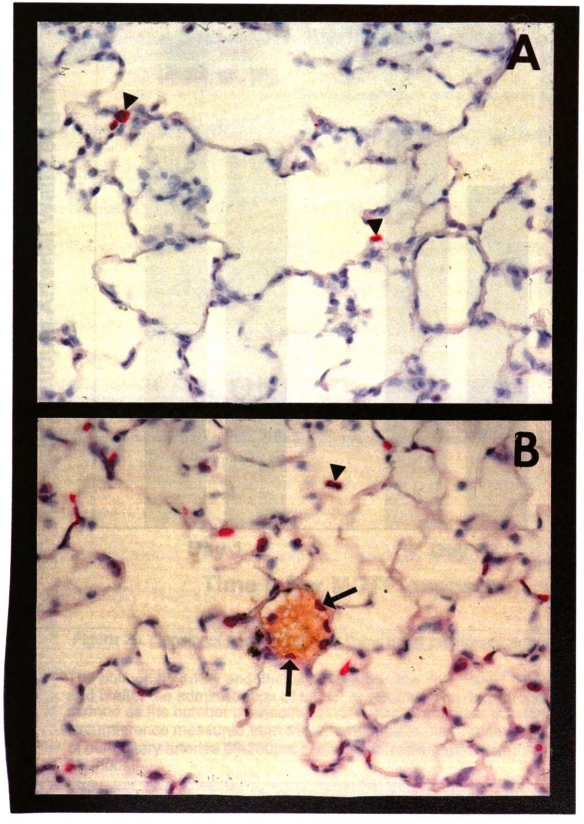

Figure 25.

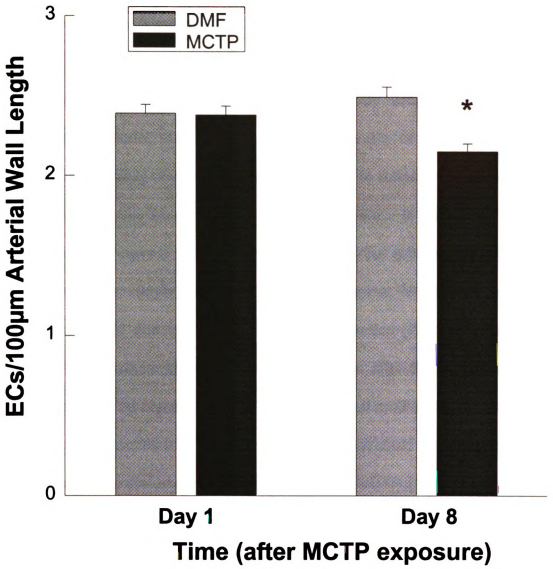

Figure 26. Density of endothelial cells lining small pulmonary arteries.

The pulmonary artery endothelial cell density was determined on days 1 and 8 after the administration of MCTP or vehicle. The density was defined as the number of endothelial cell nuclei per 100µm of arterial circumference measured from the external elastic membrane of pulmonary arteries 60-250µm in diameter [see Materials and Methods].

* = different from respective vehicle control. $p < 0.05$.
n = 153-225 arteries/treatment group/timepoint.

injury *in vivo* can be responsible for enhanced thrombogenesis or increased vascular permeability (Cotran et al, 1994).

MCTP administered intravenously to rats causes a limited, but continuous loss of endothelial cells which is accompanied by progressive pulmonary vascular leak (Reindel et al, 1990). The mechanism of increased vascular permeability is not fully understood, but it is thought to reflect the protracted loss of or damage to cells from the endothelial monolayer. *In vitro*, BEC cultures treated with MCTP have a similar degree of cell loss, but subsequent reformation of a confluent monolayer does not occur at nominal MCTP concentrations greater than 1.5μM due to inhibition of cell proliferation (Reindel et al, 1991). The pulmonary vascular endothelial cell injury seen after the administration of MCTP to rats may be compounded by the inhibition of proliferation, resulting in a deficient repair response and vascular leak that is protracted and progressive.

In the present study, rats were treated with MCTP [1] to determine how this toxicant impacts vascular endothelial cell proliferation and DNA synthesis *in vivo* and [2] to correlate events *in vivo* with the effects of MCTP on endothelial cells *in vitro* [see Chapter II]. Pulmonary vascular leak, measured as an increase in LW/BW and BALF protein, was recognized on day 3 and persisted through day 14, when right ventricular hypertrophy was evident [Figure 22]. A significant increase in vascular endothelial cell DNA synthesis, measured as BrdU incorporation, was identified on day 3 [Figure 24] which corresponded to the increase in vascular permeability. Despite the persistent upregulation of DNA

synthesis over 7-8 days [Figure 24], the number of pulmonary arterial endothelial cells at day 8 was not increased [Figure 26]. The results *in vivo* suggest that, after an MCTP-induced stimulus to proliferate [ie, endothelial cell injury and loss], endothelial cells initiate DNA synthesis but are unable to divide. The lack of cell proliferation after MCTP that follows remarkable upregulation of DNA synthesis may reflect an incomplete stimulus for cell division, or conversely, the inhibition of cell division despite the presence of a complete endothelial cell mitogen.

Mitogenic stimuli often take the form of protein growth factors which may be classified as competence or progression factors (Cotran, 1994). Competence factors can initiate cellular changes necessary for induction of the cell cycle [ie, the upregulation of early immediate genes such as Fos and Jun] (Majesky et al, 1989; Sachinidis et al, 1993) but are unable to stimulate the completion of DNA synthesis and mitosis without additional growth factors in some cell types (Ross et al, 1986; Rothman et al, 1994). Platelet derived growth factor [PDGF] is a competence factor which requires the presence of plasma or another growth protein [eg, insulin-derived growth factor] to complete mitosis in endothelial cells. PDGF is, however, a complete mitogen in smooth muscle cells (Bobik and Campbell, 1993). In contrast, progression factors induce pathways necessary for both initiation and completion of mitosis. Protein growth factors responsible for endothelial cell alterations leading to cell proliferation may be released from stimulated or injured cells or may be a component of the blood plasma (Albelda, 1990; Bobik and Campbell, 1993). PDGF released from

platelets or present in the plasma has been proposed as a possible mechanism of MCTP-induced vascular remodeling involving smooth muscle cells (Ganey et al, 1988); an interaction of PDGF with endothelial cells after injury and exacerbated by increased vascular permeabilty could result in incomplete mitogensis as is seen in the present work.

In contrast to the effect of an incomplete mitogen resulting in delayed or arrested cell proliferation, the inhibition of mitosis by MCTP in the presence of a stimulus for cell proliferation may cause DNA synthesis without subsequent cell proliferation. Several lines of data support this hypothesis. First, vascular injury similar to that produced by MCTP result in the synthesis/release of both competence and progression growth factors expected to provide a complete mitogenic stimulus (Bobik and Campbell, 1993). Second, MCTP does not interfere with DNA, RNA or protein synthesis [cell functions induced by growth stimuli and essential for mitosis] in cultured endothelial cells (Hoorn and Roth, 1992). Third, megalocytosis in hepatocytes and type II pneumocytes in the lung after MCTP and other pyrrolizidine alkaloids requires the generation of additional cell components [likely due to a mitogenic stimulus], but replication is not followed by cell division (Hsu et al, 1973; Samuel and Jago, 1975; Wilson and Segall, 1990). Understanding what growth stimuli are present after MCTP-induced endothelial cell injury, how those growth factors initiate cell division and how MCTP interferes with cell division induced by those factors is necessary to define a role for mitotic inhibition in endothelial cells by MCTP *in vivo*.

The development of technologies which will allow the analysis of cell cycle patterns in individual cells isolated directly from the pulmonary microvasculature of MCTP-treated rats will allow testing of hypotheses concerning the presence of and role of mitotic inhibition in the development of pulmonary hypertension. Until that time, the patterns of increased DNA synthesis without cell proliferation *in vivo* described in the present work suggests that MCTP may inhibit injury-induced cell proliferation *in vivo*. Inhibition of proliferation after endothelial injury may be responsible for the persistence of vascular leak. Additionally, the timecourse of increased DNA synthesis *in vivo* after MCTP administration supports the possibility that blood-borne growth factors may gain extended access to the subintimal cells of the pulmonary arteries. Such an interaction could be associated with vascular remodeling by providing a mitogenic stimulus to VSMCs.

Chapter IV

HYPERTROPHY AND PROLONGED DNA SYNTHESIS IN SMOOTH MUSCLE CELLS CHARACTERIZE PULMONARY ARTERIAL WALL THICKENING AFTER MONOCROTALINE PYRROLE TO RATS

Summary of Chapter IV

An increase in the thickness of the medial layer of pulmonary arteries constitutes a remodeling change in the vascular wall after MCT[P] which is considered important in the induction of pulmonary hypertension. The mechanism responsible for the change in medial thickness [ie, alteration in the vascular smooth muscle cells in that layer] is unknown. Defining the character of the pulmonary arterial medial layer after MCTP administration to rats was proposed as a method to 1] determine the change in smooth muscle morphology and 2] determine the effect on DNA synthesis and cell proliferation by this toxicant, the latter allowing a correlation to those changes in endothelial cells described *in vitro* [Chapter II] and *in vivo* [Chapter III]. As described in Chapter III, male, Sprague-Dawley rats were treated with MCTP [3.5mg/kg, iv] or its vehicle [dimethylformamide, DMF] and an index of vascular smooth muscle cell labeling was determined [bromodeoxyuridine incorporation]. In addition, the density of smooth muscle cells [as a determinant of cell proliferation] was measured and correlated the the arterial medial thickness. Within 5 days after MCTP administration, the thickness of the medial smooth muscle layer in arteries 60-250 μm in diameter was increased, prior to evidence of right heart hypertrophy. BrdU incorporation by VSMCs in pulmonary arteries was not different in vehicle- and MCTP-treated rats for the first 48 hours after treatment. However, MCTP caused a significant increase in DNA synthesis in VSMC on days 3-8 in arteries

up to 250 μm in diameter. Although increased DNA synthesis precedes cell proliferation, the relative number of medial VSMCs did not increase over 8 days, suggesting that hypertrophy alone was responsible for the increased thickness of the arterial media. These results demonstrate that MCTP causes thickening of the media of pulmonary vessels through VSMC hypertrophy and that the prolonged DNA synthesis which accompanies VSMC hypertrophy is not followed by proliferation. The data suggest that MCTP may initiate DNA synthesis in VSMCs but inhibit cell proliferation, similar to the mechanism proposed to occur in endothelial cells *in vivo* [Chapter III].

Introduction

Among the changes which characterize pulmonary vascular remodeling after MCTP *in vivo* is increased thickness of the medial layer of pulmonary arteries due to alterations in VSMCs (Kay and Heath, 1966; Hislop and Reid, 1974). The increase in medial thickness precedes, and is thought to be responsible for pulmonary hypertension in rats after MCT[P] (Kay and Heath, 1967; Meyrick et al, 1980). The morphologic change in VSMCs responsible for the increase in arterial medial thickeness and the mechanism responsible for that increase have not been defined.

Meyrick and Reid (1982) showed that treatment of rats with MCT caused increased incorporation of ^{3}H-thymidine in cells of pulmonary arterial walls, and

that this was associated temporally with vascular wall thickening. In that report, thickening of the arterial wall was proposed to be due in part to hyperplasia of VSMCs based on thymidine incorporation results. Reindel et al (1990) reported a notable absence of mitotic figures in pulmonary VSMCs in spite of an increase in medial thickness by 5-8 days after MCTP. The latter results suggested that the increase in vascular medial thickness may not be due to VSMC hyperplasia, but to a process which causes VSMC mass to increase through enlargement of individual cells.

In vitro, endothelial cells show a different response to the cytotoxic effect of MCTP which is dependent on the species of animal from which the cells were acquired (Reindel et al, 1991; Reindel and Roth, 1991; Hoorn et al, 1993). Regardless of the cell origin, endothelial cells exposed to MCTP and subsequently provided a growth stimulus [ie, passage of cells to a subconfluent density] become enlarged and fail to divide (Reindel and Roth, 1991). VSMCs exposed to a similar set of conditions produce additional organelles as they increase in size (Reindel and Roth, 1991), a process which has been associated with cell hypertrophy (Wang et al, 1994; Owens and Schwartz, 1983).

As described in Chapter III, hypertrophy may result from partial mitogenic activation, determined by the character of the protein growth factor. Conversely, cells exposed to MCTP may be stimulated to undergo proliferation [cell injury/loss or growth factor release] through the activation of seqential events [cell cycle] which lead to cell division [see Chapter II], but are inhibited from

completing mitosis by MCTP even though the synthesis of macromolecules continues [Chapter II] (Hoorn et al, 1992).

The present study was designed as an extention of Chapter III and used to identify changes in VSMC morphology and growth after MCTP. In addition, the results obtained were associated with mechanisms potentially involved in the development of smooth muscle cell remodeling of the vascular media.

Materials and Methods

Animals: Male, Sprague-Dawley weighing 175-225g were housed and fed as described in Chapter III.

MCTP Synthesis: Monocrotaline pyrrole was synthesized from MCT as described in Chapter II. MCTP was maintained in N, N'-dimethylformamide [DMF] under nitrogen at -20°C and was diluted to working concentrations with DMF immediately before use. The concentration of MCTP used was adjusted to allow accurate dosing at volumes less than 0.2 ml.

Treatment Protocol: On day 0, rats received a single injection of either MCTP [3.5 mg/kg] or an equivalent volume of DMF via the tail vein. Three rats per treatment group were killed on days 3, 5, 8 and 14 for the evaluation of markers of injury and pulmonary hypertension as described previously (Reindel

et al, 1990) or on days 1-8 for histopathology and immunohistochemistry. The administration of BrdU and the rationale for the dosing regimen are described in Chapter III. Prior to necropsy, animals were anesthetized with sodium pentobarbital [50 mg/kg, ip] and exsanguinated by severing the abdominal aorta. A tracheal cannula was secured in all animals (Roth, 1981), and an additional pulmonary arterial cannula was placed (Schultze et al, 1994) in animals used for histologic evaluation. Animals killed for the measurement of biochemical markers of injury were not used for histologic evaluation.

Evaluation of MCTP-Induced Lung Injury: The heart, lungs, trachea and mediastinum were removed enbloc and, prior to lavage, blotted dry and weighed. The lungs were lavaged twice with 0.9% sodium chloride solution [23 ml/kg] as previously described (Roth, 1981), and the volumes of bronchoalveolar lavage fluid [BALF] were combined and placed on ice. After lavage, the lung lobes were excised from the trachea by severing the major bronchi. The remaining heart, trachea and mediastinum were then weighed. The lung weight was determined by subtracting the weight of the heart, trachea and mediastinum from the total weight of the original tissue block removed from the thoracic cavity.

The lavage fluid was spun at 600Xg for 10 minutes to pellet the cells, and the supernatant fluid was used for quantitation of protein. BALF protein was measured by the method of Lowry et al (1951) using an EL 340 Microplate Bio Kinetics Reader [Bioteck Instruments, Winooski, VT].

Right ventricular hypertrophy was assessed as an increase in the ratio of the right heart weight to the weight of the left heart and interventricular septum [RV/{LV+S}] and used as a marker of pulmonary hypertension (Fulton et al, 1952).

Histopatholgic Evaluation and Immunohistochemistry: The procedures used for the tissue collection and preservation are described in Chapter III. Briefly, the lungs were flushed of blood with 0.9% saline, perfuse fixed with a noncrosslinking preservative [Histochoice] for 2 hours followed by immersion fixation in the same preservative for 24-36 hours. A 0.5 cm length of duodenum was harvested from each rat, fixed in Histochoice [Amresco, Solon, OH] and used as a positive control for BrdU immunohistochemistry. As previously stated, fixative perfusion of the vasculature was done to distend arteries uniformly in order to eliminate the contribution of vessel contraction to medial thickening, using a technique for vascular perfusion modified from Reindel et al (Reindel et al, 1990).

After thorough tissue fixation, sections of the midportion of each of 3 lung lobes [left, right apical and right diaphragmatic] from each rat were excised perpendicular to the mainstem bronchus and embedded in paraffin. Small, muscular pulmonary arteries were identified by their location within the peribronchiolar adventitia which differentiated them from small pulmonary veins, typically located in the parenchyma between bronchioles (Wagenvoort and

Wagenvoort, 1979). Tissue sections were stained with hematoxylin and eosin for routine histologic evaluation and elastin by the Verhoeff - Van Gieson's method, previously utilized to allow the accurate measurement of the arterial medial thickness (Hill et al, 1989; Huxtable et al, 1977; Ono and Voelkel, 1991) and ensure uniform distention of the arteries (Wagenvoort and Wagenvoort, 1979).

Additional sections of lung and duodenum were prepared for immunohistochemical examination with a mouse-derived monoclonal antibody to BrdU [Becton Dickenson, San Jose, CA] using an automated immunostainer [Leica Histostainer Ig, Leica, Inc., Deerfield, IL]. The technique is described in detail in Chapter III.

Nuclei of VSMCs labeled red under halogen light were quantified in 23-67 arteries [60-120μm diameter] or 8-28 arteries [120-250μm diameter] from each animal [3 sections of lung from each rat]. The ranges of arterial diameters were chosen to represent parenchymal arteries [<120μm] and arteries adjacent to terminal bronchioles [120-250μm], and only arteries with clearly defined endothelial cells and vascular smooth muscle cells were evaluated.

Nuclei were visualized using a Microstar IV microscope [Reichert Scientific Instruments, Buffalo, NY] and enumerated at 400X magnification. The labeling index was defined as the number of labeled VSMC nuclei/total VSMC nuclei. The VSMC labeling index was determined for each artery in one of two diameter ranges [60-120μm or 120-250μm] from 3 rats in each treatment group

[n = 69-201 or 24-84, respectively], and those values were used to calculate an average labeling index. The total number of observations per group in each of the two arterial size ranges were used for statistical analysis.

In Verhoeff-Van Gieson-stained sections, the medial thickness was measured between the internal and external elastic laminae as described by Meyrick et al (1980). The widest diameter of the artery and the diameter measured 90° perpendicular to the widest dimension were averaged as the external diameter. The average medial thickness was derived with the same sites used to measure diameter. The medial thickness ratio for each artery was calculated by the following formula [modified from Meyrick et al (1980)]:

$$\textbf{Medial Thickness Ratio} = \frac{[\text{Average Medial Thickness X 2}]}{\text{Average External Diameter}}$$

The medial thickness ratio was determined for each artery in one of two external diameter ranges [60-120μm or 120-250μm] from 3 rats in each treatment group [n = 69-201 or 24-84, respectively]. The medial thickness ratio was calculated for each treatment group [total arteries visualized in 3 rats per group] for each diameter range of arteries evaluated on each of days 1, 5 and 8.

VSMC nuclei were counted in each arterial profile examined and used to determine the VSMC density per artery in one of two diameter ranges [see above]. For each treatment group [3 rats], a total of 69-201 arteries [60-120μm

diameter arteries] or 24-84 arteries [120-250μm diameter arteries] per treatment group were evaluated on each of days 1-8 after MCTP or DMF administration.

The frequency distribution of artery diameters was determined for each of the two ranges evaluated [60-120μm and 120-250μm] to judge the uniforimity of that distribution between treatment groups. This evaluation was done to identify any misrepresentation of vessel sizes within a diameter range which may introduce bias and prevent meaningful comparisons of the medial thickness or VSMC density between treatment groups. Arteries in the diameter size range from 60-120μm were subdivided into two smaller ranges [60-90 and 91-120μm] for each treatment group [vehicle or MCTP on days 1,5 and 8]. The artery diameter distribution and the medial thickness ratio [see above] were compared between treatment groups in each of the subdivided ranges. A similar evaluation was done with arteries ranging from 121-250μm in external diameter divided into 3 subgroups.

Statistical Evaluation: Results were expressed as mean $\pm$ SEM. Data for single comparisons between treated and vehicle control were analyzed using the student's t-test (Steel and Torrie, 1980). Multiple comparisons were analyzed by one way analysis of variance [ANOVA] and Student Newman-Keuls post hoc test (Steel and Torrie, 1980). Ratios were arcsin square root-transformed prior to analysis or compared using an appropriate nonparametric test (Steel and Torrie, 1980). The criterion for significance was $p < 0.05$.

Results

Markers of Injury [Figure 22 - Chapter III]: Alterations in markers of lung injury after MCTP exposure are reported in Chapter III. Briefly, The lung weight/body weight ratio [LW/BW] [Figure 22A] and BALF protein concentration [Figure 22B] were increased by day 5 and continued to be elevated through day 14 consistent with an increase in lung interstitial and/or alveolar fluid and cellularity (44). RV/[LV+S] was increased over controls at both days 8 and 14 [Figure 22C].

Histopathology: The results of a histopathologic analysis of the lung from rats treated with MCTP are summarized in Chapter III. Briefly, significant lesions were limited to the lung of rats treated with MCTP, prevalent after day 4 and progressive through day 8, the last day of histologic evaluation. Lesions included patchy to regionally diffuse thickening of alveolar walls, the presence of alveolar protein with fibrin, hypertrophy of vascular and nonvascular lung cells, and the increase in arterial medial thickness. Figure 27 shows the relative increase in medial thickness of parenchymal and peribronchiolar arteries. Arteries between 60 and 250 μm diameter were determined to be adequately distended through evaluation of elastin-stained sections of lung. Sections of the duodenum were normal in all rats.

Figure 27. Medial thickness of small pulmonary arteries from rats treated with vehicle or MCTP.

Photomicrographs of rat lung collected 8 days after exposure to vehicle [A and C] or MCTP [B and D]. Arteries adjacent to the terminal bronchiole [A and B] and within the alveolar wall [C and D] are shown. The vascular media [arrow] and smooth muscle cell nuclei [arrowhead] are labeled in both treatment groups. All of the photomicrographs were taken at the same magnification.

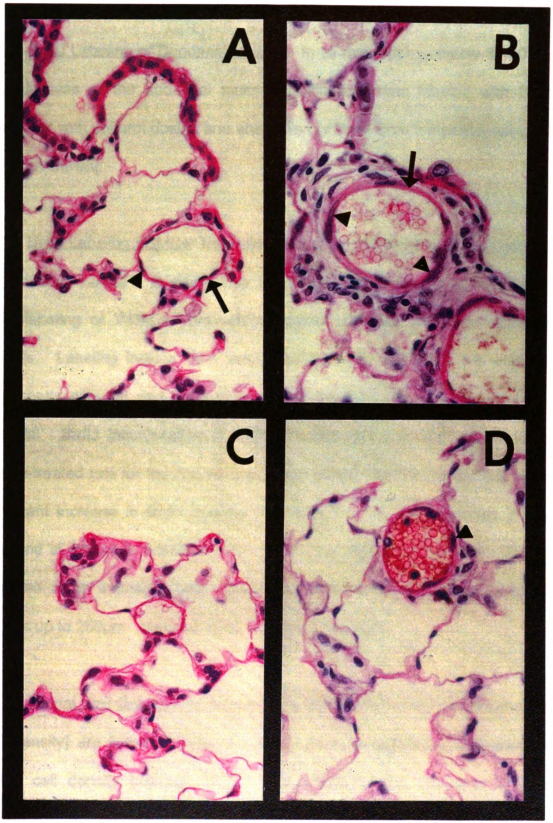

Figure 27.

BrdU Labeling of Duodenal Mucosa: In all rats, approximately 33-40% of the thickness of the duodenal mucosa [epithelium] was labeled with BrdU, consistent with uniform dosing and absorption of BrdU from the peritoneal cavity [data not shown].

BrdU Labeling VSMCs: The fraction of labeled VSMCs from untreated rats ranged from 1.5-3.5% in arteries up to 250μm in diameter [data not shown]. BrdU labeling of VSMCs from vehicle-treated rats was similar to untreated controls. Labeling indices from vehicle-treated rats from days 1-8 were not significantly different and were combined to increase the statistical power of analysis. BrdU incorporation in MCTP-treated rats was not different from vehicle-treated rats for the first 48 hours after MCTP. MCTP-treated rats had a significant increase in BrdU labeling at 3 days in 120-250μm arteries [Figure 28A] and at 4 days in arteries smaller than 120μm [Figure 28B]. BrdU labeling persisted at an increased rate through the entire 8 day evaluation period in arteries up to 250μm. Maximal labeling approached 15%.

Arterial Wall Cell [VSMC] Density: The numbers of VSMC nuclei per artery [cell density] are listed in Table 1. There were no significant differences in VSMC cell density between MCTP- and vehicle-treated rats over 8 days. Additionally, no time-dependent increase in cell density occurred for any of the treatments or artery sizes.

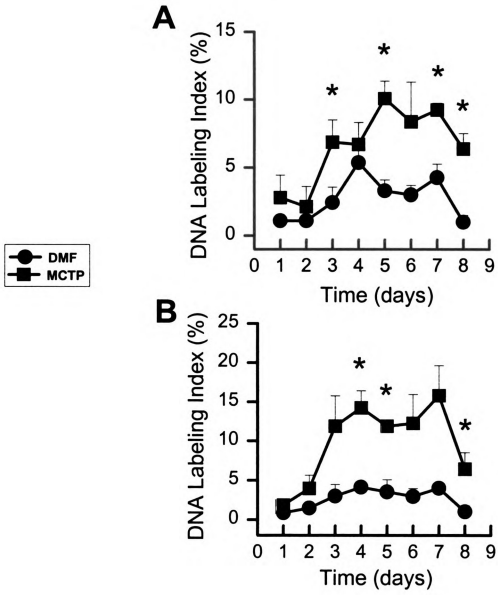

Figure 28. DNA synthesis [BrdU labeling index] of pulmonary vascular smooth muscle cells [VSMCs].

The labeling index of VSMCs in arteries with an external diameter of [**A**] 120-250μm or [**B**] less than 120μm is shown.

* = different from respective DMF control; $p < 0.05$.
n = 24-201 arteries /treatment group/timepoint.

Table 1. Density of smooth muscle cells in pulmonary arteries of MCTP-treated rats.

Days after treatment	Treatment	Arteries 60-120μm	Arteries > 120μm
		Smooth Muscle Cell Nuclei per Artery	
1	Vehicle	4.2 ± 0.5	26.7 ± 10.0
	MCTP	5.0 ± 0.3	19.0 ± 3.5
2	Vehicle	5.2 ± 0.4	22.7 ± 3.0
	MCTP	5.5 ± 0.6	26.7 ± 4.1
3	Vehicle	4.8 ± 0.3	20.7 ± 2.0
	MCTP	5.5 ± 0.4	22.3 ± 6.4
4	Vehicle	5.0 ± 0.9	18.0 ± 1.0
	MCTP	4.6 ± 0.5	18.3 ± 0.9
5	Vehicle	5.0 ± 0.8	21.0 ± 1.7
	MCTP	4.8 ± 0.7	25.0 ± 3.8
6	Vehicle	4.0 ± 0.6	21.0 ± 3.2
	MCTP	4.6 ± 0.4	25.7 ± 8.3
7	Vehicle	4.4 ± 0.5	17.7 ± 2.3
	MCTP	5.4 ± 0.5	20.0 ± 3.1
8	Vehicle	4.5 ± 0.5	19.3 ± 4.5
	MCTP	4.8 ± 0.6	23.3 ± 4.9

Results are the means ± S.E.M. for all arteries in sections of lung examined, subdivided into two groups of external diameters ranging from 60-120μm [n = 69-201] and 121-250μm [n = 24-84].

Arterial Wall Medial Thickness Ratio: The ratio of the arterial medial thickness to arterial diameter for each of the artery sizes is listed in Table 2. The medial thickness ratio was increased in MCTP-treated rats at both 5 and 8 days in arteries up to 250 μm in diameter.

Relative Distribution of Arterial Sizes: The distribution of arterial sizes within artery diameter ranges [see Materials and Methods] was determined to assess potential counting bias. A ratio of the number of arteries in a subdivided group [ie, 60-90 and 91-120μm] to the total arteries counted for a range [ie, 60-120μm] was calculated. In vessels of size 60-120μm, there were no differences between vehicle- and MCTP-exposed lungs in the size distribution of arteries evaluated at any day after treatment [Figure 29A]. Similarly, there were no consistant distribution differences within the larger range [121-250μm], although there was a tendency on day 8 for a slightly greater fraction of small vessels in the DMF group [Figure 29B].

Comparison of the Medial Thickness Ratio: The medial thickness ratio [see Materials and Methods] was compared between the subdivided groups of each diameter range [60-120 or 121-250μm] for vehicle- or MCTP-treatment groups on days 1,5 and 8. No consistent differences in medial thickness occurred between the large and small vessels within either of the original ranges

Table 2. Medial thickness of pulmonary arterial walls after exposure of rats to MCTP.

Days after treatment	Treatment	Arteries 60-120μm	Arteries > 120 μm
		Average Medial Thickness	
1-8	Vehicle	4.3 ± 0.2	5.1 ± 0.2
1	MCTP	5.2 ± 0.5	5.0 ± 0.3
5	MCTP	6.3 ± 0.7*	6.8 ± 0.5*
8	MCTP	5.5 ± 0.4*	6.5 ± 0.4*

The medial thickness was measured as the distance between the internal and external elastic laminae [see Materials and Methods]. Results are the means ± S.E.M. for all arteries in sections of lung examined from each treatment group. Artery diameters were subdivided into two size ranges consisting of vessels 60-120μm [n = 69-201] and 121-250μm [n = 24-84].

* = different from respective vehicle control.

$p < 0.05$.

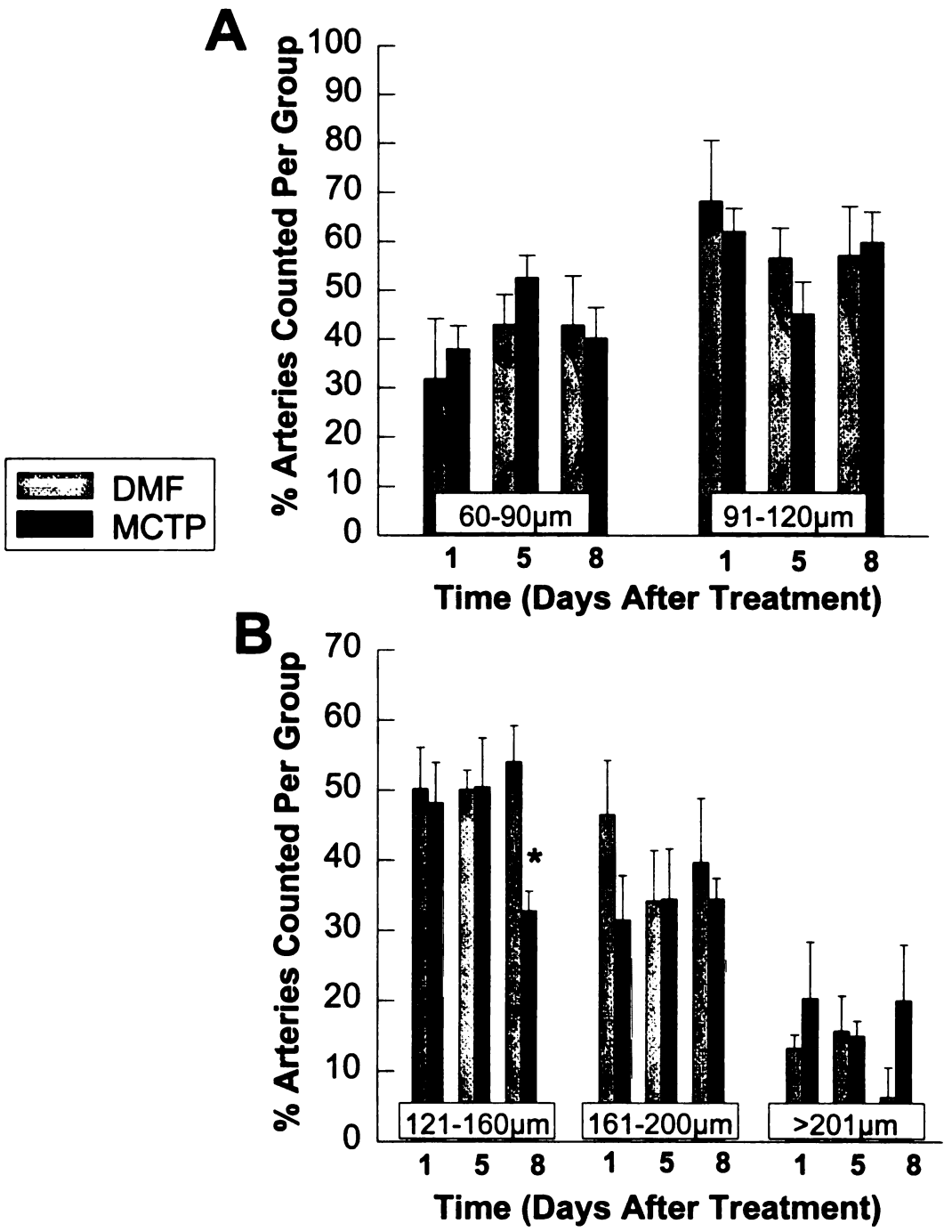

Figure 29. The frequency distribution of small pulmonary artery diameters.

The two artery size range groups [60-120 [**A**] and 121-250µm [**B**] were subdivided into two or three smaller groups [see Materials and Methods]. The distribution was compared across each of the smaller size range at days 1, 5 and 8, as well as between treatment groups on each day. The single significant difference [* in plot **B**] is addressed [see Discussion].

[Figures 30A and B]. This was true for vessels from vehicle- as well as MCTP-treated rats.

Discussion

MCTP causes pulmonary vascular remodeling which precedes a significant increase in pulmonary arterial pressure (Reindel et al, 1990). These changes occur within the first 8 days after the administration of MCTP. The present study confirms that pattern. Vascular remodeling, measured as an increase in the thickness of the medial layer of pulmonary arteries, was evident by day 5 after MCTP administration [Table 2]. Pulmonary hypertension was evaluated indirectly by the increase in right ventricular muscle weight compared to the weight of the combined left ventricular free wall and septum [RV/{LV+S}]. RV/[LV+S] was not significantly increased until post-treatment day 8 [Figure 22C].

In any histologic study of vascular remodeling, preparation artifacts, pathologic or physiologic vessel wall contraction, inadequate vascular distention or the contribution of decreased vascular compliance have the potential to preclude the accurate appraisal of medial thickening. As well, enlargement or alterations in shape or orientation of cell nuclei can influence the quantification of cell density. Although no methods exist to eliminate all potential biases

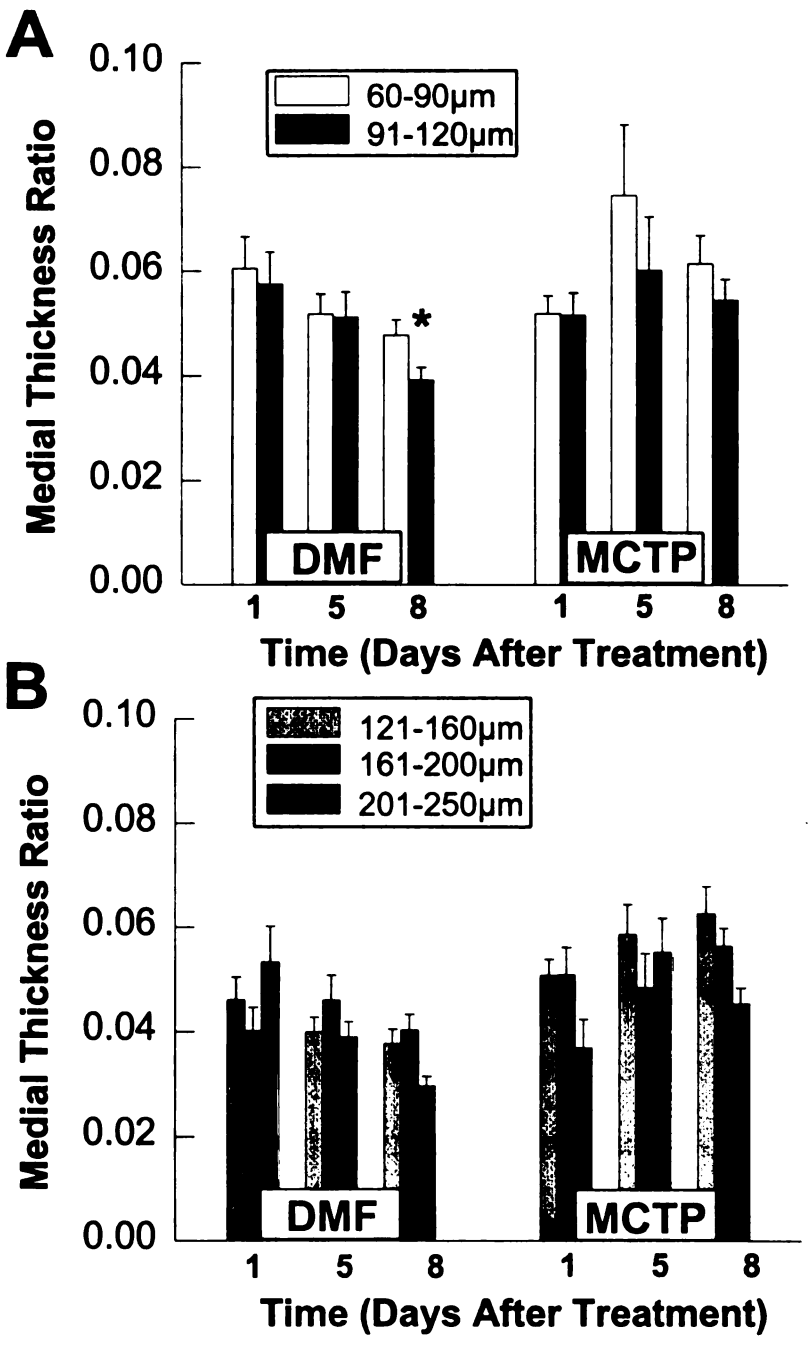

Figure 30. The medial thickness ratio of small pulmonary arteries.

Each artery size group evaluated [**A**; 60-120] and [**B**; 121-250µm] were further subdivided into smaller size groups. The medial thickness ratio was compared between the subdivided groups for vehicle [DMF] or MCTP treatment groups on days 1, 5 and 8. The single significant difference [* in plot **A**] is addressed [see Discussion].

completely in a study of this type, attempts were made to minimize misinterpretation of observed changes in pulmonary arteries after the administration of MCTP. First, biases influencing medial thickness were considered. Vascular contraction or inadequate vascular distention may cause artifactual thickening of the media. Contrasting reports have described both increased and decreased vascular contractility following MCT or MCTP (Altiere et al, 1985; Hilliker and Roth, 1985). In this study, the pulmonary circulation was fixed in a distended state using an established protocol (Reindel et al, 1990), and the uniformity of distention was confirmed by examining the elastic laminae of pulmonary arteries for the absence of cupping, an indicator of vessel wall contracture. Vascular distention was therefore considered satisfactory. Additionally, the deposition of additional extracellular matrix components in the vascular wall may increase the medial thickness or reduce compliance. In a previous study, the examination of electron micrographs of the pulmonary vasculature after MCTP administration did not reveal changes in extracellular matrix (Reindel et al, 1990) at the post-treatment times we examined.

Second, factors which may alter cellular morphology, resulting in an incorrect interpretation of VSMC density, were also considered. As described in the introduction above, the identification of hypertrophy is usually based on estimates of cell density in the tissue. In this study, the quantitation of cell nuclei and the measurement of vascular medial thickness were used to describe the morphology of VSMCs in pulmonary artery medial thickening. Nuclear

enlargement, shape change or distortion of the orientation of nuclei can result in the overrepresentation of nuclei in a tissue section and, as such, a potential bias toward overcounting. *In vitro*, application of MCTP to cells results in increased nuclear size (Reindel and Roth, 1991). If overcounting due to increased nuclear size were a significant problem, we would have expected to observe greater numbers of VSMC nuclei in MCTP-treated rats, favoring an interpretation that hyperplasia had occurred. However, the density of VSMC nuclei in arteries of MCTP-treated rats was not different from control rats at any timepoint [Table 1].

A third factor with the potential to contribute bias was the wide range of artery sizes used for comparison of effects between MCTP and its vehicle. Conceivably, the overrepresentation of arteries on one end of a range [ie, an abundance of 60-80μm diameter arteries in the 60-120μm range group] could skew the results of comparisons of that group with others containing a more normally distributed population. As well, marked differences in the artery size distribution could affect calculations to determine medial thickness and vascular smooth muscle cell density. The accurate characterization of hyperplasia or hypertrophy in this study is dependent on the uniformity of these measurements across treatment groups. The comparisons of artery diameter frequency distribution [Figure 29] and medial thickness ratios [Figure 30] showed that unequal frequency distributions did not contribute bias to the present study. A single significant difference between MCTP and vehicle-exposed arterial size

frequency was identified in the 121-250μm diameter subgroup at day 8 [overrepresentation of artery size in DMF group - Figure 29B]. This difference was matched by an equal [although not significant] overrepresentation of arteries > 201μm in the MCTP group at day 8. As well, it was determined that any contribution made by this discrepancy would favor hyperplasia and not hypertrophy in this study. In summary, the distribution of vessel sizes within the chosen ranges did not contribute to measured differences between arteries from vehicle- or MCTP-treated rats.

Treatment of rats with either MCT or MCTP results in phenotypic hypertrophy of VSMCs and a number of other cell types in the walls of pulmonary arteries (Merkow and Kleinerman, 1966; Reindel et al, 1990), but the role of hyperplasia of VSMCs in vascular remodeling has been less clear. Increased DNA synthesis [ie, ^{3}H-thymidine incorporation] noted by Meyrick and Reid (1982) was interpreted as a proliferative response to MCT. In that study, rats fed a dose of *Crotalaria spectabilis* seeds sufficient to produce pulmonary hypertension had an increase in ^{3}H-thymidine incorporation in VSMCs of large arteries at days 3 and 28-35, whereas significant VSMC labeling in small, intraacinar arteries did not occur at any time, even when evidence of pulmonary hypertension was present [ie, increased right heart weight]. Muscular pulmonary arterial wall thickness increased by 21 days after MCT, but the medial VSMC density was significantly decreased at that time, an observation not obviously consistent with VSMC proliferation. In the present study, pulmonary arteries

from 120-250μm in diameter had increased DNA labeling on day 3 which persisted through day 8 after MCTP treatment [Figure 27A]. In contrast to results seen with MCT (Meyrick and Reid, 1982), there was a similar pattern of labeling in VSMC of smaller, intraacinar arteries [Figure 27B]. Increases in the labeling index of all arteries preceded evidence of pulmonary hypertension [Figure 22C], and the change in arterial medial thickness which followed increased DNA synthesis was not accompanied by an increase in the number of arterial VSMCs [Table 1]. These results suggest that the change in arterial medial mass after MCTP is due to VSMC hypertrophy, not hyperplasia, and that the hypertrophic response is accompanied by increased DNA synthesis.

Cells normally enlarge and duplicate DNA and organelles prior to mitosis, so that each daughter cell contains a full complement of nuclear and cytoplasmic components. Once cells have passed all of the cell cycle checkpoints (Alberts et al, 1989; Nurse, 1990) synthesis of DNA subsides and mitosis usually proceeds (Laskey et al, 1989). The phenotype of VSMCs is known to change from contractile to synthetic in conjunction with the ability to proliferate (Gabbiani et al, 1984; Thyberg et al, 1983). When a differentiated cell function must continue without the interruption associated with cell division, it has been hypothesized that cells may avoid mitosis in the face of a proliferative stimulus (Owens, 1989). As such, VSMCs with the contractile phenotype may undergo hypertrophy and synthesize additional micro- and intermediate filaments and microtubules, but not divide (Wang et al, 1994). By contrast, cells with the synthetic phenotype that

undergo hypertrophy contain additional, and often enlarged, cytoplasmic organelles but fewer or smaller microfilaments (Wang et al, 1994). Accordingly, conversion of VSMCs to a phenotype capable of proliferation but associated with loss of contractile components may result in a reduced ability to maintain vascular tone.

Alterations in the structure of arteries have been well defined in animal models of systemic hypertension (Owens and Reidy, 1985; Owens and Schwartz, 1983; Owens et al, 1988b). In systemic arteries, an elevation in vascular pressure is associated with an increase in medial VSMC mass that can occur by hypertrophy (Owens and Schwartz, 1983) or hyperplasia (Owens and Reidy, 1985). The response of VSMCs to systemic hypertension appears to depend on the speed of onset and magnitude of hypertension as well as to the size or conformation of the vessel affected. VSMCs in large conduit vessels become hypertrophic and synthesize additional DNA in response to sustained elevation of the intravascular pressure (Owens and Schwartz, 1983), whereas persistent hypertension in small mesenteric arterial branches causes hyperplasia with little hypertrophy (Owens et al, 1988b). By contrast, acute systemic hypertension with endothelial denudation and vascular leak following aortic coarctation causes VSMC hyperplasia in the thoracic aorta (Owens and Reidy, 1985).

Owens and Reidy (1985) proposed that VSMC hyperplasia following endothelial cell injury in systemic hypertension might occur by exposure of

VSMCs to 1] mitogens from injured endothelial cells, 2] the effect of endothelial denudation or 3] the influx of blood-borne mitogenic factors. MCTP causes endothelial cell injury and increased permeability of the endothelium in the pulmonary microvessels *in vivo*, resulting in the escape of intravascular proteins and fluid [Figure 22B]. Subsequently, if the trends identified in models of systemic hypertension (Owens and Reidy, 1985; Owens and Schwartz, 1983; Owens et al, 1988) held true for MCTP-induced pulmonary vascular injury, VSMC hyperplasia would be the anticipated cellular response. As reported here, however, hyperplasia is not a significant feature of vascular medial thickening in pulmonary arteries after MCTP treatment [Tables 1 and 2]. MCTP appears to initiate a growth stimulus for VSMCs, but after DNA synthesis the cells do not progress to cell division.

How MCTP initiates increased DNA synthesis in VSMCs is unclear. Results of the present study indicate that the earliest increase occurs at 3 days after MCTP. At this time, endothelial cell damage and loss is minimal and alterations in pulmonary arterial pressure are not yet present (Reindel et al, 1990). The onset of pulmonary vascular leak, however, has been identified as early as 2 days after MCTP (Reindel et al, 1990) suggesting a role for mitogenic factors which have leaked from the pulmonary vasculature. Alternatively, MCTP may initiate the cellular synthesis and release of a mesenchymal growth factor through interaction with the endothelium or may directly induce a mitogenic

pathway in VSMCs. It is apparent from this study that the initial mitogenic signal occurs within the first 3 days after the administration of MCTP.

It is unclear if MCTP can or does directly interact with VSMCs *in vivo* to induce hypertrophy. MCTP, as well as other pyrrolizidine alkaloids, can inhibit mitosis and cause cell hypertrophy and karyomegaly both *in vitro* and *in vivo*. The mechanism by which mitotic inhibition occurs is unknown but presumed to follow crosslinking of DNA and protein (Wagner et al, 1993). MCTP is highly reactive and thought to interact rapidly with macromolecules within the cell, making the endothelium the first and presumedly only direct pulmonary target of the pyrrole (Mattocks, 1972). It appears possible, however, that the crosslinking associated with pyrrolizidine alkaloid exposure is not permanent and that conjugated pyrroles may be able to move from one macromolecule to another (Mattocks, 1986), making it plausible that cells beneath the endothelium [ie, VSMCs] are targets for MCTP. Consistent with this hypothesis is the response of type II pneumocytes after MCT (Wilson and Segall, 1990) or MCTP (Raczniak et al, 1979; Reindel et al, 1990) administration *in vivo*. These cells undergo marked hypertrophy and karyomegaly, possibly in response to a proliferative stimulus and mitotic inhibition induced by MCTP.

In conclusion, MCTP causes a delayed and progressive lung injury which results in pulmonary vascular remodeling and pulmonary hypertension. Vascular medial thickening appears to be the result of VSMC hypertrophy and not hyperplasia. Prior to evident cell enlargement, VSMCs undergo increased DNA

synthesis characterized by BrdU incorporation. Hyperplasia of VSMCs does not follow increased DNA synthesis and hypertrophy, suggesting incomplete mitogenesis or cell cycle inhibition prior to mitosis. It is tempting to speculate that VSMC hypertrophy and increased DNA synthesis after MCTP exposure is due to the interruption of the cell cycle machinery necessary for mitosis.

SUMMARY AND CONCLUSIONS

The pulmonary vasculature is the primary target of MCT[P] in the rat. Endothelial injury appears first in a series of alterations that lead to pulmonary hypertension. Endothelial cell damage is accompanied by pulmonary vessel leak and precedes the development of perivascular edema. Increased permeability is followed by vascular remodeling, pulmonary hypertension and cor pulmonale. The predictable order of these changes suggests that the occurrence of each event is dependent on that which precedes it [eg, vascular remodeling requires a preexisting vascular leak]. If this theory is true, then understanding the initial effect of MCT[P] on the vascular endothelium may reveal significant information about downstream events leading to pulmonary hypertension. Such a theory aided in the construction of the work done for this dissertation.

Among the MCT[P]-induced functional alterations in endothelial cells is the inhibition of cell proliferation. The formation of megalocytic cells in the liver of animals exposed to pyrrolizidine alkaloids has historically been ascribed to the inhibition of mitosis caused by this toxicant. The functional ramifications of mitotic inhibition in the development and persistence of toxicosis have not been examined. Previously, studies using cultured cells exposed to MCTP have shown that cell proliferation is inhibited and the repair of endothelial cell monolayers is delayed or prevented (Reindel and Roth, 1991). MCT[P] is known to crosslink DNA (Petry et al, 1984; Wagner et al, 1993), and the production of abnormal DNA structure can arrest the progression of cells through a replicative

cycle until repair is completed (Hartwell and Weinert, 1989). An indirect association between crosslinking and the inhibition of cell cycle progression has been suggested (Thomas et al, 1996), but identification of the mechanism by which MCT[P] inhibits mitosis has remained elusive.

The work presented in Chapter II was an attempt to define how MCTP interrupts mitosis by its action on events comprising the cell cycle. Synchronized, subconfluent BECs were exposed to MCTP during defined cell cycle phases to determine the selective sensitivity to this toxicant of events occurring during those phases. The ability of MCTP to crosslink DNA produced an expectation that the greatest sensitivity and effect would occur during S phase when DNA strands unwind to replicate. It was anticipated that the open DNA duplexes would be most vulnerable to an alkylation. The expected outcome of S phase sensitivity to MCTP was S phase arrest and the inhibition of replicative DNA synthesis, a checkpoint-controlled process in place to promote the repair of damaged DNA. In contrast to the predicted pattern, BECs were arrested in G_2-M and continued to synthesize DNA; some cells contained an amount of DNA greater than that deemed necessary for mitosis [hypertetraploid cells]. In addition, the most sensitive phase of the cell cycle to the antimitotic effect of MCTP was not during the bulk of DNA synthesis [S phase] as was expected but occurred during the G_1 [DNA synthesis preparation] and early S phases. The apparent disconnection of DNA synthesis from mitosis suggests that one or more cell functions occurring early in the cycle [G_1-early S], unrelated

to the replication of DNA strands but important in nuclear and cellular division, may be involved in cell cycle arrest. The discussion in Chapter II describes other cell cycle arrest models which inhibit mitosis through the interruption of a cell cycle checkpoint just prior to or during mitosis [Figure 6]. It is apparent that additional work must be done to identify the mechanism responsible for this pattern of cell cycle arrest after MCTP, but the groundwork established by the present work provides the basis for additional characterization.

Although Chapter II has focused thinking as to the way MCTP interferes with mitosis, theories derived from that work must be applicable to MCTP-induced vascular toxicity *in vivo* to aid in understanding this model. As stated above, current technology does not allow the collection of pure populations of vascular wall cells from small pulmonary arteries, so the evaluation of cell cycle indices in microvascular endothelial cells *in situ* is not possible. In order to make *in vivo* associations to the cell cycle data generated in cultured cells, the measurement of effects of MCTP on cell replication parameters in small pulmonary arteries of the rat was done using indirect methods.

The initial *in vivo* evaluation, described in Chapter III, was designed to determine the effect of MCTP on endothelial cell replication and DNA synthesis in pulmonary arteries. Rats treated with MCTP developed an increase in endothelial cell DNA synthesis by day 3 after exposure, an increase that persisted beyond the establishment of pulmonary hypertension [ie, increased right heart weight]. Surprisingly, the prolonged increase in DNA replication *in*

vivo was not followed by an increase in the number of endothelial cells lining pulmonary arteries. Although different methods were used to measure the effect of MCTP on DNA synthesis and cell proliferation *in vivo* and *in vitro*, a pattern of persistent DNA replication without cell division was seen in both systems. These two systems were compared to determine if the exposure to MCTP and the response observed in each could support the possibility of a similar mechanism *in vivo* and *in vitro*. The pattern of the cell cycle phase during exposure and the time course of response to exposure in each system were examined.

As was described in Chapter II, only endothelial cells leaving G_1 and starting DNA synthesis were arrested. *In vivo*, endothelial cells reside predominantly in G_0-G_1 and have a very slow turnover rate, allowing the assumption that endothelial cells in a similar cycle phase pattern were affected by MCTP in the initial moments of exposure. The slow turnover of endothelial cells *in vivo* provides an explanation for the difference in the time of response to MCTP noted in these two exposure systems. *In vitro*, BEC exposure during G_1-early S phase was followed by the rapid progression of cells through the cell cycle, induced by their subconfluent state. As such, affected cells could express the effect of mitotic inhibition within a single cell cycle [ie, 24 hours]. By contrast, the effects of MCTP on DNA synthesis and cell proliferation *in vivo* were not identified until days 3 and 8, respectively. This delayed pattern, however, closely matches the time course of initial endothelial cell injury and loss which could act as a mitogenic stimulus [ie, loss of contact inhibition] after MCTP. As described

above, the effect of MCT[P] and other PAs on cell proliferation-associated events is enhanced by the addition of a growth stimulus [ie, subconfluence - (Hoorn and Roth, 1992); hepatic necrosis - (Samuel and Jago, 1975)].

The direct involvement of inhibition of endothelial cell proliferation *in vivo* in chronic pulmonary vascular disease after MCTP remains hypothetical. Inhibition of cell proliferation can delay the repair of injury and result in the persistence of a structural or functional disturbance in an organ. The present work could not define an association between delayed endothelial monolayer repair due to the inhibition of cell proliferation and pulmonary vascular leak. However, it is easy to speculate that the loss of endothelial cells due to the cytotoxic effect of MCTP creates a conduit for the escape of fluid from the blood. In theory, the ability of the endothelium to reform the monolayer and restore selective permeability to the lung vasculature may be lost by the inhibition of cell proliferation induced by MCTP. The result could be manifest as persistent vascular leak, a consistent component of the MCTP-induced pulmonary hypertension model. Furthermore, the outcome of persistent vascular leak after MCTP may result in the exposure of subintimal cells [ie, vascular smooth muscle cells] to mitogenic stimuli present in exuded plasma, resulting in the increase in medial thickness of pulmonary arteries which precedes and is probably responsible for hypertension.

The effect of MCTP on cell proliferation and DNA synthesis in vascular cells *in vivo* was carried a step further by the examination of vascular smooth

muscle cells comprising the medial layer of small pulmonary arteries. This analysis was done both to determine the morphology of artery medial thickening after MCTP and to attempt to confirm an effect of MCTP on proliferation of subintimal cells previously proposed in other nonvascular lung cells (Wilson and Segall, 1990). After the administration of MCTP to rats, DNA synthesis increased at 3 days and persisted for up to 8 days in smooth muscle cells, with the level of DNA synthesis 2-5 times higher than respective controls during that interval. By day 8, the pulmonary arterial pressure was increased [ie, right ventricular hypertrophy] and the medial thickness of pulmonary arteries was increased, but the density of smooth muscle cells comprising the thickened medial layer was unchanged. A review of the literature describing changes in VSMCs during the development of systemic hypertension suggests that smooth muscle cell hyperplasia would be the expected outcome of MCTP-induced injury to the pulmonary vasculature [see Chapter IV]. The results presented here, however, showed that medial thickening after MCTP was not the result of cell proliferation, and, although not confirmed directly by the measurement of smooth muscle cell size, was due to hypertrophy of vascular smooth muscle cells. The result suggested that MCTP may inhibit the proliferative response of smooth muscle cells as well as endothelial cells *in vivo*. Whether MCTP is a direct mitogenic stimulus for vascular smooth muscle cells *in vivo* or interferes with the completion of mitosis in a manner similar to that reported above is unclear.

The MCT[P]-induced pulmonary vascular disease model has been compared to two human diseases which similarly lack a defined cause but result in the development of chronic vascular disease and pulmonary hypertension. PPH and ARDS can cause progressive changes in the vascular wall morphology leading to an increase in pulmonary arterial pressure similar to that seen after the administration of MCTP. To date, much of the research comparing PPH and ARDS to MCTP-induced hypertension has focused on vascular remodeling by examining events which cause a change in arterial structure, compliance and resistance. The process[es] which precedes the development of arterial lesions characteristic of PPH have not been defined; PPH-associated vascular remodeling is often well advanced before diagnosis is made and predisposing causes of PPH are largely unknown. The early stages of ARDS have been more widely characterized, yet mechanisms responsible for acute pulmonary edema, pulmonary fibrosis and hypertension have been largely unexplored. The involvement of altered cell proliferation in either PPH or ARDS has yet to be determined.

In conclusion, the present work confirms that MCTP inhibits mitosis in ECs *in vitro*, and that inhibition of mitosis occurs through a cell cycle phase-specific process. *In vivo*, MCTP induces DNA synthesis at a level expected to result in cell replication, but replication does not follow. Similarities in the cycle phases exposed *in vivo* [G_0-G_1] to those most responsive to cell cycle inhibition *in vitro* [G_1-early S] suggest that a similar mechanism may be acting in both systems.

Improvement of the present methodologies [ie, cell cycle analysis *in situ*] will be necessary to confirm like mechanisms. In addition, medial thickening [VSMC hypertrophy] associated with the development of pulmonary hypertension after MCTP may be the result of incomplete mitogenesis, or may be initiated by the inhibition of mitosis in the presence of a proliferative stimulus [ie, cell injury and/or loss]. Whether MCTP gains access to subintimal cells to induce a direct effect was not determined in the present work. In the future, the identification of direct effects of MCTP on mechanisms of proliferation in endothelial and smooth muscle cells *in vivo* will provide an understanding of not only the MCT[P] model in rats, but potentially aid in uncovering the cause[s] of other forms of chronic injury resulting in pulmonary hypertension.

BIBLIOGRAPHY

AFZELIUS, B.A. and SCHOENTAL, R. (1967). The ultrastructure of the enlarged hepatocytes induced in rats with a single oral dose of retrorsine, a pyrrolizidine (*Senecio*) alkaloid. *J. Ultrastructural Res.* **20**:328-345.

ALBELDA, S.M. (1990). Role of growth factors in pulmonary hypertension. In *The Pulmonary Circulation: Normal and Abnormal. Mechanisms, Management, and the National Registry.* (A.P. Fishman, Ed.). pp. 201-215. University of Pennsylvania Press, Philadelphia.

ALBERTS, B., BRAY, D., LEWIS, J., RAFF, M., ROBERTS, K., WATSON, J.D. (1989). In *Molecular Biology of the Cell, 2nd ed.,* (B. Alberts et al, Eds.). Garland Publishing, New York.

ALLEN, J.R. and CARSTENS, L.A. (1970a). Clinical signs and pathologic changes in Crotalaria spectabilis-intoxicated rats. *Am. J. Vet. Res.* **31**(6):1059-1070.

ALLEN, J.R. and CARSTENS, L.A. (1970b). Pulmonary vascular occlusions initiated by endothelial lysis in monocrotaline-intoxicated rats. *Exp. Mol. Pathol.* **13**:159-171.

ALLEN, J.R. and CHESNEY, C.F. (1972). Effect of age on development of cor pulmonale in nonhuman primates following pyrrolizidine alkaloid intoxication. *Exp. Mol. Pathol.* **17**:220-232.

ALLEN, J.R., CARSTENS, L.A., OLSON, B.E. (1967). Veno-occlusive disease in *Macaca speciosa* monkeys. *Am. J. Pathol.* **50**(4):653-667

ALLEN, J.R., CARSTENS, L.A., NORBACK, D.H. (1970a). Ultrastructural and biochemical changes in the liver of monocrotaline intoxicated chickens. *Toxicol. Appl. Pharmacol.* **16**:800-806.

ALLEN, J.R., CARSTENS, L.A., NORBACK, D.H., LOH, P.M. (1970b). Ultrastructural and biochemical changes associated with pyrrolizidine-induced hepatic megalocytosis. *Cancer Res.* **30**:1857-1866.

ALLEN, J.R., CHESNEY, C.F., FRAZEE, W.J. (1972). Modifications of pyrrolizidine alkaloid intoxication resulting from altered hepatic microsomal enzymes. *Toxicol. Appl. Pharmacol.* **23**:470-479.

ALLEN, J.R., HSU, I-C., CARSTENS, L.A. (1975). Dehydroretronecine-induced rhabdomyosarcomas in rats. *Cancer Res.* **35**:997-1002.

ALTIERE, R.J., OLSON, J.W., GILLESPIE, M.N. (1986). Altered pulmonary vascular smooth muscle responsiveness in monocrotaline-induced pulmonary hypertension. *J. Pharmacol. Exp. Ther.* **236**(2):390-395.

ANDERSON, E.G., SIMON, G., REID, L. (1973). Primary and thrombo-embolic pulmonary hypertension: A quantitative pathological study. *J. Pathol.* **110**:273-293.

ANDREASSEN, P.R. and MARGOLIS, R.L. (1994). Microtubule dependency on $p34^{cdc2}$ inactivation and mitotic exit in mammalian cells. *J. Cell Biol.* **127**(3):789-802.

ARCOT, S.S., LIPKE, D.W., GILLESPIE, M.N., OLSON, J.W. (1993). Alterations of growth factor transcripts in rat lungs during development of monocrotaline-induced pulmonary hypertension. *Biochem. Pharmacol.* **46**(6):1086-1091.

ARMSTRONG, S.J., ZUCKERMAN, A.J., BIRD, R.G. (1972). Induction of morphological changes in human embryo liver cells by the pyrrolizidine alkaloid lasiocarpine. *Br. J. Exp. Pathol.* **53**:145-149.

ARSECULERATNE, S.N., GUNATILAKA, A.A.L., PANABOKKE, R.G. (1981). Studies on medicinal plants of Sri Lanka: Occurrence of pyrrolizidine alkaloids and hepatotoxic properties in some traditional medicinal herbs. *J. Ethnopharmacol.* **4**:159-177.

ARSECULERATNE, S.N., GUNATILAKA, A.A.L., PANABOKKE, R.G. (1985). Studies on medicinal plants of Sri Lanka. Part 14: Toxicity of some traditional medicinal herbs. *J. Ethnopharmacol.* **13**:323-335.

ATKINSON, B.F., KATZ, A.S., KNIGHT, D., PIETRA, G.G., FISHMAN, A.P. (1977). Monocrotaline-induced pulmonary hypertension in beagle puppies. *Lab. Invest.* **36**:354.

BAGBY, S.P., O'REILLY, M.M., KIRK, E.A., MITCHELL, L.H., STENBERG, P.E., MAKLER, M.T., BAKKE, A.C. (1992). EGF is incomplete mitogen in porcine aortic smooth muscle cells: DNA synthesis without cell division. *Am. J. Physiol.* **262**:C578-C588.

BARNES, J.M., MAGEE, P.N., SCHOENTAL, R. (1964). Lesions in the lungs and livers of rats poisoned with the pyrrolizidine alkaloid fulvine and its N-oxide. *J. Path. Bact.* **88**:521-531.

BAYBUTT, R.C., AZIZ, S.M., FAGERLAND, J.A., OLSON, J.W., GILLESPIE, M.N. (1994). Monocrotaline alters type II pneumocyte morphology and polyamine regulation. *Toxicol. Appl. Pharmacol.* **129**:188-195.

BERGMEYER, H.U. and BRENT, E. (1974). Lactate dehydrogenase UV assay with pyruvate and NADH. In *Methods of Enzymatic Analysis, Vol. 2.* (H.U. Bergmeyer, Ed.). pp 574-579. Academic Press, New York.

BHUYAN, B.K. and GROPPI, V.E. (1989). Cell cycle specific inhibitors. *Pharmacol. Ther.* **42**:307-348.

BJORNSSON, T.D., DRYJSKI, M., TLUCZEK, J., MENNIE, R., RONAN, J., MELLIN, T.N., THOMAS, K.A. (1991). Acidic fibroblast growth factor promotes vascular repair. *Proc. Natl. Acad. Sci. USA* **88**:8651-8655.

BOBIK, A. and CAMPBELL, J.H. (1993). Vascular derived growth factors: Cell biology, pathophysiology, and pharmacology. *Pharmacol. Rev.* **45**(1):1-42.

BOTNEY, M.D., BAHADORI, L., GOLD, L.I. (1994). Vascular remodeling in primary pulmonary hypertension: Potential role for transforming growth factor-β. *Am. J. Pathol.* **144**(2):286-295.

BOWDEN, D.H. (1983). Cell turnover in the lung. *Am. Rev. Respir. Dis.* **128**:S46-S48.

BRAS, G., BERRY, D.M., GYÖRGY, P. (1957). Plants as ætiological factor in veno-occlusive disease of the liver. *Lancet* **I**(272):960-962.

BRUGGEMAN, I.M. and VAN DER HOEVEN, J.C.M. (1985). Induction of SCEs by some pyrrolizidine alkaloids in V79 Chinese hamster cells co-cultured with chick embryo hepatocytes. *Mutation Res.* **142**:209-212.

BRUNER, L.H., HILLIKER, K.S., ROTH, R.A. (1983). Pulmonary hypertension and ECG changes from monocrotaline pyrrole in the rat. *Am. J. Physiol.* **245**:H300-H306.

BRUNER, L.H., CARPENTER, L.J., HAMLOW, P., ROTH, R.A. (1986). Effect of mixed function oxidase inducer and inhibitor on monocrotaline pyrrole pneumotoxicity. *Toxicol. Appl. Pharmacol.* **85**:416-427.

BUHLER, D.H., MIRANDA, C.L., KEDZIERSKI, B., REED, R.L. (1990). Mechanisms for pyrrolizidine alkaloid activation and detoxification. In *Biological Reactive Intermediates IV.* (C. M. Witmer et al, Ed.). pp.597-603. Plenum Press, New York.

BULL, L.B. (1955). The histological evidence of liver damage from pyrrolizidine alkaloids: Megalocytosis of the liver cells and Inclusion globules. *Aust. Vet. J.* **31**:33-40.

BULL, L.B. and DICK, A.T. (1959). The chronic pathological effects on the liver of the rat of the pyrrolizidine alkaloids heliotrine, lasiocarpine, and their N-oxides. *J. Path. Bact.* **78**:483-502.

BULL, L.B. and DICK, A.T. (1960). The function of total dose in the production of chronic lethal liver disease in rats by periodic injections of the pyrrolizidine alkaloid, heliotrine. *Aust. J. Exp. Biol.* **38**:515-524.

BULL, L.B., CULVENOR, C.C.J., DICK, A.T. (1968). *The Pyrrolizidine Alkaloids: Their Chemistry, Pathogenicity and Other Biological Properties*. (A. Neuberger and E.L. Tatum., Eds). North-Holland Publishing Co. Amsterdam.

BUTLER, W.H. (1970). An ultrastructural study of the pulmonary lesion induced by pyrrole derivatives of the pyrrolizidine alkaloids. *J. Pathol.* **102**:15-19.

BUTLER, W.H., MATTOCKS. A.R., BARNES, J.M. (1970). Lesions in the liver and lungs of rats given pyrrole derivatives of pyrrolizidine alkaloids. *J. Pathol.* **100**:169-175.

CACOUB, P., DORENT, R., NATAF, P., HOUPPE, J.P., PIETTE, J.C., GODEAU, P., GANDJBAKHCH, I. (1995). Pulmonary hypertension and dexfenfluramine. *Eur. J. Clin. Pharmacol.* **48**:81-83.

CAMPBELL, J.H., RENNICK, R.E., KALEVITCH, S.G., CAMPBELL, G.R. (1992). Heparan sulfate-degrading enzymes induce modulation of smooth muscle phenotype. *Exp. Cell Res.* **200**:156-167.

CANDRIAN, U., LÜTHY, J., SCHLATTER, C. (1985). In vivo covalent binding of retronecine-labelled [^{3}H]seneciphylline and [^{3}H]senecionine to DNA of rat liver, lung and kidney. *Chem. -Biol. Interactions* **54**:57-69.

CHEEKE, P.R. (1988). Toxicity and metabolism of pyrrolizidine alkaloids. *J. Anim. Sci.* **66**:2343-2350.

CHEEKE, P.R. (1989). Pyrrolizidine alkaloid toxicity and metabolism in laboratory animals and livestock. In *Toxicants of Plant Origin - Volume I: Alkaloids*. (P.R. Cheeke, Ed.). pp 1-22. CRC Press, Inc., Boca Raton.

CHEEKE, P.R. (1994). A review of the functional and evolutionary roles of the liver in the detoxification of poisonous plants, with special reference to pyrrolizidine alkaloids. *Vet. Human Toxicol.* **36**(3):240-247.

CHEEKE, P.R. and PIERSON-GOEGER, M.L. (1983). Toxicity of *Senecio jacobaea* and pyrrolizidine alkaloids in various laboratory animals and avian species. *Toxicol. Lett.* **18**:343-349.

CHESNEY, C.F. and ALLEN, J.R. (1973a). Monocrotaline-induced pulmonary vascular lesions in nonhuman primates. *Cardiovascular Res.* **7**:508-518.

CHESNEY, C.F. and ALLEN, J.R. (1973b). Resistance of the guinea pig to pyrrolizidine alkaloid intoxication. *Toxicol. Appl. Pharmacol.* **26**:385-392.

CHESNEY, C.F., ALLEN, J.R., HSU, I-C. (1974a). Right ventricular hypertrophy in monocrotaline pyrrole treated rats. *Exp. Mol. Pathol.* **20**:257-268.

CHESNEY, C.F., HSU, I-C., ALLEN, J.R. (1974b). Modifications of the *in vitro* metabolism of the hepatotoxic pyrrolizidine alkaloid, monocrotaline. *Res. Commun. Chem. Path. Pharmacol.* **8**(3):567-570.

CHRISTIE, G.S. (1958). Liver damage in acute heliotrine poisoning: 1. Structural changes. *Aust. J. Exp. Biol.* **36**:405-412.

CLOWES, A.W., REIDY, M.A., CLOWES, M.M. (1983). Kinetics of cellular proliferation after arterial injury: I. Smooth muscle growth in the absence of endothelium. *Lab. Invest.* **49**(3):327-333.

COLLINS, T, POBER, J.S., GIMBRONE Jr., M.A., HAMMACHER, A., BETSHOLTZ, C., WESTERMARK, B., HELDIN, C-H. (1987). Cultured human endothelial cells express platelet-derived growth factor. *Am. J. Pathol.* **127**:7-12.

COOMBER, B.L. (1992). Influence of mitomycin C on endothelial monolayer regeneration *in vitro*. *J. Cell. Biochem.* **50**:293-300.

COTRAN, R.S., KUMAR, V., ROBBINS, S.L. (1994). In *Robbins Pathologic Basis of Disease*, 5th Edition. (R.S. Cotran, V. Kumar, S.L. Robbins, Ed.) W.B. Saunders Co., Philadelphia, PA.

CULVENOR, C.C.J. (1980). Alkaloids and human disease. In *Toxicology in the Tropics*. (B.L. Smith and E.A. Bababunmi, Eds.) pp 124-141. Taylor and Francis, Ltd., London.

CULVENOR, C.C.J., DANN, A.T., DICK, A.T. (1962). Alkylation as the mechanism by which the hepatotoxic pyrrolizidine alkaloids act on cell nuclei. *Nature* **195**:570-573.

CULVENOR, C.C.J., DOWNING, D.T., EDGAR, J.A. (1969). Pyrrolizidine alkaloids as alkylating and antimitotic agents. *Ann. N.Y. Acad. Sci.* **168**:837-847.

CULVENOR, C.C.J., EDGAR, J.A., JAGO, M.V., OUTTERIDGE, A., PETERSON, J.E., SMITH, L.W. (1976). Hepato- and pneumotoxicity of pyrrolizidine alkaloids and derivatives in relation to molecular structure. *Chem. - Biol. Interactions* **12**:299-324.

CUNNINGHAM, A.J. (1991). Acute respiratory distress syndrome - Two decades later. *Yale J. Biol. Med.* **64**:387-402.

CUEVAS, P., GONZALEZ, A.M., CARCELLER, F., BAIRD, A. (1991). Vascular response to basic fibroblast growth factor when infused onto the normal adventitia or into the injured media of the rat carotid artery. *Circ. Res.* **69**:360-369.

DATTA, N.S., WILLIAMS, J.L., CALDWELL, J., CURRY, A.M., ASHCRAFT, E.K., LONG, M.W. (1996). Novel alterations in CDK1/Cyclin B1 kinase complex formation occur during the acquisition of a polyploid DNA content. *Mol. Biol. Cell* **7**:209-223.

DAVIDSON, J. (1935). The action of retrorsine on rats liver. *J. Pathol.* **40**:285-295.

DAVIES, P., BURKE, G., REID, L. (1986). The structure of the wall of the rat intraacinar pulmonary artery: An electron microscopic study of microdissected preparations. *Microvascular Res.* **32**:50-63.

DELEVE, L., WANG, X., KUHLENKAMP, J.F., KAPLOWITZ, N. (1996). Toxicity of azathioprine and monocrotaline in murine sinusoidal endothelial cells and hepatocytes: The role of glutathione and relevance to hepatic venoocclusive disease. *Hepatology* **23**:589-599.

DEYO, J.A. and KERKVLIET, N.I. (1990). Immunotoxicity of the pyrrolizidine alkaloid monocrotaline following subchronic administration to C57BL/6 mice. *Fundam. Appl. Toxicol.* **14**:842-849.

DEYO, J.A. and KERKVLIET, N.I. (1991). Tier-2 studies on monocrotaline immunotoxicity in C57BL/6 mice. *Toxicology* **70**:313-325.

DEYO, J.A., REED, R.L., BUHLER, D.R., KERKVLIET, N.I. (1994). Role of metabolism in monocrotaline-induced immunotoxicity in C57BL/6 mice. *Toxicology* **94**:209-222.

DICKENSON, J.O., COOKE, M.P., KING, R.R., MOHAMED, R.A. (1976). Milk transfer of pyrrolizidine alkaloids in cattle. *J. Amer. Vet. Med. Assoc.* **169**(11):1192-1196.

DOLBEARE, F., GRATZNER, H., PALLAVINCINI, M.G., GRAY, J.W. (1983). Flow cytometric measurement of total DNA content and incorporated bromodeoxyuridine. *Proc. Natl. Acad. Sci. USA* **80**:5573-5577.

DORÉE, M., GALAS, S. (1994). The cyclin-dependent protein kinases and the control of cell division. *FASEB. J.* **8**:1114-1121.

DOWNING, D.T. and PETERSON, J.E. (1968). Quantitative assessment of the persistent antimitotic effect of certain hepatotoxic pyrrolizidine alkaloids on rat liver. *Aust. J. Exp. Biol. Med. Sci.* **46**:493-502.

DUEKER, S.R., LAMÈ, J.W., MORIN, D., WILSON, D.W., SEGALL, H.J. (1992a). Guinea pig and rat microsomal metabolism of monocrotaline. *Drug Metab. Dispos.* **20**(2):275-280.

DUEKER, S.R., LAMÈ, J.W., SEGALL, H.J. (1992b). Hydrolysis of pyrrolizidine alkaloids by guinea pig hepatic carboxylesterases. *Toxicol. Appl. Pharmacol.* **117**:116-121.

ELLEDGE, S.J. (1996). Cell cycle checkpoints: Preventing an identity crisis. *Science* **274**:1664-1671.

ENGELBERG, H. (1989). Endothelium in health and disease. *Semin. Thromb. Hemost.* **15**(2):178-182.

EPSTEIN, R.B., MIN, K.W., ANDERSON,S.L., SYZEK, L. (1992). A canine model for hepatic veno-occlusive disease. *Transplantation* **54**:12-16.

ESTEP, J.E., LAMÈ, M.W., SEGALL, H.J. (1990a). Excretion and blood radioactivity levels following [^{14}C]senecionine administration to the rat. *Toxicology* **64**:179-189.

ESTEP, J.E., LAMÈ, M.W., JONES, A.D., SEGALL, H.J. (1990b). N-acetylcysteine-conjugated pyrrole identified in rat urine following administration of two pyrrolizidine alkaloids, monocrotaline and senecionine. *Toxicol. Lett.* **54**:61-69.

ESTEP, J.E., LAMÈ, M.W., MORIN, D., JONES, A.D., WILSON, D.W., SEGALL, H.J. (1991). [^{14}C]monocrotaline kinetics and metabolism in the rat. *Drug Metab. Dispos.* **19**(1):135-139.

ETTENSON, D.S. and GOTLIEB, A.I. (1992). Centrosomes, microtubule, and microfilaments in the reendothelialization and remodeling of double-sided *in vitro* wounds. *Lab. Invest.* **66**(6):722-733.

ETTENSON, D.S. and GOTLIEB, A.I. (1994). Endothelial wounds with disruption in cell migration repair primarily by cell proliferation. *Microvascular Res.* **48**:328-337.

FARHAT, M.Y., CHEN, M-F., BHATTI, T., IQBAL, A., CATHAPERMAL, S., RAMWELL, P.W. (1993). Protection by oestradiol against the development of cardiovascular changes associated with monocrotaline pulmonary hypertension in rats. *Br. J. Pharmacol.* **110**:719-723.

FISHMAN, A.P. and PIETRA, G.G. (1980). Primary pulmonary hypertension. *Ann. Rev. Med.* **31**:421-431.

FRAYSSINET, C. and MOULÈ, Y. (1969). Effect of lasiocarpine on transcription in liver cells. *Nature* **223**:1269-1270.

FULTON, R.M., HUTCHINSON, E.C., JONES, A.M. (1952). Ventricular weight in cardiac hypertrophy. *Br. Heart J.* **14**:413-420.

GABBIANI, G., KOCKER, O., BLOOM, W.S., VANDEKERCKHOVE, J., WEBER, K. (1984). Actin expression in smooth muscle cells of rat aortic intimal thickening, human atheromatous plaque and cultured rat aortic media. *J. Clin. Invest.* **73**:148-152.

GANEY, P.E., FINK, G.D., ROTH, R.A. (1985). The effect of dietary restriction and altered sodium intake on the cardiopulmonary toxicity or monocrotaline pyrrole. *Toxicol. Appl. Pharmacol.* **78**:55-62.

GANEY, P.E., HILLIKER-SPRUGEL, K., HADLEY, K.B., ROTH, R.A. (1986). Monocrotaline pyrrole-induced cardiopulmonary toxicity is not altered by metergoline or ketanserin. *J. Pharmacol. Exp. Ther.* **237**(1):226-231.

GANEY, P.E., HILLIKER-SPRUGEL, K., WHITE, S.M., WAGNER, J.G., ROTH, R.A. (1988). Pulmonary hypertension due to monocrotaline pyrrole is reduced by moderate thrombocytopenia. *Am. J. Physiol.* **255**:H1165-H1172.

GANEY, P.E., and ROTH, R.A. (1987). Thromboxane does not mediate pulmonary vascular response to monocrotaline pyrrole. *Am. J. Physiol.* **252**:H743-H748.

GANEY, P.E. and ROTH, R.A. (1988a). 6-Keto prostaglandin $F_{1\alpha}$ and thromboxane B_2 in isolated, buffer-perfused lungs from monocrotaline pyrrole-treated rats. *Exp. Lung Res.* **12**:195-206.

GANEY, P.E. and ROTH, R.A. (1988b). 6-Ketoprostaglandin $F_{1\alpha}$ and thromboxane B_2 in isolated, blood-perfused lungs from monocrotaline pyrrole-treated rats. *J. Toxicol. Environ. Health* **23**:127-137.

GHANEM, J. and HERSHKO, C. (1981). Veno-occlusive disease and primary hepatic vein thrombosis in Israeli Arabs. *Israel J. Med. Sci.* **17**(5):339-347.

GHODSI, F. and WILL, J.A. (1981). Changes in pulmonary structure and function induced by monocrotaline intoxication. *Am. J. Physiol.* **240**:H149-H155.

GILLESPIE, M.N., DYER, K.K., OLSON, J.W., O'CONNOR, W.N., ALTIERE, R.J. (1985a). α-Difluoromethylornithine, an inhibitor of polyamine synthesis, attenuates monocrotaline-induced pulmonary vascular hyperresponsiveness in isolated perfused rat lungs. *Res. Commun. Chem. Pathol. Pharmacol.* **50**(3):365-378.

GILLESPIE, M.N., FREDERICK, W.B., ALTIERE, R.J., OLSON, J.W., KIMMEL, E.C. (1985b). Pulmonary mechanical, ventilatory, and gas exchange abnormalities in rats with monocrotaline-induced pulmonary hypertension. *Exp. Lung. Res.* **8**:191-199.

GILLESPIE, M.N., OLSON, J.W., REINSEL, C.N., O'CONNOR, W.N., ALTIERE, R.J. (1986). Vascular hyperresponsiveness in perfused lungs from monocrotaline-treated rats. *Am. J. Physiol.* **251**:H109-H114.

GILLESPIE, M.N., GOLDBLUM, S.E., COHEN, D.A., McCLAIN, C.J. (1988). Interleukin 1 bioactivity in the lungs of rats with monocrotaline-induced pulmonary hypertension. *Proc. Soc. Exp. Biol. Med.* **187**:26-32.

GILLESPIE, M.N., OLSON, J.W., HENNIG, B., COHEN, D.A., McCLAIN, C.J., GOLDBLUM, S.E. (1989a). Monokine-induced lung injury in rats: Similarities to monocrotaline-induced pneumotoxicity. *Toxicol. Appl. Pharmacol.* **98**:134-143.

GILLISPIE, M.N., RIPPETOE, P.E., HAVEN, C.A., SHIAO, R-T., ORLINSKA, U., MALEY, B.E., OLSON, J.W. (1989b). Polyamines and epidermal growth factor in monocrotaline-induced pulmonary hypertension. *Am. Rev. Respir. Dis.* **140**:1463-1466.

GILLIS, C.N. (1973). Metabolism of vasoactive hormones by the lung. *Anesthesiology* **39**:626-632.

GILLIS, C.N., HUXTABLE, R.J., ROTH, R.A. (1978). Effects of monocrotaline pretreatment of rats on removal of 5-hydroxytryptamine and noradrenaline by perfused lung. *Br. J. Pharmacol.* **63**:435-443.

GLOWAZ, S.L., MICHNIKA, M., HUXTABLE, R.J. (1992). Detection of a reactive pyrrole in the hepatic metabolism of the pyrrolizidine alkaloid, monocrotaline. *Toxicol. Appl. Pharmacol.* **115**:168-173.

GOEGER, D.E., CHEEKE, P.R., SCHMITZ, J.A., BUHLER, D.R. (1982). Toxicity of tansey ragwort (*Senecio jacobaea*) to goats. *Am. J. Vet. Res.* **43**(2):252-254.

GOLDBERG, I.D., STEMERMAN, M.B., SCHNIPPER, L.E., RANSIL, B.J., CROOKS, G.W., FUHRO, R.L. (1979). Vascular smooth muscle cell kinetics: A new assay for studying patterns of cell proliferation *in vivo*. *Science* **205**:920-922.

GOLDENTHAL, E.I., D'AGUANNO, W.D., LYNCH, J.F. (1964). Hormonal modification of the sex differences following monocrotaline administration. *Toxicol. Appl. Pharmacol.* **6**:434-441.

GRAY, J.W., DOLBEARE, F., PALLAVINCINI, M.G., BEISKER, W., WALDMAN, F. (1986). Cell cycle analysis using flow cytometry. *Int. J. Radiat. Biol.* **49**(2):237-255.

GREEN, C.R. and CHRISTIE, G.S. (1961). Malformations in foetal rats induced by the pyrrolizidine alkaloid, heliotrine. *Br. J. Exp. Pathol.* **42**:369-378.

GROTENDORST, G.R., CHANG, T., SEPPÄ, H.E.J., KLEINMAN, H.K., MARTIN, G.R. (1982). Platelet-derived growth factor is a chemoattractant for vascular smooth muscle cells. *J. Cell. Physiol.* **113**:261-266.

HACKER, A.D. (1992). Inhibition of deoxyribonucleic acid synthesis by difluoromethylornithine: Role of polyamine metabolism in monocrotaline-induced pulmonary hypertension. *Biochem. Pharmacol.* **44**(5):965-971.

HACKER, A.D. (1993). Dietary restriction, polyamines and monocrotaline-induced pulmonary hypertension. *Biochem. Pharmacol.* **45**(12):2475-2481.

HAMILTON, J.A., VAIRO, G., COCKS, B.G. (1992). Inhibition of S-phase progression in macrophages is linked to G1/S-phase suppression of DNA synthesis genes. *J. Immunol.* **148**(12):4028-4035.

HARDING, J.D.J., LEWIS, G., DONE, G.T., ALLCROFT, R. (1964). Experimental poisoning by Senecio jacobaea in pigs. *Path. Vet.* **1**:204-220.

HARRIS, P.N., ANDERSON, R.C., CHEN, K.K. (1942). The action of monocrotaline and retronecine. *J. Pharmacol. Exp. Ther.* **75**:78-82.

HARTWELL, L.H., WEINERT, T.A. (1989). Checkpoints: Controls that ensure the order of cell cycle events. *Science* **246**:629-634.

HAWN, M.T., UMAR, A., CARETHERS, J.M., GIANCARLO, M., KUNKEL, T.A., BOLAND, C.R., KOI, M. (1995). Evidence for a connection between the mismatch repair system and the G2 cell cycle checkpoint. *Cancer Res.* **55**:3721-3725.

HAYASHI, Y. and LALICH, J.J. (1967). Renal and pulmonary alterations induced in rats by a single injection of monocrotaline. *Proc. Soc. Exp. Biol. Med.* **124**:392-396.

HAYASHI, Y., KATO, M., OTSUKA, H. (1979). Inhibitory effects of diet-reduction on monocrotaline intoxication in rats. *Toxicol. Lett.* **3**:151-155.

HAYASHI, Y., KOKUBO, T., TAKAHASHI, M., FURUKAWA, F., OTSUKA, H., HASHIMOTO, K. (1984). Correlative morphological and biochemical studies on monocrotaline-induced pulmonary alterations in rats. *Toxicol. Lett.* **21**:65-71.

HEATH, D. (1992). The rat is a poor model for the study of human pulmonary hypertension. *Cardioscience* **3**(1):1-6.

HEATH, D., SHABA, J., WILLIAMS, A., SMITH, P., KOMBE, A. (1975). A pulmonary hypertension-producing plant from Tanzania. *Thorax* **30**:399-404.

HEATH, D. and SMITH, P. (1977). Pulmonary vascular disease. *Med. Clin. North Am.* **61**(6):1279-1307.

HEATH, D. and SMITH, P. (1979). Pulmonary vascular disease secondary to lung disease. In *Pulmonary Vascular Diseases.* (K.M. Moser, Ed.) pp 387-426. Marcel Dekker, Inc. New York.

HEBY, O. (1981). Role of polyamines in the control of cell proliferation and differentiation. *Differentiation* **19**:1-20.

HENDRICKS, J.D., SINNHUBER, R.O., HENDERSON, M.C., BUHLER, D.R. (1981). Liver and kidney pathology in rainbow trout (*Salmo gairdneri*) exposed to dietary pyrrolizidine (*Senecio*) alkaloids. *Exp. Mol. Pathol.* **35**:170-183.

HERBST, H., MILANI, S., SCHUPPAN, D., STEIN, H. (1991). Temporal and spatial patterns of proto-oncogene expression at early stages of toxic liver injury in the rat. *Lab. Invest.* **65**(3):324-333.

HILL, N.S., JEDERLINIC, P., GAGNON, J. (1989). Supplemental oxygen reduces right ventricular hypertrophy in monocrotaline-injected rats. *J. Appl. Physiol.* **66**(4):1642-1648.

HILLIKER, K.S., BELL, T.G., ROTH, R.A. (1982). Pneumotoxicity and thrombocytopenia after single injection of monocrotaline. *Am. J. Physiol.* **242**:H573-H579.

HILLIKER, K.S., GARCIA, C.M., ROTH, R.A. (1983). Effects of monocrotaline and monocrotaline pyrrole on 5-hydroxytrptamine and paraquat uptake by lung slices. *Res. Commun. Chem. Path. Pharmacol.* **40**(2):179-197.

HILLIKER, K.S., BELL, T.G., LORIMER, D., ROTH, R.A. (1984). Effects of thrombocytopenia on monocrotaline pyrrole-induced pulmonary hypertension. *Am. J. Physiol.* **246**:H747-H753.

HILLIKER, K.S. and ROTH, R.A. (1984). Alteration of monocrotaline pyrrole-induced cardiopulmonary effects in rats by hydrallazine, dexamethasone or sulphinpyrazone. *Br. J. Pharmacol.* **82**:375-380.

HILLIKER, K.S. and ROTH, R.A. (1985a). Increased vascular responsiveness in lungs of rats with pulmonary hypertension induced by monocrotaline pyrrole. *Am. Rev. Respir. Dis.* **131**:46-50.

HILLIKER, K.S. and ROTH, R.A. (1985b). Injury to the isolated, perfused lung by exposure *in vitro* to monocrotaline pyrrole. *Exp. Lung Res.* **8**:201-212.

HINCKS, J.R., KIM, H-Y., SEGALL, H.G., MOLYNEUX, R.J., STERMITZ, F.R., COULOMBE Jr., R.A. (1991). DNA cross-linking in mammalian cells by pyrrolizidine alkaloids: Structure-activity relationships. *Toxicol. Appl. Pharmacol.* **111**:90-98.

HIRONO, I., MORI, H., YAMADA, K., HIRATA, Y., HAGA, M., TATEMATSU, H., KANIE, S. (1977). Carcinogenic activity of petasitenine, a new pyrrolizidine alkaloid isolated from *Petasites japonicus* maxim. *J. Natl. Cancer Inst.* **58**(4):1155-1157.

HISLOP, A. and REID, L. (1974). Arterial changes in *Crotalaria spectabilis*-induced pulmonary hypertension in rats. *Br. J. Exp. Pathol.* **55**:153-163.

HOLTER, J.F., WEILAND, J.E., PACHT, E.R., GADEK, J.E., DAVIS, W.B. (1986). Protein permeability in the adult respiratory distress syndrome: Loss of size selectivity of the alveolar epithelium. *J. Clin. Invest.* **78**:1513-1522.

HOOPER, P.T. (1974). The pathology of *Senecio jacobaea* poisoning of mice. *J. Pathol.* 113(4):227-230.

HOOPER, P.T.and SCANLON, W.A. (1977). *Crotalaria retusa* poisoning of pigs and poultry. *Aust. Vet. J.* **53**:109-114.

HOORN, C.M. (1994). Effects of mitomycin C on RNA and protein synthesis in cultured endothelium. *FASEB J.* **8**(4 pt4):A148 (abstract).

HOORN, C.M. and ROTH, R.A. (1992). Monocrotaline pyrrole alters DNA, RNA and protein synthesis in pulmonary artery endothelial cells. *Am. J. Physiol.* **262**:L740-L747.

HOORN, C.M. and ROTH, R.A. (1993). Monocrotaline pyrrole-induced changes in angiotensin-converting enzyme activity of cultured pulmonary artery endothelial cells. *Br. J. Pharmacol.* **110**:597-602.

HOORN, C.M., WAGNER, J.W., ROTH, R.A.(1993). Effects of monocrotaline pyrrole on cultured rat pulmonary endothelial cells. *Toxicol. Appl. Pharmacol.* **120**:281-287.

HOORN, C.M., WAGNER, J.G., PETRY, T.W., ROTH, R.A. (1995). Toxicity of mitomycin C toward cultured pulmonary artery endothelium. *Toxicol. Appl. Pharmacol.* **130**:87-94.

HOOSON, J. and GRASSO, P. (1976). Cytotoxic and carcinogenic response to monocrotaline pyrrole. *J. Pathol.* **118**:121-128.

HSU, I-C., CHESNEY, C.F., ALLEN, J.R. (1973). Chronic effects of monocrotaline pyrrole on hepatic mitosis and DNA synthesis. *Proc. Soc. Exp. Biol. Med.* **147**:1133-1136.

HSU, I-C., ROBERTSON, K.A., ALLEN J.R. (1976). Tissue distribution, binding properties and lesions produced by dehydroretronecine in the nonhuman primate. *Chem. -Biol. Interactions* **12**:19-28.

HUBERMAN, J.A. (1981). New views of the biochemistry of eukaryotic DNA replication revealed by aphidicolin, an unusual inhibitor of DNA polymerase α. *Cell* **23**:647-648.

HURLEY, J.V., JAGO, M.V. (1975). Pulmonary edema in rats given dehydromonocrotaline: A topographic and electron microscopic study. *J. Pathol.* **117**:23-32.

HUXTABLE, R.J. (1980). Herbal teas and toxins: Novel aspects of pyrrolizidine poisoning in the United States. *Prosp. Biol. Med.* **24**(1):1-14.

HUXTABLE, R.J. (1989). Human health implications of pyrrolizidine alkaloids and herbs containing them. In *Toxicants of Plant Origin - Volume I: Alkaloids*. (P. R. Cheeke, Ed.). pp 41-86. CRC Press, Inc., Boca Raton.

HUXTABLE, R.J. (1990). Activation and pulmonary toxicity of pyrrolizidine alkaloids. *Pharmacol. Ther.* **47**:371-389.

HUXTABLE, R.J., PAPLANUS, S., LAUGHARN, J. (1977). The prevention of monocrotaline-induced right ventricular hypertrophy. *Chest* **71**(Suppl.):308-312.

HUXTABLE, R., CIARAMITARO, D., EISENSTEIN, D. (1978). The effect of a pyrrolizidine alkaloid, monocrotaline, and a pyrrole, dehydroretronecine, on the biochemical functions of the pulmonary endothelium. *Mol. Pharmacol.* **14**:1189-1203.

HUXTABLE, R.J., BOWERS, R., MATTOCKS, A.R., MICHNICKA, M. (1990). Sulfur conjugates as putative pneumotoxic metabolites of the pyrrolizidine alkaloid, monocrotaline. In *Biological Reactive Intermediates IV*. (C. M. Witmer, R.R. Snyder, D.J. Jollow, G.F. Kalf, J.J. Kocsis, I.G. Sipes, Eds). pp.605-611. Plenum Press, New York.

ILKIW, R., TODOROVICH-HUNTER, L., MARUYAMA, K., SHIN, J., RABINOVITCH, M. (1989). SC-39026, a serine elastase inhibitor, prevents muscularization of peripheral arteries, suggesting a mechanism of monocrotaline-induced pulmonary hypertension. *Circ. Res.* **64**:814-825.

ISHIDA, R., SATO, M., NARITA, T., UTSUMI, K.R., NISHIMOTO, T., MORITA T., HAGATA, H., ANDOH, T. (1994). Inhibition of DNA topoisomerase II by ICRF-193 induces polyploidization by uncoupling chromosome dynamics from other cell cycle events. *J. Cell Biol.* **126**(6):1341-1351.

ITO, K., NAKASHIMA, T., MURAKAMI, K., MURAKAMI, T. (1988). Altered function of pulmonary endothelium following monocrotaline-induced lung vascular injury in rats. *Br. J. Pharmacol.* **94**:1175-1183.

JACKSON, C.L. and SCHWARTZ, S.M. (1992). Pharmacology of smooth muscle cell replication. *Hypertension* **20**:713-736.

JAGO, M.V. (1969). The development of the hepatic megalocytosis of chronic pyrrolizidine alkaloid poisoning. *Am. J. Pathol.* **56**(3):405-422.

JAGO, M.V. (1970). A method for the assessment of the chronic hepatotoxicity of pyrrolizidine alkaloids. *Aust. J. Exp. Biol. Med. Sci.* **48**:93-103.

JAWIEN, A., BOWEN-POPE, D.F., LINDER, V., SCHWARTZ, S.M., CLOWES, A.W. (1992). Platelet-derived growth factor promotes smooth muscle migration and intimal thickening in a rat model of balloon angioplasty. *J. Clin Invest.* **89**:507-511.

JOHNSON, A.E. and MOLYNEUX, R.J. (1984). Toxicity of threadleaf groundsel (*Senecio douglasii* var *longilobus*) to cattle. *Am. J. Vet. Res.* **45**(1):26-31.

JOHNSON, A.E., MOLYNEUX, R.J., STUART, L.D. (1985). Toxicity of Riddel's groundsel (*Senecio riddellii*) to cattle. *Am. J. Vet. Res.* **46**(3):577-582.

JONES, R. and REID, L. (1991). Pulmonary vascular changes in adult respiratory distress syndrome. In *Adult Respiratory Distress Syndrome.* (E.A. Artigas, F. Lemaire, P.M. Suter, W.M. Zapol, Eds). Pp 33-43. Churchill Livingstone, UK.

KAMEJI, R., OTSUKA, H., HAYASHI, Y. (1980). Increase of collagen synthesis in pulmonary arteries of monocrotaline-treated rats. *Experimentia* **36**:441-442.

KANAI, Y., HORI, S., TANAKA, T., YASUOKA, M., WATANABE, K., AIKAWA, N., HOSODA, Y. (1993). Role of 5-hydroxytryptamine in the progression of monocrotaline-induced pulmonary hypertension in rats. *Cardiovascular Res.* **27**:1619-1623.

KATAYAMA, Y., HATANAKA, K., HAYASHI, T., ONODA, K., YADA, I., NAMIKAWA, S.,YUASA, H., KUSAGAWA, M., MARUYAMA, K., KITABATAKE, M. (1994). Effects of inhaled nitric oxide in rats with chemically-induced pulmonary hypertension. *Resp. Physiol.* **97**:301-307.

KATO, T., KITAMURA, H., KANISAWA, M. (1989). Comparative effects of isosorbide dinitrate, prednisolone, indomethacin and elastase on the development of monocrotaline-induced pulmonary hypertension. *Exp. Mol. Pathol.* **50**:303-315.

KAUFMANN, W.K. and PAULES, R.S. (1996). DNA damage and cell cycle checkpoints. *FASEB J.* **10**:238-247.

KAY, J.M. and HEATH, D. (1966). Observations on the pulmonary arteries and heart weight of rats fed on *Crotalaria spectabilis* seeds. *J. Path. Bact.* **92**:385-394.

KAY, J.M. and HEATH, D. (1969). *Crotalaria spectabilis*: The pulmonary hypertension plant. Charles C. Thomas Publishing, Springfield, Illinois.

KAY, J.M., HARRIS, P., HEATH, D. (1967). Pulmonary hypertension produced in rats by ingestion of Crotalaria spectabilis seeds. *Thorax* **22**:176-179.

KAY, J.M., SMITH, P., HEATH, D. (1969). Electron microscopy of *Crotalaria* pulmonary hypertension. *Thorax* **24**:511-526.

KAY, J.M., HEATH, D., SMITH, P., BRAS, G., SUMMERELL, J. (1971). Fulvine and the pulmonary circulation. *Thorax* **26**:249-261.

KAY, J.M., SUYAMA, K.L., KEANE, P.M. (1982). Failure to show decrease in small pulmonary blood vessels in rats with experimental pulmonary hypertension. *Thorax* **37**:927-930.

KAY, J.M., KEANE, P.M., SUYAMA, K.L. (1985). Pulmonary hypertension induced in rats by monocrotaline and chronic hypoxia is reduced by p-chlorophenylalanine. *Respiration* **47**:48-56.

KHARBANDA, S., YUAN, Z-M., TANEJA, N., WEICHSELBAUM, R., KUFE, D. (1994). P56/p53^{lyn} tyrosine kinase activation in mammalian cells treated with mitomycin C. *Oncogene* **9**:3005-3011.

KIDO, M., HIROSE, T., TANAKA, K., KUROZUMI, T., SHOYAMA, Y. (1981). Increased alveolar-capillary membrane permeability by monocrotaline. *Japan. J. Med.* **20**(3):170-179.

KIM, H-Y., STERMITZ, F.R., MOLYNEUX, R.J., WILSON, D.W., TAYLOR, D., COULOMBE Jr., R.A. (1993). Structural influences on pyrrolizidine alkaloid-induced cytopathology. *Toxicol. Appl. Pharmacol.* **122**:61-69.

KIYATAKE, K., KANNEKO, N., OKADA, O., KAKUSAKA, I., NAGAO, K., KURIYAMA, T. (1992). Role of liver microsome for sexual difference in monocrotaline treated rats. A*m. Rev. Respir. Dis.* **145**:A620.

KOVACH, J.S., AMES, R.R., POWIS, G., MOERTEL, C.G., HAHN, R.G., CREAGAN, E.T. (1979). Toxicity and pharmacokinetics of a pyrrolizidine alkaloid, indicine N-oxide, in humans. *Cancer Res.* **39**:4540-4544.

KUMANA, C.R., NG, M., LIN, H.J., KO, W., WU, P-C., TODD, D. (1983). Hepatic veno-occlusive disease due to toxic alkaloid in herbal tea. *Lancet* **II**(8363):1360-1361.

KUMANA, C.R., NG, M., LIN, H.J., KO, W., WU, P-C., TODD, D. (1985). Herbal tea induced hepatic veno-occlusive disease: Quantification of toxic alkaloid exposure in adults. *Gut* **26**:101-104.

KUROZUMI, T., TANAKA, K., KIDO, M., SHOYAMA, Y. (1983). Monocrotaline-induced renal lesions. *Exp. Mol. Pathol.* **39**:377-386.

LAFRANCONI, W.M. and HUXTABLE, R.J. (1983). Changes in angiotensin-converting enzyme activity in lungs damaged by the pyrrolizidine alkaloid monocrotaline. *Thorax* **38**:307-309.

LAFRANCONI, W.M. and HUXTABLE, R.J. (1984). Hepatic metabolism and pulmonary toxicity of monocrotaline using isolated perfused liver and lung. *Biochem. Pharmacol.* **33**(15):2479-2484.

LAFRANCONI, M.W., OHKUMA, S., HUXTABLE, R.J. (1985). Biliary excretion of novel pneumotoxic metabolites of the pyrrolizidine alkaloid, monocrotaline. *Toxicon* **23**(6):983-992.

LALICH, J.J. and MERKOW, L. (1961). Pulmonary arteritis produced in rats by feeding *Crotalaria spectabilis*. *Lab. Invest.* **10**(4):744-750.

LALICH, J.L., JOHNSON, W.D., RACZNIAK, T.J., SHUMAKER, R.C. (1977). Fibrin thrombosis in monocrotaline pyrrole-induced cor pulmonale in rats. *Arch. Pathol. Lab. Med.* **101**:69-73.

LAMÈ, M.W., MORIN, D., JONES, A.D., SEGALL, H.J., WILSON, D.W. (1990). Isolation and identification of a pyrrolic glutathione conjugate of the pyrrolizidine alkaloid monocrotaline. *Toxicol. Lett.* **51**:321-329.

LAMÈ, M.W., JONES, A.D., MORIN, D., SEGALL, H.J. (1991). Metabolism of [^{14}C]monocrotaline by isolated perfused rat liver. *Drug Metab. Dispos.* **19**(2):516-524.

LAMÈ, M.W., JONES, A.D., MORIN, D., SEGALL, H.J., WILSON, D.W. (1995). Biliary excretion of pyrrolic metabolites of [^{14}C]monocrotaline in the rat. *Drug Metab. Dispos.* **23**(3):422-429.

LAMY, M., FALLAT, R.J., KOENIGER, E., DIETRICH, H-P., RATLIFF, J.L., EBERHART, R.C., TUCKER, H.J., HILL, J.D. (1976). Pathologic features and mechanisms of hypoxemia in adult respiratory distress syndrome. *Am. Rev. Respir. Dis.* **114**:267-284.

LANGLEBEN, D. and REID, L.M. (1985). Effect of methylprednisolone on monocrotaline-induced pulmonary vascular disease and right ventricular hypertrophy. *Lab. Invest.* **52**(3):298-303.

LANGLEBEN, D., CARALHO, A.C.A., REID, L.M. (1986). The platelet thrombaxane inhibitor, dazmegrel, does not reduce monocrotaline-induced pulmonary hypertension. *Am. Rev. Respir. Dis.* **133**:789-791.

LANGLEBEN, D., SZAREK, J.L., COFLESKY, J.T., JONES, R.C., REID, L.M., EVANS, J.N. (1988). Altered artery mechanics and structure in monocrotaline pulmonary hypertension. *J. Appl. Physiol.* **65**(5):2326-2331.

LANIER, T.L., BERGER, E.K., EACHO, P.I. (1989). Comparison of 5-bromo-2-deoxyuridine and [3H]thymidine for studies of hepatocellular proliferation in rodents. *Carcinogenesis* **10**(7):1341-1343.

LASKEY, R.A., FAIRMAN, M.P., BLOW, J.J. (1989). S phase of the cell cycle. *Science* **246**:609-613.

LAUFE, M.D., SIMON, R.H., FLINT, A., KELLER, J.B. (1986). Adult respiratory distress syndrome in neutropenic patients. *Am. J. Med.* **80**:1022-1026.

LESSARD, P., WILSON, W.D., OLANDER, H.J., ROGERS, Q.R., MENDEL, V.E. (1986). Clinicopathologic study of horses surviving pyrrolizidine alkaloid (*Senecio vulgaris*) toxicosis. *Am. J. Vet. Res.* **47**(8):1776-1780.

LINDNER, V., MAJACK, R.A., REIDY, M.A. (1990). Basic fibroblast growth factor stimulates endothelial regrowth and proliferation in denuded arteries. *J. Clin. Invest.* **85**:2004-2008.

LINDNER, V., LAPPI, D.A., BAIRD, A., MAJACK, R.A., REIDY, M.A. (1991). Role of basic fibroblast growth factor in vascular lesion formation. *Circ. Res.* **68**:106-113.

LIPKE, D.W., ARCOT, S.S., GILLESPIE, M.N., OLSON, J.W. (1993). Temporal alterations in specific basement membrane components in lungs from monocrotaline-treated rats. *Am. J. Respir. Cell Mol. Biol.* **9**:418-428.

LOWRY, O.H., ROSEBROUGH, N.J., FARR, A.L., RANDALL, R.J. (1951). Protein measurement with the folin phenol reagent. *J. Biol. Chem.* **193**:265-275.

MADDEN, J.A., KELLER, P.A., EFFROS, R.M., SEAVITTE, C., CHOY, J.S., HACKER, A.D. (1994). Responses to pressure and vasoactive agents by isolated pulmonary arteries from monocrotaline-treated rats. *J. Appl. Physiol.* **76**(4):1589-1593.

MAJEWSKY, M.W., DAEMEN, M.J.A.P., SCHWARTZ, S.M. (1990). α_1-adernergic stimulation of platelet-derived growth factor A-chain gene expression in rat aorta. *J. Biol. Chem.* **265**:1082-1088.

MARTIN, P.A., THORBURN, J.J., HUTCHINSON, S., BRAS, G., MILLER, C.G. (1972). Preliminary findings of chromosomal studies on rats and humans with veno-occlusive disease. *Br. J. Exp. Pathol.* **53**:374-380.

MARUYAMA, J., MARUYAMA, K., MITANI,Y., KITABATAKE, M., YAMAUCHI, T., MIYASAKA, K. (1997). Continuous low-dose NO inhalation does not prevent monocrotaline-induced pulmonary hypertension in rats. *Am. J. Physiol.* **272**:H517-H524.

MATHEW, R., ZEBALLOW, G.A., TUN H., GEWITZ, M.H. (1995). Role of nitric oxide and endothelin-1 in monocrotaline-induced pulmonary hypertension in rats. *Cardiovascular Res.* **30**:739-746.

MATSUKAWA, Y., NARUI, N., SAKAI, T., SATOMI, Y., YOSHIDA, M., MATSUMOTO, K., NISHINO, H., AOIKE, A. (1993). Genistein arrests cell cycle progression at G2-M. *Cancer Res.* **53**:1328-1331.

MATTOCKS, A.R. (1968). Toxicity of pyrrolizidine alkaloids. *Nature* **217**:723-728.

MATTOCKS, A.R. (1969). Dihydropyrrolizidine derivatives from unsaturated pyrrolizidine alkaloids. *J. Chem. Soc. Lond.* **C**:1155-1162.

MATTOCKS, A.R. (1970). Role of the acid moieties in the toxic actions of pyrrolizidine alkaloids on liver and lung. *Nature* **228**:174-175.

MATTOCKS, A.R. (1971a). The occurrence and analysis of pyrrolizidine alkaloid N-oxides. *Xenobiotica* **1**(4/5):451-453.

MATTOCKS, A.R. (1971b). Hepatotoxic effects due to pyrrolizidine alkaloid N-oxides. *Xenobiotica* **1**(4/5):563-565.

MATTOCKS, A.R. (1972a). Acute hepatotoxicity and pyrrolic metabolites in rats dosed with pyrrolizidine alkaloids. *Chem. -Biol. Interactions* **5**:227-242.

MATTOCKS, A.R. (1972b). Toxicity and metabolism of Senecio alkaloids. In *Phytochemical Ecology. Annual proceedings of the Phytochemical Society.* **No. 8**. pp 179-200. (J.B. Harborne, Ed.). Academic Press, London.

MATTOCKS, A.R. (1986). *Chemistry and Toxicology of Pyrrolizidine Alkaloids.* (A.R. Mattocks, Ed.). Academic Press, London.

MATTOCKS, A.R. and CABRAL, J.R.P. (1982). Carcinogenicity of some pyrrolic pyrrolizidine alkaloid metabolites and analogues. *Cancer Lett.* **17**:61-66.

MATTOCKS, A.R., DRIVER, H.E., BARBOUR, R.H., ROBINS, D.J. (1986). Metabolism and toxicity of synthetic analogues of macrocyclic diester pyrrolizidine alkaloids. *Chem. -Biol. Interactions* **58**:95-108.

MATTOCKS, A.R., JUKES, R., BROWN, J. (1989). Simple procedures for preparing putative toxic metabolites of pyrrolizidine alkaloids. *Toxicon* **27**(5):561-567.

MATTOCKS, A.R. and JUKES, R. (1990a). Trapping and measurement of short-lived alkylating agents in a recirculating flow system. *Chem. -Biol. Interactions* **76**:19-30.

MATTOCKS, A.R. and JUKES, R. (1990b). Recovery of the pyrrolic nucleus of pyrrolizidine alkaloid metabolites from sulfur conjugates in tissues and body fluids. *Chem. -Biol. Interactions* **75**:225-239.

MATTOCKS, A.R. and LEGG, R.F. (1980). Antimitotic activity of dehydroretronecine, a pyrrolizidine alkaloid metabolite, and some analogous compounds, in a rat liver parenchymal cell line. *Chem. -Biol. Interactions* **30**:325-336.

MATTOCKS, A.R. and WHITE, I.N.H. (1970). Estimation of metabolites of pyrrolizidine alkaloids in animal tissues. *Anal. Biochem.* **38**:529-535.

MATTOCKS, A.R. and WHITE, I.N.H. (1971). The conversion of pyrrolizidine alkaloids to N-oxides and dihydropyrrolizidine derivatives by rat liver microsomes in vitro. *Chem. -Biol. Interactions* **3**:383-396.

MATTOCKS, A.R. and WHITE, I.N.H. (1973). Toxic effects of pyrrolic metabolites in the liver of young rats given the pyrrolizidine alkaloid retrorsine. *Chem. -Biol. Interactions.* **6**:297-306.

MAUNDER, R.J., HACKMAN, R.C., RIFF,E., ALBERT, R.K., SPRINGMEYER, S.C. (1986). Occurrence of adult respiratory distress syndrome in neutropenic patients. *Am. Rev. Resp. Dis.* **133**:313-316.

McGEE, J.O'D., PATRICK, R.S., WOOD, C.B., BLUMGART, L.H. (1976). A case of veno-occlusive disease of the liver in Britain associated with herbal tea consumption. *J. Clin. Pathol.* **29**:788-794.

McGRATH, J.P.M., DUNCAN, J.R., MUNNELL, J.F. (1975). Crotalaria spectabilis toxicity in swine: Characterization of the renal glomerular lesion. *J. Comp. Pathol.* **85**:185-194.

MCLEAN, E.K. (1970). The toxic actions of pyrrolizidine (*senecio*) alkaloids. *Pharmacol. Rev.* **22**(4):429-483.

MENDEL, V.E., WITT, M.R., GITCHELL, B.S., GRIBBLE, D.N., ROGERS, Q.R., SEGALL, H.J., KNIGHT, H.D. (1988). Pyrrolizidine alkaloid-induced liver disease in horses: An early diagnosis. *Am. J. Vet. Res.* **49**(4):572-578.

MERKOW, L. and KLEINERMAN, J. (1966). An electron microscopic study of pulmonary vasculitis induced by monocrotaline. *Lab. Invest.* **15**(3):547-564.

MEYRICK, B., GAMBLE, W., REID, L. (1980). Development of *Crotalaria* pulmonary hypertension: Hemodynamic and structural study. *Am. J. Physiol.* **239**:H692-H702.

MEYRICK, B. and REID, L. (1979). Development of pulmonary arterial changes in rats fed *Crotalaria spectabilis*. *Am. J. Pathol.* **94**:37-50.

MEYRICK, B.O. and REID, L.M. (1982). *Crotalaria*-induced pulmonary hypertension: Uptake of ^{3}H-thymidine by cells of the pulmonary circulation and alveolar walls. *Am. J. Pathol.* **106**:84-94.

MILLER, W.C., RICE, D.L., KREUSEL, R.G., BEDROSSIAN, C.W.M. (1978). Monocrotaline model of noncardiogenic pulmonary edema in dogs. *J. Appl. Physiol.* **45**(6):962-965.

MIRANDA, C.L., REED, R.L., GUENGERICH, F.P., BUHLER, D.R. (1991). Role of cytochrome P450IIIA4 in the metabolism of the pyrrolizidine alkaloid senecionine in human liver. *Carcinogenesis* **12**(3):515-519.

MIYATA, M., UENO, Y., SEKINE, H., ITO, O., SAKUMA, F., KIOKE, H., NISHIO, S., NISHIMAKI, T., KASUKAWA, R. (1996). Protective effect of beraprost sodium, a stable prostacyclin analogue, in development of monocrotaline-induced pulmonary hypertension. *J. Card. Pharmacol.* **27**:20-26.

MIYAUCHI, T., YORIKANE, R., SAKAI, S., SAKURAI, T., OKADA, M., NISHIKIBE, M., YANO, M., YAMAGUCHI, I., SUGISHITA, Y., GOTO, K. (1993). Contribution of endogenous endothelin-1 to the progression of cardiopulmonary alterations in rats with monocrotaline-induced pulmonary hypertension. *Circ. Res.* **73**:887-897.

MOHABBAT, O., YOUNOS, M.S., MERZAD, A.A., SRIVASTAVA, R.N., SEDIQ, G.G., ARAM, G.N. (1976). An outbreak of veno-occlusive disease in north-western Afghanistan. *Lancet* **II**(7980):269-271.

MOLTENI, A., WARD, W.F., TS'AO, C-H., PORT, C.D., SOLLIDAY, N.H. (1984). Monocrotaline-induced pulmonary endothelial dysfunction in rats. *Proc. Soc. Exp. Biol. Med.* **176**:88-94.

MOLTENI, A., WARD, W.F., TS'AO, C-H., SOLLIDAY, N.H., DUNNE, M. (1985). Monocrotaline-induced pulmonary fibrosis in rats: Amelioration by Captopril and Penicillamine. *Proc. Soc. Exp. Biol. Med.* **180**:112-120.

MOLTENI, A., WARD, W.F., TS'AO, C-H., SOLLIDAY, N.H. (1986). Monocrotaline-induced cardiopulmonary damage in rats: Amelioration by the angiotensin-converting enzyme inhibitor CL242817. *Proc. Soc. Exp. Biol. Med.* **182**:483-493.

MOLTENI, A., WARD, W.F., TS'AO, C-H., HINZ, J.M. (1989). Monocrotaline-induced cardiopulmonary injury in rats: Modification by the neutrophil elastase inhibitor SC39026. *Biochem. Pharmacol.* **38**(15):2411-2419.

MONKS, T.J., ANDERS, M.W., DEKANT, W., STEVENS, J.L., LAU, S.S., VAN BLADEREN, P.J. (1990). Glutathione conjugate mediated toxicities. *Toxicol. Appl. Pharmacol.* **106**:1-19.

MOOI, W.J. (1987). Pathology of pulmonary hypertension. *Transplantation Proc.* **19**(5):4373-4374.

MORI, H., SUGIE, S., YOSHIMI, N., ASADA, Y., FURUYA, T., WILLIAMS, G.M. (1985). Genotoxicity of a variety of pyrrolizidine alkaloids in the hepatocyte primary culture-DNA repair test using rat, mouse, and hamster hepatocytes. *Cancer Res.* **45**:3125-3129.

MÜELLER, L., KASPER, P., KAUFMANN, G. (1992). The clastogenic potential in vitro of pyrrolizidine alkaloids employing hepatocyte metabolism. *Mutation Res.* **282**:169-176.

NAKAMURA, T., MASUDA, K., MATSUMOTO, S., OKU, T., MANDA, T., MORI, J., SHIMOMURA, K. (1989). Effect of FK973, a new tumor antibiotic, on the cell cycle of L1210 cells *in vitro*. *Japan. J. Pharmacol.* **49**:317-324.

NEWBERNE, P.M. and ROGERS, A.E. (1973). Nutrition, monocrotaline, and aflatoxin B1 in liver carcinogenesis. *Plant Foods for Man* **1**:23-31.

NIWA, H., OGAWA,T., OKAMOTO, O., YAMADA, K. (1991). Alkylation of nucleosides by dehydromonocrotaline, the putative toxic metabolite of the carcinogenic pyrrolizidine alkaloid monocrotaline. *Tetrahedron Lett.* **32**(7):927-930.

NORBURY, C., BLOW, J., NURSE, P. (1991). Regulatory phosphorylation of the $p34^{cdc2}$ protein kinase in vertebrates. *EMBO J.* **10**(11):3321-3329.

NUGENT, M.A., KARNOVSKY, N.J., EDELMAN, E.R. (1993). Vascular cell-derived heparan sulfate shows coupled inhibition of basic fibroblast growth factor binding and mitogenesis in vascular smooth muscle cells. *Circ. Res.* **73**:1051-1060.

NURSE, P. (1990). Universal control mechanism regulating onset of M-phase. *Nature* **344**:503-507.

O'CONNOR, P.M., FERRIS, D.K., WHITE, G.A., PINES, J., HUNTER, T., LONGO, D.L., KOHN, K.W. (1992). Relationship between cdc2 kinase, DNA cross-linking, and cell cycle perturbations induced by nitrogen mustard. *Cell Growth Differ.* **3**:43-52.

ODRIOZOLA, E., CAMPERO, C., CASARO, A., LOPEZ, T., OLIVIERI, G., MELUCCI, O. (1994). Pyrrolizidine alkaloidosis in Argentinean cattle caused by *Senecio selloi*. *Vet. Human Toxicol.* **36**(3):205-208.

O'FARRELL, M.K. and DEALTRY, G.B. (1992). *Cell Biology - Labfax*. G.B. Dealtry and D. Rickwood, Eds). Pp 205-210. Bios Scientific Publishers, Ltd. Oxford.

OKADA, M., YAMASHITA, C., OKADA, M., OKADA, K. (1995a). Establishment of canine pulmonary hypertension with dehydromonocrotaline: Importance of a larger animal model for lung transplantation. *Transplantation* **60**(1):9-13.

OKADA, M., YAMASHITA, C., OKADA, M., OKADA, K. (1995b). Endothelin receptor antagonists in a beagle model of pulmonary hypertension: Contribution to possible potential therapy? *J. Am. Coll. Cardiol.* **25**:1213-1217.

OKADA, M., YAMASHITA, C., OKADA, M., OKADA, K. (1995c). A dehydromonocrotaline-induced pulmonary hypertension model in the beagle. *J. Thorac. Cardiovasc. Surg.* **110**:546-547.

OLSON, J.W., ALTIERE, R.J., GILLESPIE, M.N. (1984a). Prolonged activation of rat lung ornithine decarboxylase in monocrotaline-induced pulmonary hypertension. *Biochem. Pharmacol.* **33**(22):3633-3637.

OLSON, J.W., HACKER, A.D., ALTIERE, R.J., GILLESPIE, M.W. (1984b). Polyamines and the development of monocrotaline-induced pulmonary hypertension. *Am. J. Physiol.* **247**:H682-H685.

OLSON, J.W., ATKINSON, J.E., HACKER, A.D., ALTIERE, R.J., GILLESPIE, M.N. (1985). Suppression of polyamine biosynthesis prevents monocrotaline-induced pulmonary edema and arterial medial thickening. *Toxicol. Appl. Pharmacol.* **81**:91-99.

OLSON, J.W., GEBB, S.A., ORLINSKA, U., GILLESPIE, M.W. (1989a). Polyamine synthesis in rat lungs injured with alpha-naphylthiourea. *Toxicology* **55**:317-326.

OLSON, J.W., ORLINSKA, U., GILLESPIE, M.W. (1989b). Polyamine synthesis blockade in monocrotaline-induced pneumotoxicity. *Biochem. Pharmacol.* **38**(17):2903-2910.

ONO, S. and VOELKEL, N.F. (1991). PAF antagonists inhibit monocrotaline-induced lung injury and pulmonary hypertension. *J. Appl. Physiol.* **71**(6):2483-2492.

ONO, S. and VOELKEL, N.F. (1992). PAF receptor blockade inhibits vascular changes in the rat monocrotaline model. *Lung* **170**:31-40.

ORLINSKA, U., OLSON, J.W., GILLESPIE, M.W. (1988). Polyamine content in pulmonary arteries from rats with monocrotaline-induced pulmonary hypertension. *Res. Commun. Chem. Pathol. Pharmacol.* **62**(2):187-194.

OWENS, G.K. (1989). Control of hypertrophic versus hyperplastic growth of vascular smooth muscle cells. *Am. J. Physiol.* **257**:H1755-H1765.

OWENS, G.K. (1991). Role of contractile agonists in growth regulation of vascular smooth muscle cells. In *Cellular and Molecular Mechanisms in Hypertension*. (R.H. Cox, Ed.). pp71-79. Plenum Press, New York.

OWENS, G.K. and REIDY, M.A. (1985). Hyperplastic growth response of vascular smooth muscle cells following induction of acute hypertension in rats by aortic coarctation. *Circ. Res.* **57**:695-705.

OWENS, G.K. and SCHWARTZ, S.M. (1983). Vascular smooth muscle cell hypertrophy and hyperploidy in the Goldblatt hypertensive rat. *Circ. Res.* **53**:491-501.

OWENS, G.K., GEISTERFER, A.A.T., WEI-HWA YANG, Y., KOMORIYA, A. (1988a). Transforming growth factor-β-induced growth inhibition and cellular hypertrophy in cultured vascular smooth muscle cells. *J. Cell Biol.* **107**:771-780.

OWENS, G.K., SCHWARTZ, S.M., McCANNA, M. (1988b). Evaluation of medial hypertrophy in resistance vessels of spontaneously hypertensive rats. *Hypertension* **11**:198-207.

PALEVSKY, H.I. and FISHMAN, A.P. (1992). Pulmonary hypertension. In *Vascular Medicine: A Textbook of Vascular Biology and Diseases*. (J. Loscalzo, M.A. Creager, V.J. Dzau, Eds.) pp 957-973. Little, Brown and Company, Boston.

PAN, L.C., LAMÈ, M.W., MORIN, D., WILSON, D.W., SEGALL, H.J. (1991). Red blood cells augment transport of reactive metabolites of monocrotaline from liver to lung in isolated and tandem liver and lung preparations. *Toxicol. Appl. Pharmacol.* **110**:336-346.

PAN, L.C., WILSON, D.W., LAMÈ, M.W., JONES, A.D., SEGALL, H.J. (1993). Cor pulmonale is caused by monocrotaline and dehydromonocrotaline, but not by glutathione or cysteine conjugates of dihydropyrrolizine. *Toxicol. Appl. Pharmacol.* **118**:87-97.

PARDEE, A.B. (1989). G1 events and regulation of cell proliferation. *Science* **246**:603-608.

PARKINSON, A. (1995). Biotransformation of xenobiotics. In *Casarett and Doull's - Toxicology: The Basic Science of Poisons*, 5th ED. (C.D. Klassen, M.O. Amdur, J. Doull, Eds.) pp 113-186. McGraw-Hill, New York.

PECKHAM, J.C., SANGSTER, L.T., JONES Jr., O.H. (1974). *Crotalaria spectabilis* poisoning in swine. *J. Am. Vet. Med. Assoc.* **165**(7):633-638.

PEEPER, D.S., VAN DER EB, A.J., ZANTEMA, A. (1994). The G_1/S cell-cycle checkpoint in eukaryotic cells. *Biochim. Biophys. Acta.* **1198**:215-230.

PETERSON, J.E. (1965). Effects of the pyrrolizidine alkaloid, lasiocarpine N-oxide, on nuclear and cell division in the liver of rats. *J. Path. Bact.* **89**:153-171.

PETERSON, J.E., SAMUEL, A., JAGO, M.V. (1972). Pathological effects of dehydroheliotridine, a metabolite of heliotridine-based pyrrolizidine alkaloids, in the young rat. *J. Pathol.* **107**:175-189.

PETRY, T.W., BOWDEN, G.T., HUXTABLE, R.J., SIPES, I.G. (1984). Characterization of hepatic DNA damage induced in rats by the pyrrolizidine alkaloid monocrotaline. *Cancer Res.* **44**:1505-1509.

PETRY, T.W. and SIPES, I.G. (1989). Modulation of monocrotaline-induced hepatic genotoxicity in rats. *Carcinogenesis* **8**(3):415-419.

PIETRA, G.G. and RÜTTNER, J.R. (1987). Specificity of pulmonary vascular lesions in primary pulmonary hypertension: A reappraisal. *Respiration* **52**:81-85.

PLESTINA, R. and STONER, H.B. (1972). Pulmonary edema in rats given monocrotaline pyrrole. *J. Pathol.* **106**:235-249.

POLLACK, A. (1990). Flow cytometric cell-kinetic analysis by simultaneously staining nuclei with propidium iodide and fluorescein isothiocyanate. *Meth. Cell. Biol.* **33**:315-323.

POWIS, G., AMES, M.M., KOVACH, J.S. (1979). Relationship of the reductive metabolism of indicine N-oxide to its antitumor activity. *Res. Commun. Chem. Pathol. Pharmacol.* **24**(3):559-569.

PRINGLE, J.K., BRIGHT, J.M., DUNCAN, R.B., KERR, L., LINNABARY, R.D., TARRIER, M.P. (1991). Pulmonary hypertension in a group of dairy calves. *J. Am. Vet. Med. Assoc.* **198**(5):857-861.

RACZNIAK, T.J., SHUMAKER, R.C., ALLEN, J.R., WILL, J.A., LALICH, J.J. (1979). Pathophysiology of dehydromonocrotaline-induced pulmonary fibrosis in the beagle. *Respiration* **37**:252-260.

RAGHOW, R. (1994). The role of extracellular matrix in post inflammatory wound healing and fibrosis. *FASEB J.* **8**:823-831.

RATNOFF, O.D. anD MIRICK, G.S. (1949). Influence of sex upon the lethal effects of an hepatotoxic alkaloid, monocrotaline. *Bull. Johns Hopkins Hosp.* **84**:507-523.

REDDY, G.V.P. (1994). Cell cycle: Regulatory events in G1 to S transition of mammalian cells. *J. Cell. Biochem.* **54**:379-386.

REID, L. (1990). Vascular remodeling. In *The Pulmonary Circulation: Normal and Abnormal. Mechanisms, Management, and the National Registry.* (A.P. Fishman, Ed.) pp 259-282. University of Pennsylvania Press, Philadelphia.

REID, L. and MEYRICK, B. (1982). Microcirculation: Definition and organization at tissue level. *Ann. N.Y. Acad. Sci.* **384**:3-20.

REIDY, M.A. (1992). Factors controlling smooth-muscle cell proliferation. *Arch. Pathol. Lab. Med.* **116**:1276-1280.

REINDEL, J.F., GANEY, P.E., WAGNER, J.G., SLOCOMBE, R.F., ROTH, R.A. (1990). Development of morphologic, hemodynamic and biochemical changes in lungs of rats given monocrotaline pyrrole. *Toxicol. Appl. Pharmacol.* **106**:179-200.

REINDEL, J.F., HOORN, C.M., WAGNER, J.G., ROTH, R.A. (1991). Comparison of response of bovine and porcine pulmonary arterial endothelial cells to monocrotaline pyrrole. *Am. J. Physiol.* **261**:L406-L414.

REINDEL, J.F. and ROTH, R.A. (1991). The effects of monocrotaline pyrrole on cultured bovine pulmonary artery endothelial and smooth muscle cells. *Am. J. Pathol.* **138**(3):707-719.

RIABOWOL, K., DRAETTA, G., BRIZUELA, L., VANDRE, D., BEACH, D. (1989). The cdc2 kinase is a nuclear protein that is essential for mitosis in mammalian cells. *Cell* **57**:393-401.

RICH, S. and BRUNDAGE, B.H. (1989). Pulmonary hypertension: A cellular basis for understanding the pathophysiology and treatment. *J. Am. Coll. Cardiol.* **14**:545-550.

RIDKER, P.M., OHKUMA, S., McDERMOTT, W.V., TREY, C., HUXTABLE, R.J. (1985). Hepatic venocclusive disease associated with the consumption of pyrrolizidine-containing dietary supplements. *Gastroenterology* **88**:1050-1054.

ROBERTSON, K.A., SEMOUR, J.L., HSIA, M-T., ALLEN, J.R. (1977). Covalent interaction of dehydroretronecine, a carcinogenic metabolite of the pyrrolizidine alkaloid monocrotaline, with cysteine and glutathione. *Cancer Res.* **37**:3141-3144.

ROGERS, A.E. and NEWBERNE, P.M. (1971). Lasiocarpine: Factors influencing its toxicity and effects on liver cell division. *Toxicol. Appl. Pharmacol.* **18**:356-366.

ROGERS, J.M. and KAVLOCK, R.J. (1995). Developmental toxicology. In *Casarett and Doull's - Toxicology: The Basic Science of Poisons*, 5th ED. (C.D. Klassen, M.O. Amdur, J. Doull, Eds.) pp 301-331. McGraw-Hill, New York.

ROITMAN, J.N. (1981). Comfrey and liver damage. *Lancet* I(8226):944.

ROSENFELD, I. and BEATH, O.A. (1945). Tissue changes induced by *Senecio riddellii. Am. J. Clin. Pathol.* **15**:407-412.

ROSENBERG, H.C. and RABINOVITCH, M. (1988). Endothelial injury and vascular reactivity in monocrotaline pulmonary hypertension. *Am. J. Physiol.* **255**:H1484-H1491.

ROSS, J.S. (1996). DNA ploidy and cell cycle analysis in pathology. J.S. Ross, Ed.). Igaku-Shoin, New York.

ROSS, R., RAINES, E.W., BOWEN-POPE, D.F. (1986). The biology of platelet-derived growth factor. *Cell* **46**:155-169.

ROTH, R.A. (1981). Effect of pneumotoxicants on lactate dehydrogenase activity in airways of rats. *Toxicol. Appl. Pharmacol.* **57**:69-78.

ROTH, R.A. and REINDEL, J.F. (1990). Lung vascular injury from monocrotaline pyrrole, a putative hepatic metabolite. In *Biological Reactive Intermediates IV.* (C. M. Witmer, R.R. Snyder, D.J. Jollow, G.F. Kalf, J.J. Kocsis, I.G. Sipes, Eds). pp 477-487. Plenum Press, New York.

ROTH, R.A., WHITE, S.M., REINDEL, J.F. (1989). Mechanisms of lung injury and pulmonary hypertension from monocrotaline: An hypothesis. *Comm. Toxicol.* **3**(2):131-144.

ROTHMAN, A., WOLNER, B., BUTTON, D., TAYLOR, P. (1994). Immediate-early gene expression in response to hypertrophic and proliferative stimuli in pulmonary arterial smooth muscle cells. *J. Biol. Chem.* **269**(9):6399-6404.

RUBIN, L.J., PALEVSKY, H.I., FISHMAN, A. (1996). Pulmonary hypertension. In *Pulmonary Hypertension in Vascular Medicine: A Textbook of Vascular Biology and Diseases.* (J. Loscalzo, M.A. Creager, V.J. Dzau, Eds). Pp 951-964. Little, Brown and Co. Boston.

RYAN, U.S. (1990). Endothelial processing of biologically active materials. In *The Pulmonary Circulation: Normal and Abnormal. Mechanisms, Management, and the National Registry.* (A.P. Fishman, Ed) pp 69-83. University of Pennsylvania Press, Philadelphia.

SACHINIDIS, A., SCHULTE, K., KO, Y., MEYER ZU BRICKWEDDE, M.K., HOPPE, V., HOPPE, J., VETTER, H. (1993). The induction of early response genes in rat smooth muscle cells by PDGF-AA is not sufficient to stimulate DNA synthesis. *FEBS Lett.* **319**(3):221-224.

SAMUEL, A., and JAGO, M.V. (1975). Localization in the cell cycle of the antimitotic action of the pyrrolizidine alkaloid, lasiocarpine and of its metabolite dehydroheliotridine. *Chem. -Biol. Interactions* **10**:185-197.

SANDERSON, B.J.S. and CLARK, A.M. (1993). Micronuclei in adult and foetal mice exposed in vivo to heliotrine, urethane, monocrotaline, and benzidine. *Mutation Res.* **285**:27-33.

SCHOENTAL, R. and HEAD, M.A. (1955). Pathological changes in rats as a result of treatment with monocrotaline. *Br. J. Cancer* **9**:229-237.

SCHOENTAL, R. and MAGEE, P.N. (1957). Chronic liver changes in rats after a single dose of lasiocarpine, a pyrrolizidine (*Senecio*) alkaloid. *J. Path. Bact.* **74**:305-319.

SCHOENTAL, R. and MAGEE, P.N. (1959). Further observations on the subacute and chronic liver changes in rats after a single dose of various pyrrolizidine (*Senecio*) alkaloids. *J. Path. Bact.* **78**:471-482.

SCHOENTAL, R. and MATTOCKS, A.R. (1960). Hepatotoxic activity of semi-synthetic analogues of pyrrolizidine alkaloids. *Nature* **185**:842-843.

SCHRAUFNAGEL, D.E. (1990). Monocrotaline-induced angiogenesis: Differences in the bronchial and pulmonary vasculature. *Am. J. Pathol.* **137**(5):1083-1090.

SCHULTZE, A.E. and ROTH, R.A. (1993). Fibronolytic activity in blood and lungs of rats treated with monocrotaline pyrrole. *Toxicol. Appl. Pharmacol.* **121**:129-137.

SCHULTZE, A.E., WAGNER, J.G., ROTH, R.A. (1991). An evaluation of procoagulant activity in the peripheral blood of rats treated with monocrotaline pyrrole. *Toxicol. Appl. Pharmacol.* **109**:421-431.

SCHULTZE, A.E., GUNAGA, K.P., WAGNER, J.G., HOORN, C.M., MOOREHEAD, W.R., ROTH, R.A. (1994). Lactate dehydrogenase activity and isozyme patterns in tissues and bronchoalveolar lavage fluid from rats treated with monocrotaline pyrrole. *Toxicol. Appl. Pharmacol.* **126**:301-310.

SCHULTZE, A.E., EMEIS, J.J., ROTH, R.A. (1996). Cellular fibronectin and von Willebrand factor concentrations in plasma of rats treated with monocrotaline pyrrole. *Biochem. Pharmacol.* **51**:187-191.

SCHULTZE, A.E., WAGNER, J.G., WHITE, S.M., ROTH, R.A. (1991b). Early indications of monocrotaline pyrrole-induced lung injury in rats. *Toxicol. Appl. Pharmacol.* **109**:41-51.

SCHWARTZ, S.M. and BENDITT, E.P. (1976). Clustering of replicating cells in aortic endothelium. *Proc. Natl. Acad. Sci. USA* **73**(2):651-653.

SCHWARTZ, S.M., GAJDUSEK, C.M., REIDY, M.A., SELDEN III, S.C., HAUDENSCHILD, C.C. (1980). Maintenance of integrity in aortic endothelium. *Fed. Proc.* **39**:2618-2625.

SEAMAN, J.T. (1987). Pyrrolizidine alkaloid poisoning of sheep in New South Wales. *Aust. Vet. J.* **64**:164-167.

SHEPRO, D. and MOREL, N.M.L. (1993). Pericyte physiology. *FASEB J.* **7**:1031-1038.

SHUBAT, P.J., BANNER Jr., W., HUXTABLE, R.J. (1987). Pulmonary vascular responses induced by the pyrrolizidine alkaloid, monocrotaline, in rats. *Toxicon* **25**(9):995-1002.

SHUBAT, P.J., HUBBARD, A.K., HUXTABLE, R.J. (1989). Dose-response relationship in intoxication by the pyrrolizidine alkaloid monocrotaline. *J. Toxicol. Environ. Health.* **28**:445-460.

SHULMAN, H.M., LUK, K., DEEG, H.J., SHUMAN, W.B., STORB, R. (1987). Induction of hepatic veno-occlusive disease in dogs. *Am. J. Pathol.* **126**:114-125.

SHUMAKER, R.C., ROBERTSON, K.A., HSU, I-C., ALLEN, J.R. (1976). Neoplastic transformation in tissues of rats exposed to monocrotaline or dehydroretronecine. *J. Natl. Cancer Inst.* **56**:787-790.

SKILLETER, D.N., MATTOCKS, A.R., NEAL, G.E. (1988). Sensitivity of different phases of the cell cycle to selected hepatotoxins in cultured liver-derived (BL9L) cells. *Xenobiotica* **18**(6):699-705.

SMITH, L.W. and CULVENOR, C.C.J. (1981). Plant sources of hepatotoxic pyrrolizidine alkaloids. *J. Nat. Prod.* **44**(2):129-152.

SMITH, P. and HEATH, D. (1978). Evagination of vascular smooth muscle cells during the early stages of Crotalaria pulmonary hypertension. *J. Pathol.* **124**:177-183.

SMITH, P., HEATH, D., KAY, J.M., WRIGHT, J.S., McKENDRICK, C.S. (1973). Pulmonary arterial pressure and structure in the patas monkey after prolonged administration of aminorex fumarate. *Cardiovascular Res.* **7**:30-38.

SNOW, R.L., DAVIES, P., PONTOPPIDAN, H., ZAPOL, W.M., REID, L. (1982). Pulmonary vascular remodeling in adult respiratory distress syndrome. *Am. Rev. Respir. Dis.* **126**:887-892.

SPERL, W., STUPPNER, H., GASSNER, I., JUDMAIER, W., DIETZE, O., VOGEL, W. (1995). Reversible hepatic veno-occlusive disease in an infant after consumption of pyrrolizidine-containing herbal tea. *Eur. J. Pediatr.* **154**:112-116.

STEEL, R.G.D. and TORRIE, J.H. (1980). *Principles and procedures of statistics, a biomedical approach.* McGraw-Hill, Inc., New York.

STENMARK, K.R., MORGANROTH, M.L., REMIGIO, L.K., VOELKEL, N.F., MURPHY, R.C., HENSON, P.M., MATHIAS, M.M., REEVES, J.T. (1985). Alveolar inflammation and arachidonate metabolism in monocrotaline-induced pulmonary hypertension. *Am. J. Physiol.* **248**:H859-H866.

STEVENS, P.M. (1982) General assessment and support of the adult respiratory distress syndrome. *Ann. N. Y. Acad. Sci.* **384**:477-487.

STILLMAN, A.E., HUXTABLE, R.J., CONSROE, P., KOHNEN, P., SMITH, S. (1977). Hepatic veno-occlusive disease due to pyrrolizidine (Senecio) poisoning in Arizona. *Gastroenterology* **73**:349-352.

STILLMAN, B. (1996). Cell cycle control of DNA replication. *Science* **274**:1659-1663.

STUART, K.L. and BRAS, G. (1957). Veno-occlusive disease of the liver. *Q. J. Med.* **26**(103):291-315.

SUGITA, T., HYERS, T.M., DAUBER, I.M., WAGNER, W.W., McMURTRY, I.F., REEVES, J.T. (1983). Lung vessel leak precedes right ventricular hypertrophy in monocrotaline-treated rats. J. *Appl. Physiol.* **54**(2):371-374.

SULLMAN, S.F. and ZUCKERMAN, A.J. (1969). The effect of heliotrine, a pyrrolizidine alkaloid, on human liver cells in culture. *Br. J. Exp. Pathol.* **50**:361-370.

SVOBODA, D., REDDY, J., BUNYARATVEJ, S. (1971). Hepatic megalocytosis in chronic lasiocarpine poisoning. *Am. J. Pathol.* **65**(2):399-409.

TAKANARI, H. and IZUTSU, K. (1983). Studies on endoreduplication III. Endoreduplication induced by mitomycin C in PHA-stimulated tonsillar lymphocyte cultures. *Mutation. Res.* **107**:297-306.

TANDON, B.N., TANDON, H.D., TANDON, R.K., NARNDRANATHAN, M., HOSHI, Y.K. (1976). An epidemic of veno-occlusive disease of liver in central India. *Lancet* **II**(7980):271-272.

TELFORD, W.G., KING, L.E., FRAKER, P.J. (1991). Evaluation of glucocorticoid-induced DNA fragmentation in mouse thymocytes by flow cytometry. *Cell Prolif.* **24**(5):447-459.

THOMAS, H.C., LAMÉ, M.W., WILSON, D.W., SEGALL, H.J. (1996). Cell cycle alterations associated with covalent binding of monocrotaline pyrrole to pulmonary artery endothelial cell DNA. *Toxicol. Appl. Pharmacol.* **141**:319-329.

TODOROVICH-HUNTER, L., DODO, H., YE, C., MCCREADY, L., KEELEY, F.W., RABINOVITCH, M. (1992). Increased pulmonary artery elastolytic activity in adult rats with monocrotaline-induced progressive hypertensive pulmonary vascular disease compared with infant rats with nonprogressive disease. *Am. Rev. Respir. Dis.* **146**:213-223.

TODD, L., MULLEN, M., OLLEY, P.M., RABINOVITCH, M. (1985). Pulmonary toxicity of monocrotaline differs at critical periods of lung development. *Pediatr. Res.* **19**(7):731-737.

TOUVAY,C., VILAIN, B., CARRÉ, C., MANCIA-HUERTA, J.M., BRAQUET, P. (1995). Effect of limonene and sobrerol on monocrotaline-induced lung alterations and pulmonary hypertension. *Int. Arch. Allergy Immunol.* **107**:272-274.

TURNER, J.H. and LALICH, J.J. (1965). Experimental cor pulmonale in the rat. *Arch. Pathol.* **79**:409-419.

THYBERG, J., PALMBERG, L., NILSSON, J., KSIAZEK, T., SJÒLUND, M. (1983). Phenotype modulation in primary cultures of arterial smooth muscle cells: On the role of platelet-derived growth factor. *Differentiation* **25**:156-167.

USUI, T., YOSHIDA, M., ABE, K., OSADA, H., ISONO, K., BEPPU, T. (1991). Uncoupled cell cycle without mitosis induced by a protein kinase inhibitor. *J. Cell Biol.* **115**(5):1275-1282.

VALDIVIA, E., LALICH, J.J., HAYASHI, Y., SONNAD, J. (1967a). Alterations in pulmonary alveoli after a single injection of monocrotaline. *Arch. Pathol.* **84**:64-76.

VALDIVIA, E., SONNAD, J., HAYASHI, Y., LALICH, J.J. (1967b). Experimental interstitial pulmonary edema. *Angiology* **18**:378-383.

VINDELØV, L., and CHRISTENSEN, I.J. (1990). An integrated set of methods for routine flow cytometric DNA analysis. *Methods Cell. Biol.* **33**:127-137.

VITA, J.A., KEANEY Jr., J.F., LOSCALZO, J. (1996). Endothelial dysfunction in vascular disease. In *Pulmonary Hypertension in Vascular Medicine: A Textbook of Vascular Biology and Diseases.* (J. Loscalzo, M.A. Creager, V.J. Dzau, Eds). pp 245-263. Little, Brown and Co. Boston.

WAGENVOORT, C.A., DINGEMENS, K.P., LOTGERING, G.G. (1974a). Electron microscopy of pulmonary vasculature after application of fulvine. *Thorax* **29**:511-521.

WAGENVOORT, C.A. and WAGENVOORT, N., DIJK, H.J. (1974b). Effect of fulvine on pulmonary arteries and veins of the rat. *Thorax* **29**:522-529.

WAGENVOORT, C.A. and WAGENVOORT, N. (1979). Pulmonary vascular bed: Normal anatomy and responses to disease. In *Pulmonary Vascular Diseases.* (K.M Moser, Ed.). pp 1-109. Marcel Dekker, Inc., New York..

WAGNER, J.G., PETRY, T.W., ROTH, R.A. (1993). Characterization of monocrotaline pyrrole-induced DNA cross-linking in pulmonary artery endothelium. *Am. J. Physiol.* **264**:L517-L522.

WANG, J., ESSNER, E., SHICHI, H. (1994). Ultrastructural and immunocytochemical studies of smooth muscle cells in iris arterioles of rats with experimental autoimmune uvoretinitis. *Exp. Mol. Pathol.* **61**:153-163.

WEHNER, F.C., THIEL, P.G., VAN RENSBURG, S.J. (1979). Mutagenicity of alkaloids in the *Salmonella*/microsome system. *Mutation Res.* **66**:187-190.

WHITE, I.N.H. (1976). The role of liver glutathione in the acute toxicity of retrorsine to rats. *Chem. -Biol. Interactions* **13**:333-342.

WHITE, I.N.H. and MATTOCKS, A.R. (1971). Some factors affecting the conversion of pyrrolizidine alkaloids to N-oxides and to pyrrolic derivatives *in vitro*. *Xenobiotica* **1**(4/5):503-505.

WHITE, I.N.H., MATTOCKS, A.R., BUTLER, W.H. (1973). The conversion of the pyrrolizidine alkaloid retrorsine to pyrrolic derivatives in vivo and in vitro and its acute toxicity to various animal species. *Chem. -Biol. Interactions* **6**:207-218.

WHITE, R.D., SWICK, R.A., CHEEKE, P.R. (1983). Effects of microsomal enzyme induction on the toxicity of pyrrolizidine (*Senecio*) alkaloids. *J. Toxicol. Environ. Health* **12**:633-640.

WHITE, S.M. and ROTH, R.A. (1988). Pulmonary platelet sequestration is increased following monocrotaline pyrrole treatment of rats. *Toxicol. Appl. Pharmacol.* **96**:465-475.

WHITE, S.M., WAGNER, J.G., ROTH, R.A. (1989). Effects of altered platelet number on pulmonary hypertension and platelet sequestration in monocrotaline pyrrole-treated rats. *Toxicol. Appl. Pharmacol.* **99**:302-313.

WILLIAMS, D.E., REED, R.L., KEDZIERSKI, B., DANNAN, G.A., GUENGERICH, F.P., BUHLER, D.R. (1989). Bioactivation and detoxication of the pyrrolizidine alkaloid senecionine by cytochrome P-450 enzymes in rat liver. *Drug Metab. Dispos.* **17**(4):387-392.

WILLIAMS, G.M. and MORI, H. (1980). Genotoxicity of pyrrolizidine alkaloids in the hepatocyte primary culture/DNA repair test. *Mutation Res.* **79**:1-5.

WILSON, D.W. and SEGALL, H.J. (1990). Changes in type II cell populations in monocrotaline pneumotoxicity. *Am. J. Pathol.* **136**(6):1293-1299.

WILSON, D.W., SEGALL, H.J., PAN, L.C.W., DUNSTON, S.K. (1989). Progressive inflammatory and structural changes in the pulmonary vasculature of monocrotaline-treated rats. *Microvascular Res.* **38**:57-80.

WILSON, D.W., SEGALL, H.J., PAN, L.C., LAMÈ, M.W., ESTEP, J.E., MORIN, D. (1992). Mechanisms and pathology of monocrotaline pulmonary toxicity. *Crit. Rev. Toxicol.* **22**(5/6):307-325.

WINTER, C.K. and SEGALL, H.J. (1989). Metabolism of pyrrolizidine alkaloids. In *Toxicants of Plant Origin - Volume I: Alkaloids*. (P. R. Cheeke, Ed.). pp 23-40. CRC Press, Inc., Boca Raton.

WINTER, H., SEAWRIGHT, A.A., MATTOCKS, A.R., JUKES, R., TSHEWANG, U., GURUNG, B.J. (1990). Pyrrolizidine alkaloid poisoning in yaks. First report and confirmation by identification of sulphur-bound pyrrolic metabolites of the alkaloids in preserved liver tissue. *Aust. Vet. J.* **67**(11):411-412.

WONG, M.K.K., and GOTLIEB, A.I. (1984). *In vitro* reendothelialization of a single-cell wound: Role of microfilament bundles in rapid lamellipodia-mediated wound closure. *Lab. Invest.* **51**(1):75-81.

WONG, M.K.K., and GOTLIEB, A.I. (1988). The reorganization of microfilaments, centrisomes, and microtubules during in vitro small wound reendothelialization. *J. Cell Biol.* **107**:1777-1783.

WYNFORD-THOMAS, D. and WILLIAMS, E.D. (1986). Use of bromodeoxyuridine for cell kinetic studies in intact animals. *Cell Tissue Kinet.* **19**:179-182.

YAMANAKA, H., NAGAO, M., SUGIMURA, T. (1979). Mutagenicity of pyrrolizidine alkaloids in the *Salmonella*/mammalian-microsome test. *Mutation Res.* **68**:211-216.

YAN, C.C. and HUXTABLE, R.J. (1994). Quantitation of the hepatic release of metabolites of the pyrrolizidine alkaloid, monocrotaline. *Toxicol. Appl. Pharmacol.* **127**:58-63.

YAN, C.C. and HUXTABLE, R.J. (1995a).The relationship between the concentration of the pyrrolizidine alkaloid monocrotaline and the pattern of metabolites released from the isolated liver. *Toxicol. Appl. Pharmacol.* **130**:1-8

YAN, C.C. and HUXTABLE, R.J. (1995b). Relationship between glutathione concentration and metabolism of the pyrrolizidine alkaloid, monocrotaline, in the isolated, perfused liver. *Toxicol. Appl. Pharmacol.* **130**:132-139.

YAN, C.C. and HUXTABLE, R.J. (1996). Effects of taurine and guanidinoethane sulfonate on toxicity of the pyrrolizidine alkaloid monocrotaline. *Biochem. Pharmacol.* **51**:321-329.

YE, C. and RABINOVITCH, M. (1991). Inhibition of elastolysis by SC-37698 reduces development and progression of monocrotaline pulmonary hypertension. *Am. J. Physiol.* **261**:H1255-H1267.

ZALKOW, L.H., BONETTI, S., GELBAUM, L., GORDON, M.M., PATIL, B.B., SHANI, A., VAN DERVEER, D. (1979). Pyrrolizidine alkaloids from middle eastern plants. *J. Nat. Prod.* **42**(6):603-614.

ZHOU, K.-R. and LAI, Y.-L. (1992). α-Difluoromethylornithine attenuates monocrotaline-induced airway/lung dysfunction. *J. Appl. Physiol.* **72**(5):1914-1921.

ZHU, L., WIGLE, D., HINEK, A., KOBAYASHI, J., YE, C., ZUKER, M., DODO, H., KEELEY, F.W., RABINOVITCH, M. (1994). The endogenous vascular elastase that governs development and progression of monocrotaline-induced pulmonary hypertension in rats is a novel enzyme related to the serine proteinase adipsin. *J. Clin. Invest.* **94**:1163-1171.

ZUCKER, R.M., ADAMS, D.J., BAIR, K.W., ELSTEIN, K.H. (1991). Polyploidy induction as a consequence of topoisomerase inhibition. *Biochem. Pharmacol.* **42**(11):2199-2208.